

2.2 Natural Conditions along Kirinda Coast

In this paragraph, data on the natural conditions found along the Kirinda coast collected for this Study are described.

2.2.1 Coast and Submarine Topography

(1) Submarine Topography

Four bathymetric surveys around the Harbour have been conducted to date. Two of them were in May 1988 and March 1989 for this Study, as shown in Appendix C. Another one was in February 1983 before the construction of the Harbour. The other was in November 1986 after siltation blocked the Harbour. The results of these surveys are shown three-dimensionally in Fig.2.2.1 (1)-(6). The figures show the water depth changes between the surveys. Locations of accumulated and eroded areas are indicated.

Fig.2.2.1 (1) shows the results comparing the data for between February 1983 and November 1986. It is considered acceptable that this result indicates characteristic of changes in the SW monsoon season, though the data were not obtained in the same year. From Fig.2.2.1, it is apparent that the areas where sand accumulated in this period are 1) the north side coast of Kirinda Point (hereinafter referred to the Point), 2) along a line between the rocky area in front of the Point and the mouth of the Harbour, 3) the basin in the Harbour. Erosion took place along the coast north of the Harbour. As to location 2), it became apparent from both sets of data that this location became shallower over the period.

Fig.2.2.2 (2) shows the results of comparing the data for between February 1983 and May 1988. Both were sets of data after the NE monsoon season. The data after construction of the Harbour shows two bank-shape shallow areas with accumulation appearing along the bank. On the other hand, a eroded area appeared at the north side of the

Harbour.

Fig.2.2.2 (3) shows the results of comparing the data for between February 1983 and March 1989. Both sets were also data after the NE monsoon season. The distribution of accumulation and erosion is almost the same as in the results in Fig.2.2.2 (1), but the accumulation in the area from the mouth of the Harbour to the offshore does not appear in Fig.2.2.2 (1).

Fig.2.2.2 (4) shows the results of comparing the data for between November 1986 and May 1988. It is considered that this also shows the characteristics of sea bottom changes after the NE monsoon season. The remarkable indication from the data obtained in May 1988 is that two bank-shaped shallow areas were found. One of these, located in the south side had also been found in the two previous surveys and had progressed toward the rocky area in front of the Point. This bank-shaped shallow area had significantly eroded in two years. The other had progressed from the north side of the Harbour to the offshore though it was not present in the results of February 1983.

Fig.2.2.2 (5) shows the results of comparing the data for between November 1986 and March 1989. These two sets of data were obtained before and after the NE monsoon season. The area from the north side beach of the Harbour to the offshore through the mouth of the Harbour was accreted and the area in front of Main Breakwater of the Harbour was eroded.

Fig.2.2.2 (6) shows the results of comparing the data for between May 1988 and March 1989. As the last survey was conducted just at the end of the NE monsoon season, an area of accumulation was found in the north coast of the Harbour, around the Point and in front of the mouth of the Harbour. The areas other than those were found to have been eroded.

The accreted and eroded locations after comparing all four of these bathymetric survey results are summarized in Table 2.2.1. From this table, the following items are noteworthy ;

- 1) There was a bank-shaped shallow area progressing from the rocky area in front of the Point to the Harbour in every survey. This progressed in the period from 1983 to 1986 but there was no progress after 1986. In this area, a strong current was observed in the field survey and the hydraulic model test mentioned in the following chapter. Based on this, it is considered that this area is the steady route of littoral drift.
- 2) Another bank-shaped shallow area progressing from the mouth of the Harbour to the offshore appeared in 1988 and progressed thereafter.
- 3) The area along the Main Breakwater and pocket beach was accreted suddenly but there were no changes after 1986. As to the area along the Main Breakwater, this showed a tendency to preferential erosion.
- 4) The beach area to the north side of the Harbour showed a tendency for erosion to occur in the SW monsoon season and accumulation in the NE. The tendency over the long term was one of erosion.
- 5) The location in front of the Point showed a tendency of both erosion and accumulation.

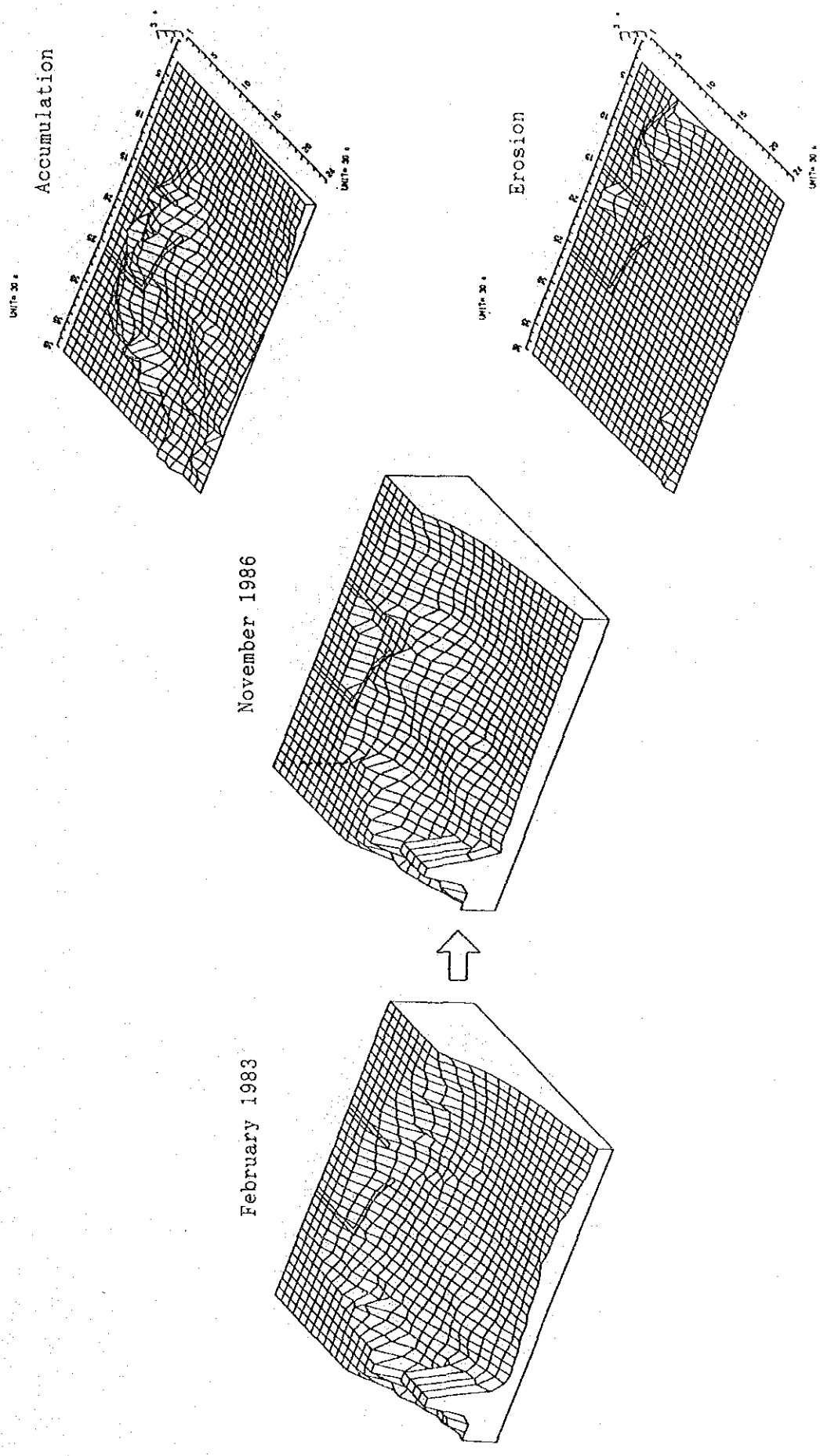


Fig. 2.2.1 (1) Submarine Topography (February 1983, November 1986)

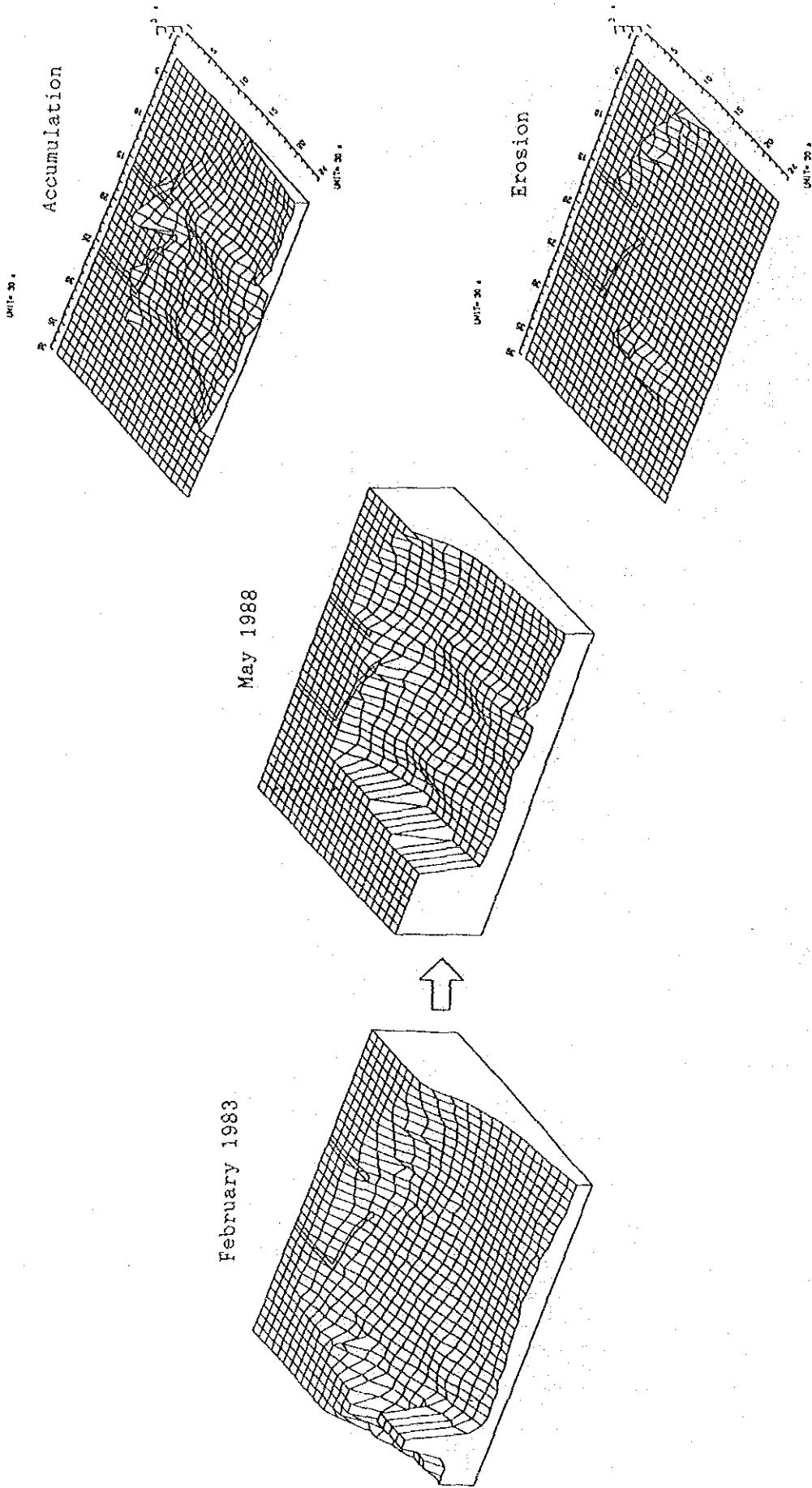


Fig. 2.2.1 (2) Submarine Topography (February 1983, May 1988)

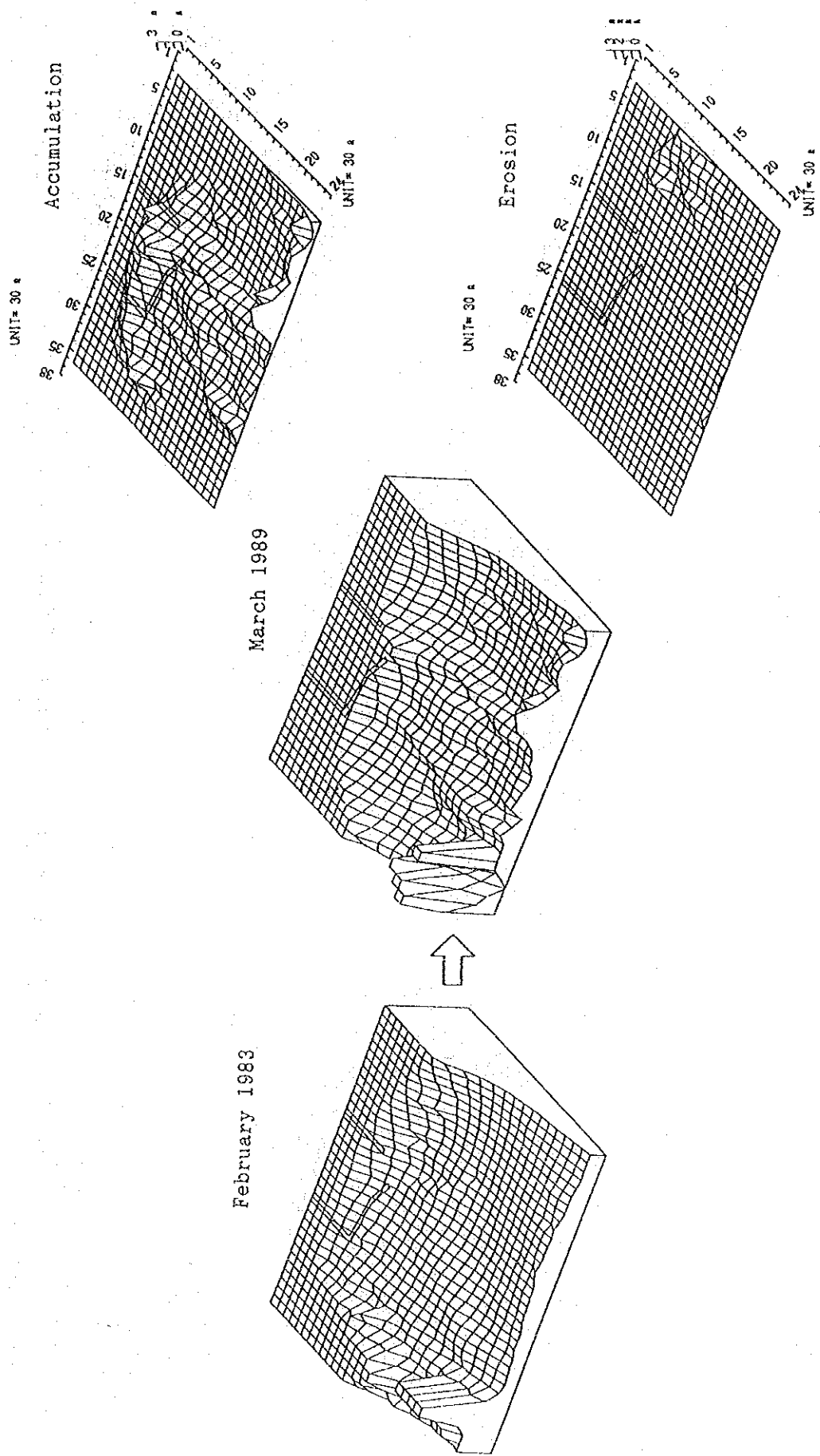


Fig. 2.2.1 (3) Submarine Topography (February 1983, March 1989)

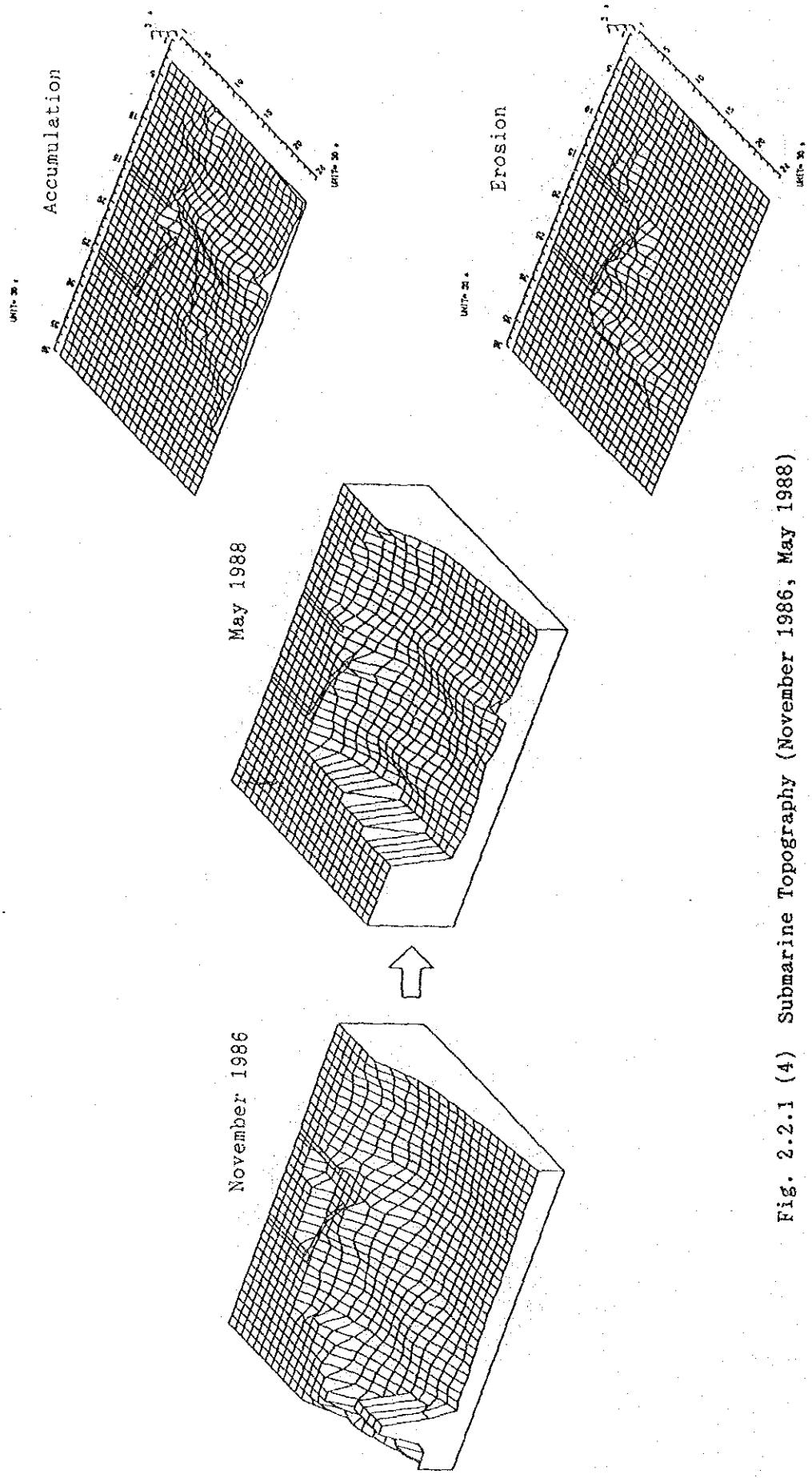


Fig. 2.2.1 (4) Submarine Topography (November 1986, May 1988)

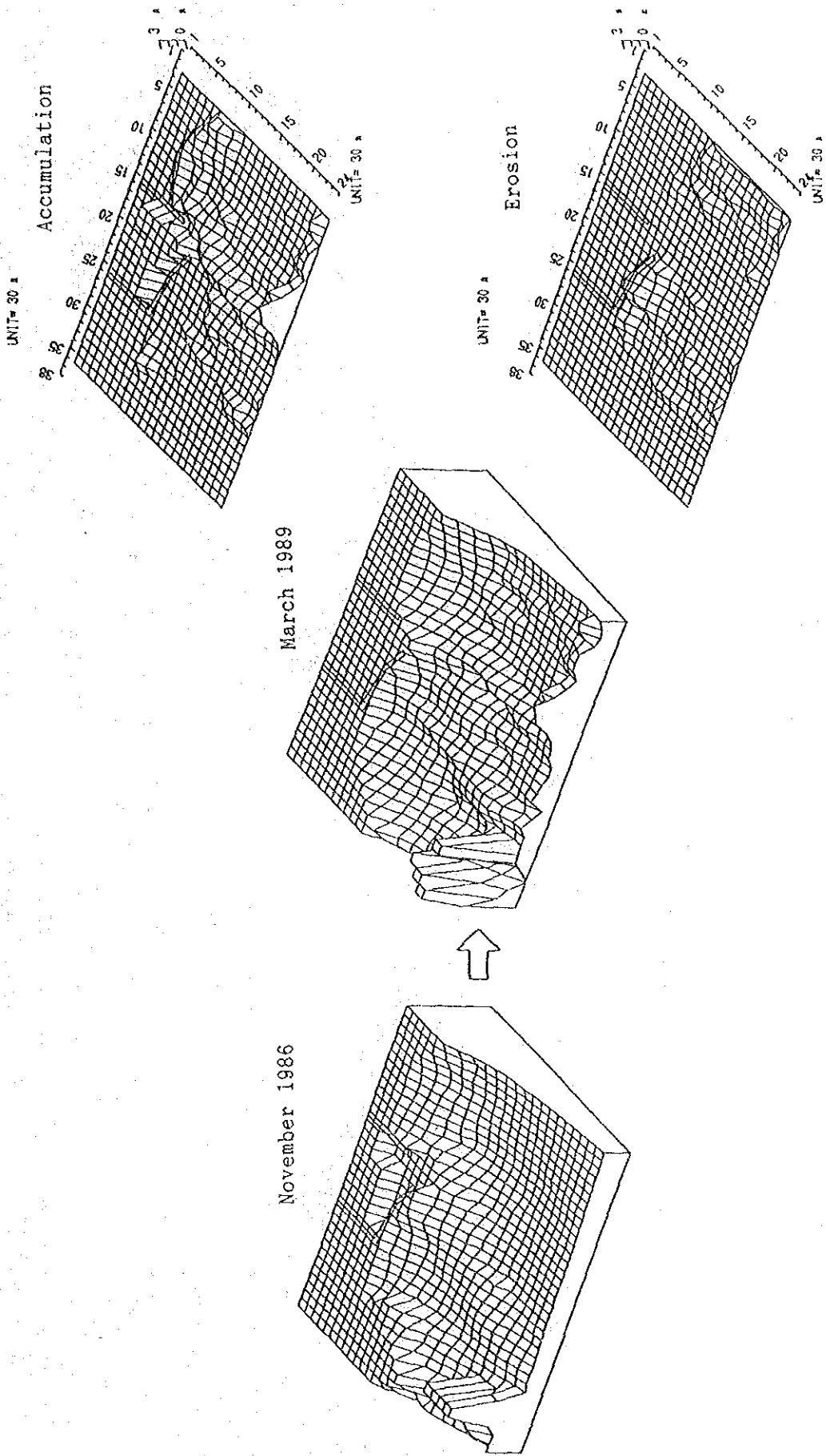


Fig. 2.2.1 (5) Submarine Topography (November 1986, March 1989)

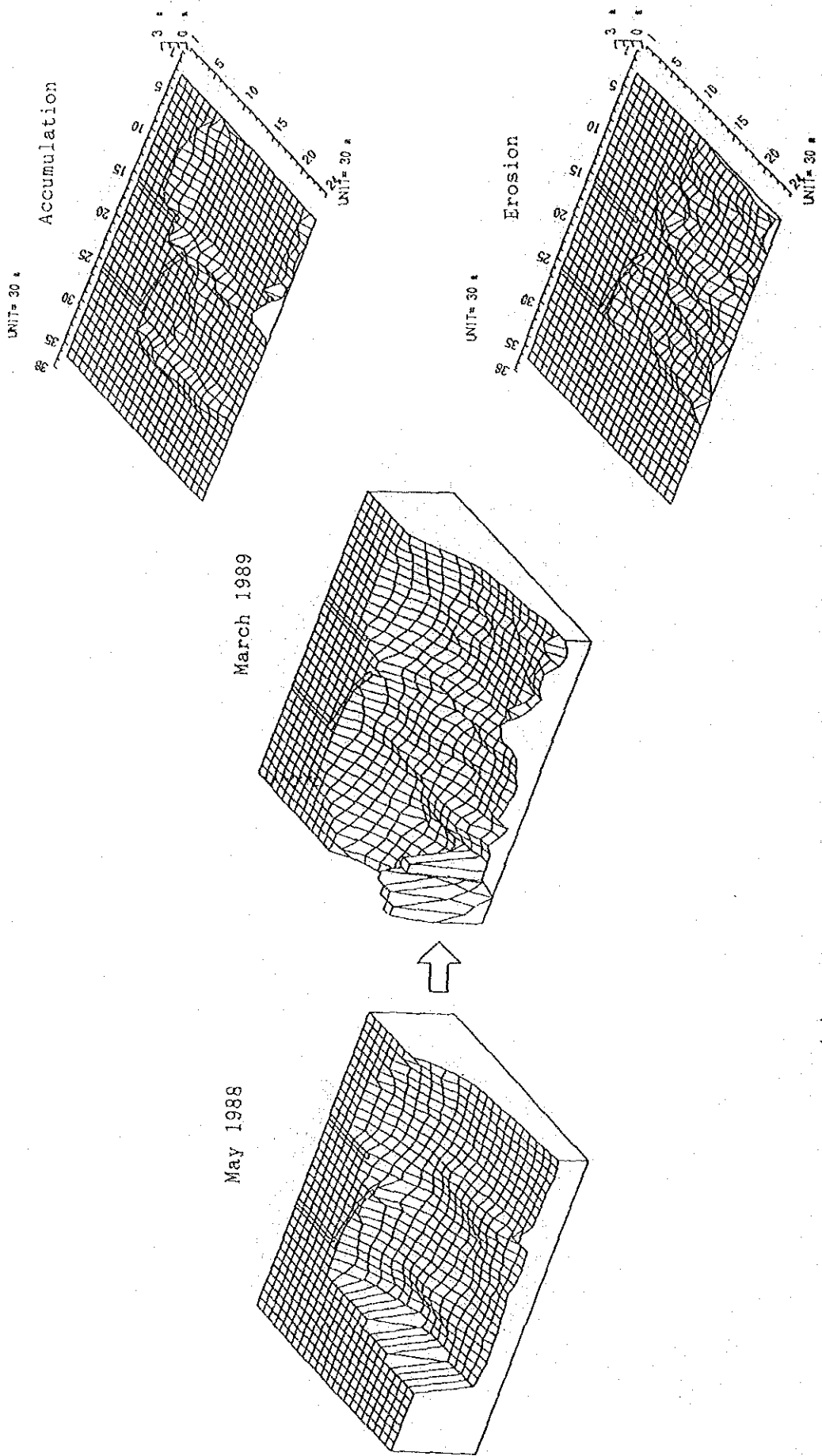


Fig. 2.2.1 (6) Submarine Topography (May 1988, March 1989)

Table 2.2.1 Main Accumulated and Eroded Locations between Surveys

February 1983	November 1986	May 1988	March 1989
<ul style="list-style-type: none"> * north side beach 	<ul style="list-style-type: none"> * along the Kirinda Point * from the Kirinda Point to mouth of the Harbour * front of the main breakwater 	<ul style="list-style-type: none"> * from the Kirinda Point to mouth of the Harbour * offshore from the mouth of Harbour * front of the main breakwater * offshore from the mouth of Harbour 	<ul style="list-style-type: none"> * pocket beach * inside the Harbour * from the Kirinda Point to mouth of the Harbour * offshore from the mouth of Harbour
<ul style="list-style-type: none"> * north side beach 	<ul style="list-style-type: none"> * along the Kirinda Point * front of the main breakwater * north side beach 	<ul style="list-style-type: none"> * offshore from the mouth of Harbour 	<ul style="list-style-type: none"> * offshore from the mouth of Harbour * north side beach
<ul style="list-style-type: none"> * north side beach * along the Kirinda Point 	<ul style="list-style-type: none"> * along the Kirinda Point * front of the main breakwater * north side beach 	<ul style="list-style-type: none"> * front of main breakwater * wide area of offshore 	<ul style="list-style-type: none"> * along the Kirinda Point * offshore from the mouth of Harbour * north side beach
<ul style="list-style-type: none"> * north side beach 	<ul style="list-style-type: none"> * front of the main breakwater * offshore of north side beach 	<ul style="list-style-type: none"> * front of main breakwater * wide area of offshore 	<ul style="list-style-type: none"> * front of main breakwater * wide area of offshore

Eroded Locations

Accumulated Locations

(2) Beach Topography

Shoreline surveys were conducted four times in the May, August, November of 1988 and March of 1989. The survey lines are shown in Fig.2.2.2. The results on selected survey lines are shown in Fig.2.2.3. and all the results are summarized in Fig.2.2.4 as a distribution of five stages, namely, notable accumulation, accumulation, stable, erosion and notable erosion. The following are apparent from Fig.2.2.4.

- 1) A tendency to erosion was dominant for the period from May to August of 1988 and accumulation from November 1988 to March 1989. For the period from August to November of 1988, the beach was stable.
- 2) The north coast which is 600 to 1000 meters distance from the Existing Groyne apparently showed a tendency to erosion in the SW monsoon season and accumulation in the NE.
- 3) The north coast more than 1 km away from the Existing Groyne showed a tendency toward erosion through out the survey period of this Study.
- 4) The area of the pocket beach showed a tendency to erosion in the SW monsoon season and accumulation in the NE.
- 5) The coast north of Drava Point showed a tendency to erosion in the SW monsoon season and accumulation in the NE.

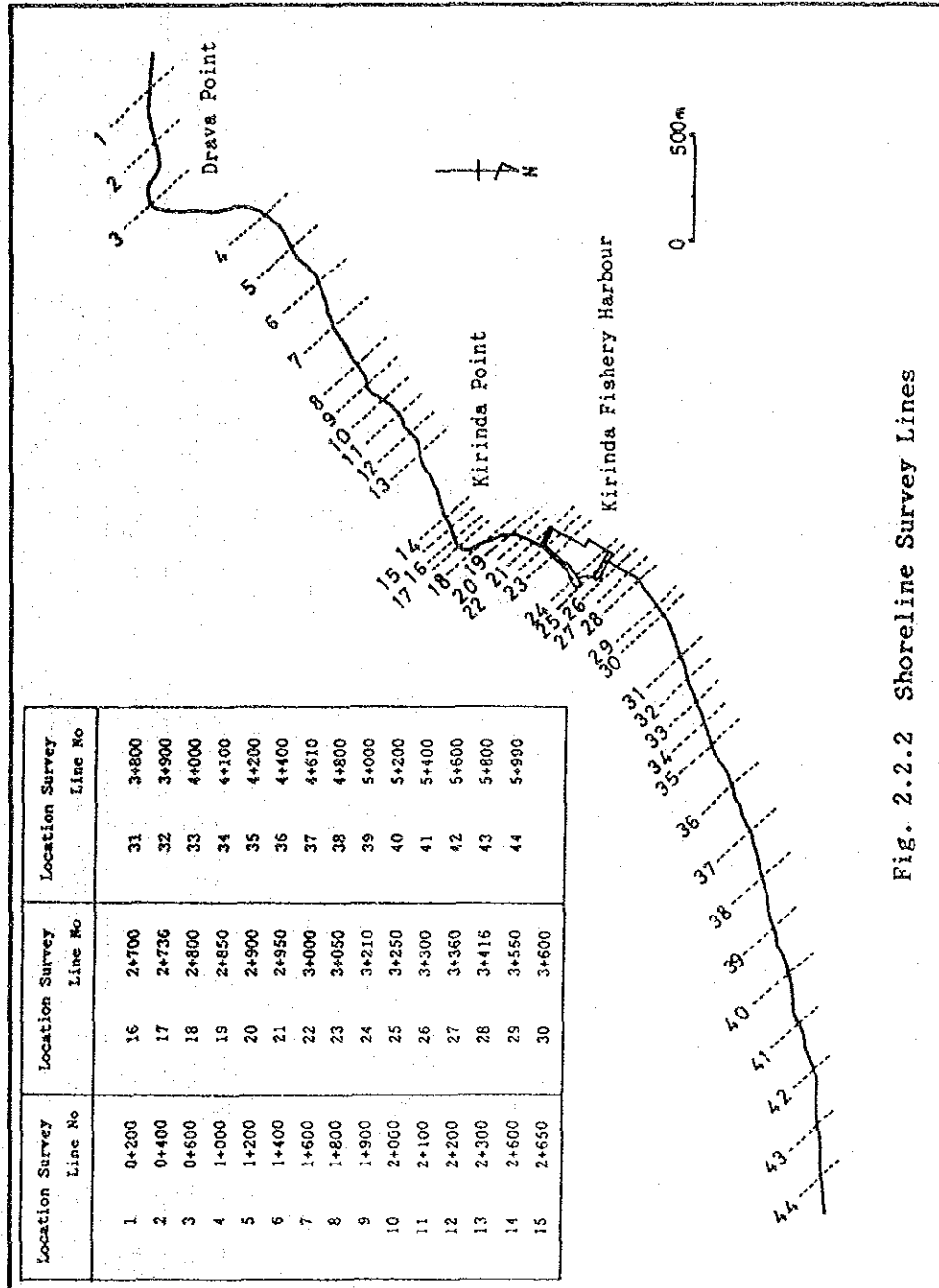


Fig. 2.2.2 Shoreline Survey Lines

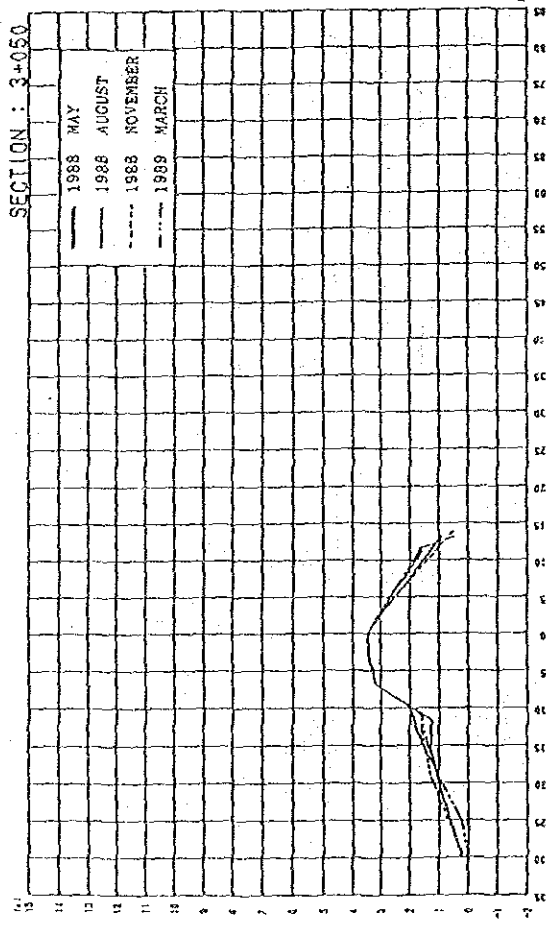
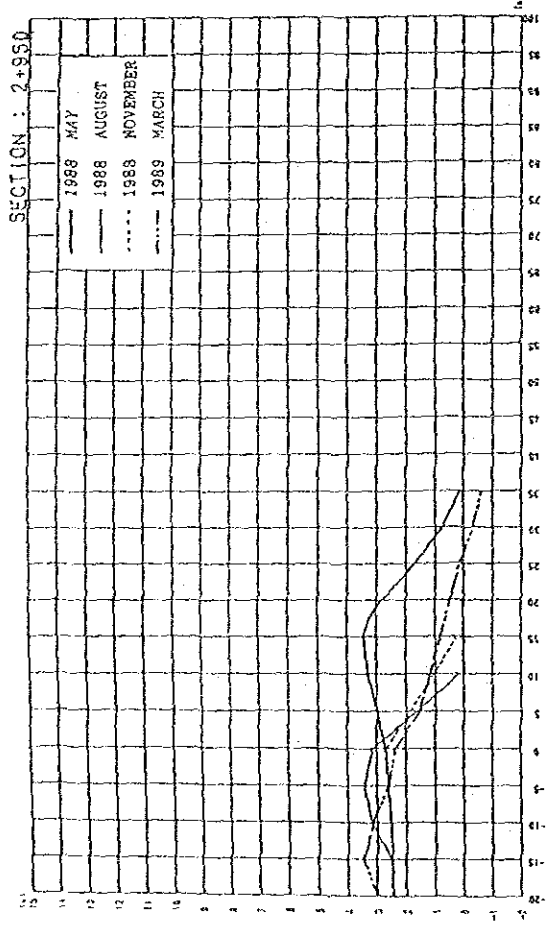
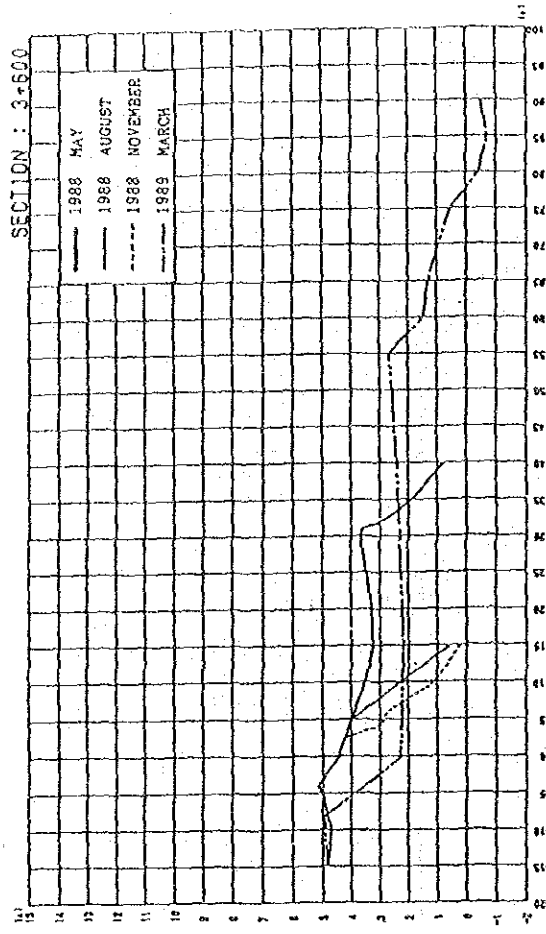
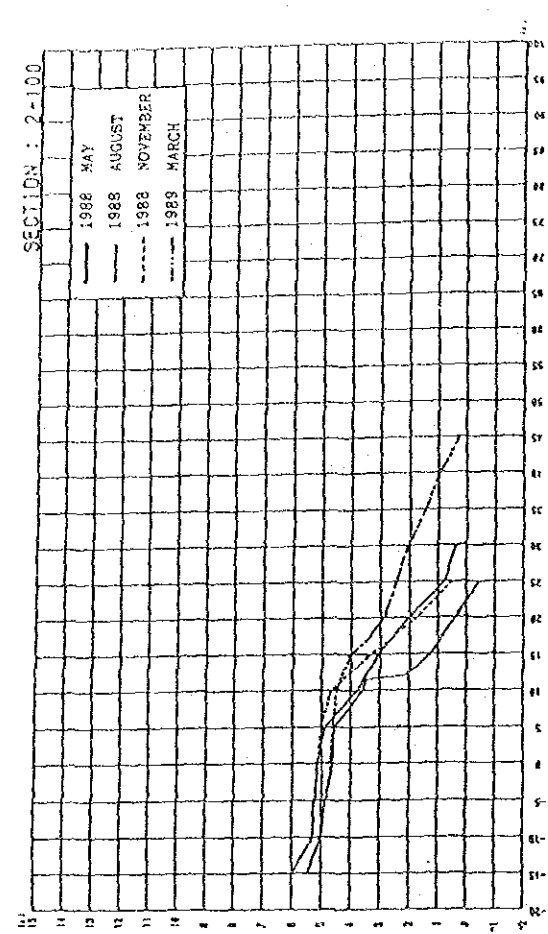


Fig. 2.2.3 Changes of Selected Beaches

Survey Line	Locations	May' 88	Aug' 88	Nov' 88	Mar' 89
0-066		●	←	△	→
0-200		●	←	○	→
0-400		+	←	▲	→

0-600	DORAVA POINT	+	+		
1-000		+	+		△
1-200		▲	○		△
1-400		●	△		○
1-600		▲	+		●
1-800		+	+		△
1-900		+	+		△

2-000		+	+		△
2-100		△	+		△
2-200		+	+		+
2-300		+	+		●
2-650		+	+		●
2-700	KIRINDA POINT	+	←	+	→
2-730		+	+		+
2-800		+	●		
2-850	West End of Pocket Beach	+	+		○
2-900		●	△		●
2-950	East End of Pocket Beach	▲	+		+

3-000	Front of South Breakwater	+	+		△
3-050	Front of South Breakwater	+	+		+
3-200	Front of South Breakwater	+	+		+
3-300	West End of East Beach	●	+		○
3-360		▲	●		○
3-416		▲	+		○
3-550		△	+		○
3-600		▲	+		○
3-800		▲	●		○
3-900		▲	+		○

4-000		●	+		●
4-100		●	△		●
4-200		●	△		●
4-400		+	+		●
4-610		+	+		
4-800		●	△		●

5-000		+	+		●
5-200		+	+		
5-400		+	+		△
5-600		+	△		+
5-800		△	+		●
5-990		+	+		▲

Legend ○ Remarkable Accumulation
 △ Accumulation
 + Stable
 ▲ Erosion
 ● Remarkable Erosion

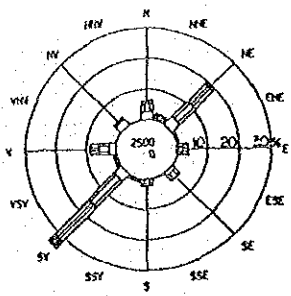
Fig. 2.2.4 Tendency of Accumulation and Erosion at Each Survey Line

2.2.2 Wind

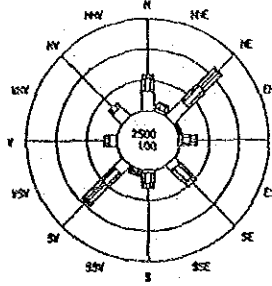
Wind roses at Hambantota and Kirinda are shown in Fig.2.2.5 and 2.2.6 respectively.

Wind data on Hambantota was obtained at Hambantota meteorological station located on a hill near the coast so it suffered no topographical influence. The observation period taken was for the six years from 1983 to 1988. Wind data for Kirinda was observed at the top of a water tank in the Harbour for ten months from May 1988 to February 1989 throughout this Study. A simple wind meter was used and observation was conducted at three hour intervals from 6 AM to 6 PM.

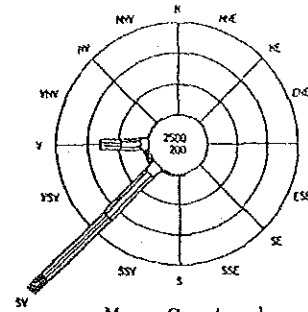
The results show the typical tendency of the so-called trade winds which blow dominantly from the SW direction in the SW monsoon season, and from the NE direction in the NE. The distribution range of wind direction is very limited. The tendency through a year was that, the SW direction is dominant and strong winds blow from the SW. As to the off monsoon season, March through April, again conditions were a typical, but in October to November there was a tendency toward the SW monsoon season conditions rather than those of the off.



Total

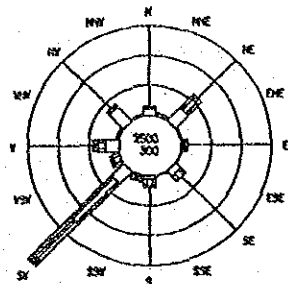
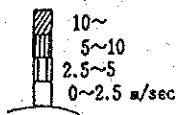


March - April

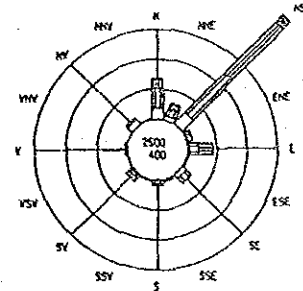


May-September
(SW monsoon season)

Legend
wind speed

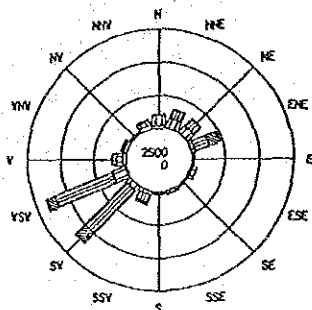


October - November

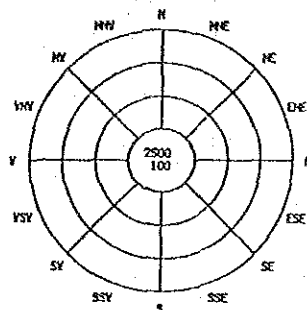


December - February
(NE monsoon season)

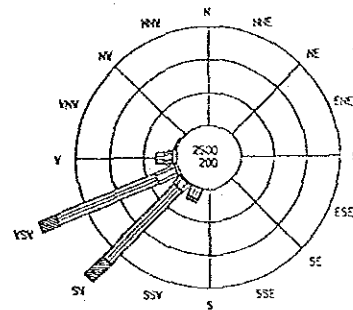
Fig. 2.2.5 Wind Roses (Hambantota, 1983 - 1988)



Total

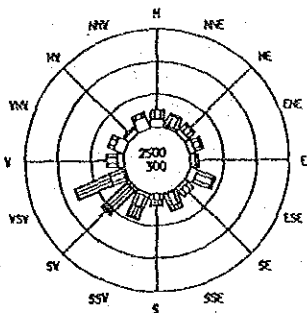
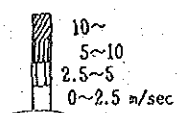


March - April

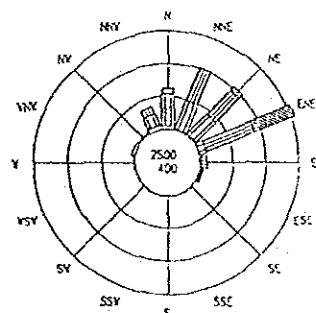


May - September
(SW monsoon season)

Legend
wind speed



October - November



December - February
(NE monsoon season)

Fig. 2.2.6 Wind Roses (Kirinda, May 1988 - February 1989)

2.2.3 Tide

In this Study it was difficult to find a suitable place for tide observation around the Harbour so the tide at Kirinda was turned out to examine the water surface data obtained by a pressure type wave recorder and the tide observation data using a Fuess tide gauge conducted at the quay in Tangalla Fishery Harbour located about 60 km far from Kirinda. The observation using a pressure type wave recorder was carried out for one month from August 1988 to September 1989 and for about one month from February 1989 to March 1989. And these were recorded every two hours interval. On the other hand, the observation at Tangalla Fishery Harbour using a Fuess tide gauge was carried out for seven months from August 1988 to February 1989, but even here, due to the influence of waves, conditions for observation were not so good. Using the data for one month from 8:30 on 20th of August 1988 to 6:30 on 20th of September obtained by a wave recorder and data for one month from 0:00 on 7th of September 1988 to 7:00 on 8th of October 1988 obtained by a Fuess tide gauge, the mean sea level and four tidal constituents (M2, S2, O1, K1) were analyzed. These four tidal constituents were compared with those of other locations in Sri Lanka as shown in Fig.2.2.7 and verified through examination. The tidal constituents of Kirinda, Tangalla and another locations are listed in Table 2.2.2 and heights of tides are shown in Fig.2.2.8. From the results, it is apparent that the tide types at Colombo, Galle, Tangalla and Kirinda are almost the same although the tidal ranges are slightly different.

In Sri Lanka, one characteristic is that there is a large time difference in the tides between the east and west sides of the Island. For example, at Point Pedro, the tide changes like an east side tide type but at Jaffna, although it is near Point Pedro, the tide changes to be a west side tide type. In the southern parts of the Island, the tidal constituents are known only the west side of Galle. And there are also known the data on time difference of tide and ratio of ranges at Hambantota compared with Colombo. The data shows that the tide at Hambantota show changes like a west side tide type. Accordingly, the tide at Tangalla should show the changes of a west side tide type and also the

tide at Kirinda so that this tendency corresponds to the results of observations gained through this Study. The ratio of tide ranges becomes small as the location goes east side.

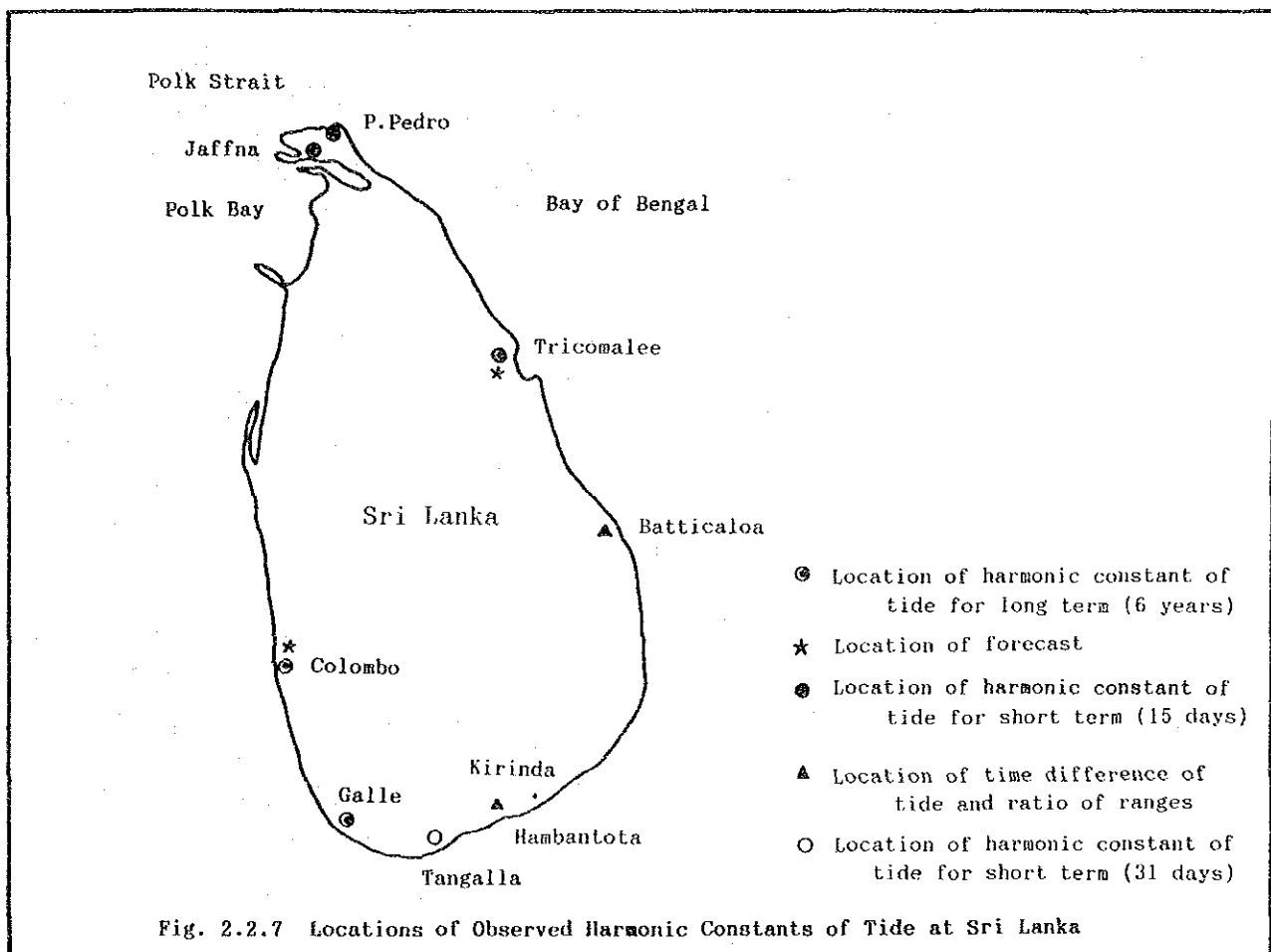


Table 2.2.2 Main Harmonic Constants of Tide in Sri Lanka

	Colombo		Galle		Tangalla		Kirinda		Tricomalee	
	H'cm	K°	H'cm	K°	H'cm	K°	H'cm	K°	H'cm	K°
M 2	17.6	50	16.1	57	13.7	60.8	7.7	72.0	17.7	241
S 2	11.9	95	11.0	94	8.2	96.4	5.8	97.4	6.4	265
K 1	7.3	33	5.1	18	4.2	48.8	4.6	357.1	6.6	331
O 1	2.9	62	1.4	76	0.7	1.0	0.4	322.8	2.0	309
Sa	9.5	308	10.7	309					7.5	268
Ssa	4.1	111	3.9	116					6.2	134
Hm+Hs	29.5		27.1		21.9		13.5		24.1	
H +Ho	10.2		6.5		4.9		5.0		8.6	
Hm-Hs	5.7		5.1		5.5		1.8		11.3	
H'+Ho/Hm+Hs	0.35		0.24		0.22		0.37		0.36	
Hm-Hs/Hm+Hs	0.19		0.19		0.25		0.14		0.47	
Hm+Hs+H'+Hs	39.7		33.6		26.8		18.5		32.7	
Z 0	37.8		33.8						31.4	
$\kappa_s - \kappa_m$	45		37		35.6		25		24	
$\kappa' - \kappa_o$	-29		-58		47.8		34		22	
Hs/Hm	0.68		0.68		0.60		0.76		0.36	
Ho/H	0.40		0.27		0.17		0.09		0.30	
M.H.W.I.	1h-43m		1h-58m		2h-06m		2h-29m		8h-19m	

Time Differences of Tide and Ratio of Ranges from Colombo

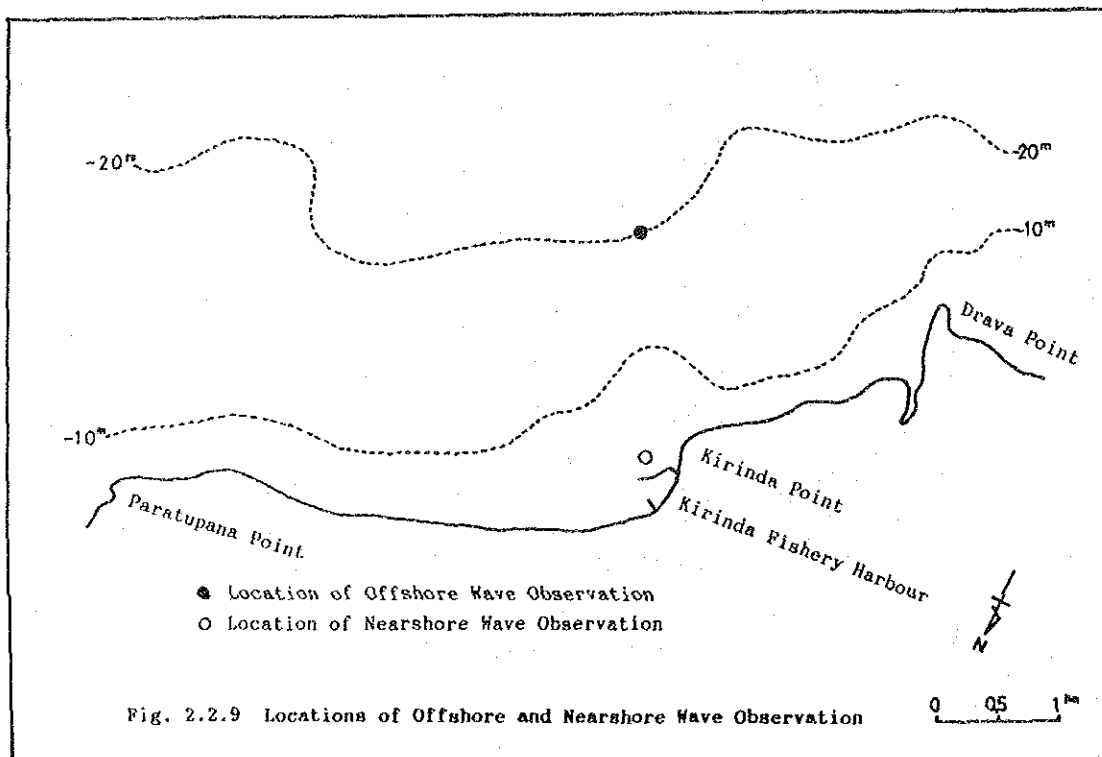
	Colombo	Galle	Tangalla	Hambantota	Kirinda
Time Differences of Tide	0 min	+15min	+23min	+20min	+46min
Ratio of Ranges	1	0.92	0.74	0.65	0.46

2.2.4 Waves

The offshore wave height and wave direction were observed at 20 m depth located offshore from the Point from May 1988 to March 1989 using a buoy type wave recorder (a wave rider) and a magnetic current meter. Also, the nearshore wave height and wave direction were observed in front of the Main Breakwater of the Harbour for one month from the middle of August to the middle of September, 1988 and for the month of March 1989 using pressure type wave recorders and magnetic current meters.

At the offshore, the wave height was observed for 20 min durations in three hour intervals, and the current, for 8 min in 6 hour intervals. In the nearshore, the wave height was observed for 9 min in 2 hour intervals during the SW monsoon season, and for 17 min in 2 hour intervals during the NE monsoon season.

The locations observed in both the offshore and nearshore are shown in Fig.2.2.9.



(1) Characteristics of Offshore Waves

Monthly and seasonal frequency distributions of the wave heights are shown in Fig.2.2.3 (1) - (2). The frequency distributions of wave heights over ten months showed a wave height ranging from 1.0 - 1.2 m as the most frequent and this occupied 31.1 % of the total. A wave height ranging over 0.6 - 1.6 m duly occupied 96.0 % of the total. This shows that the wave heights in Kirinda were mostly confined within 1.0 m and heights of more than 1.6 m or less than 0.6 m wave height constituted of less than 5 %.

In general, the waves occurring in the SW monsoon season were bigger than those in the NE monsoon season. Waves in the SW monsoon season were frequent in the wave range 1.0 -1.6 m while in the NE monsoon season they were frequently in the range of 0.6 - 1.2 m.

The maximum and minimum of the monthly maximum wave heights (H_{max}), 1/10 maximum wave height ($H_{1/10}$), significant wave height (H_s), average wave period (T_z) and significant wave period (T_s) are shown in Table 2.2.4. From this Table, it can be seen out that the maximum of the maximum wave heights was 3.36 m recorded at 9 AM on 15th September 1988, and the maximum of the significant wave heights was 1.95 m recorded at 3 PM on 23rd May 1988 through this Study. Comparing this to the data obtained at Galle Harbour from 1985 to 1986 where the maximum significant wave height was 3.5 m and the frequency distribution of significant wave height over 2.0 m was almost 23 % in the SW monsoon season, it is considered that waves occurring around the Harbour were not so large and the reason for this was due to the refraction effect resulting from the Galle coast being almost perpendicular to the south-west direction while on the other hand the Kirinda coast is parallel to the south-west direction, so the energy of waves is dispersed.

The monthly and seasonal frequency distributions of the wave period are shown in Table 2.2.5 (1) - (2). The frequency distribution of the wave periods for 10 months showed that most of total (92 %) was in the rank of 6 - 10 sec with waves with a rank of 7 - 9 sec occupying 52 % of the total. As to the seasonal frequency distribution of wave period, waves ranking in the 7 - 10 sec were frequent in the SW monsoon season and 5 - 8 sec in the NE monsoon season. There was a tendency for the wave period in the SW monsoon period to be longer than that in the NE monsoon season.

It is known generally that wave periods recorded by a buoy type wave recorder are shorter than the real wave period. An example of a comparison between the average period obtained with a wave rider and one of a wave motion component of current obtained with a magnetic current meter which was installed just near the wave rider is shown in Table 2.2.6 (1) - (2). The results show that the average period obtained with the wave rider was dominant at 4 - 8 sec rank while that with the current meter was dominant at 8 - 12 sec. There was a difference of about 4 sec. It is considered that the wave motion component measured with the current meter is strongly influenced by the swell component due to the attenuation of wind waves which have short wave periods.

The wave direction was determined as that direction of the composite current which had a wave motion component separate from the current records obtained by a magnetic current meter. The monthly and seasonal wave directions are shown in Table 2.2.7 (1) - (2). The angles in the Table are in degrees measured clockwise starting from the north, i.e. zero indicates the direction of north and 180 degrees is south. The distribution of the wave direction through out one year was in a limited range. The wave direction was 90 % from the south within a 15 degree variation. As to the seasonal wave direction, more than 95 % was from the south or within 15 degrees from the south in the SW monsoon season and the same direction in the NE monsoon season decreased to 74 %. The frequency distribution on the east side direction from 165 degrees was 4.2 % in the SW monsoon

season and this increased to 26.3 % in the NE monsoon season.

Typical wave spectra observed in this Study are shown in Fig.2.2.10 (1) - (3). There was a peak around the wave period of 10 - 16 sec throughout the year as shown in Fig.2.2.10 (1) and this peak was dominant in the SW monsoon season. Even when there were other secondary peaks around the short wave period of 4 - 7 sec shown in Fig.2.2.10 (2), the peak of 10 - 16 sec still remained more dominant than the 4 - 7 sec. However, in the case of the NE monsoon season, sometimes shorter peaks became dominant as shown in Fig.2.2.10 (3). There was a tendency for changes in the short period component to often be diurnal like the wind. Throughout one year, especially in the NE monsoon season, the short period component became bigger in the daytime and an corresponding increment in the wave height resulted.

As described before, the dominant wave direction was also from the south in the NE monsoon season while the dominant wind direction was from NNE - ENE in the same season. As the wave direction of the short period component of a wind wave must correspond to the direction of the wind, it is considered that waves in the NE monsoon season are composition of swells which are continuous through the year coming from south and the wind waves coming from the NE monsoon season. As to the spectra of waves in the NE monsoon season, it was possible to separate the long period components and short period components using a boundary of frequency 0.125 Hz (wave period 8.0 sec). The wave heights and wave periods of both components were calculated using the following with zero and secondary moments of frequency spectra respectively.

$$H_s = 4.0 \sqrt{m_0},$$
$$T_s = 1.1 \sqrt{m_0 / m_2}$$

in which,

$$m_0 = \int_0^{\infty} S(f) df$$
$$m_2 = \int_0^{\infty} f^2 S(f) df$$

The separated frequency distributions of the swell and wind waves are shown in Table 2.2.8 (1) - (2). However, the above calculation was conducted using the only following data.

3/Dec. 15:00 - 4/Dec. 18:00	12/Dec. 21:00 - 15/Dec. 6:00
28/Dec. 6:00 - 31/Dec. 12:00	12/Jan. 12:00 - 15/Jan. 15:00
22/Jan. 3:00 - 24/Jan. 12:00	29/Jan. 9:00 - 31/Jan. 21:00
3/Feb. 6:00 - 4/Feb. 18:00	19/Feb. 6:00 - 20/Feb. 6:00
23/Feb. 18:00 - 26/Feb. 21:00	

Table 2.2.3 (1) Monthly Frequency Distribution of Wave Height

Wave Height Hs (m)	May '88		Jun '88		Jul '88		Aug '88		Sep '88		Oct '88		Nov '88		Dec '88		Jan '89		Feb '89	
	Rec	%	Rec	%	Rec	%	Rec	%	Rec	%	Rec	%	Rec	%	Rec	%	Rec	%	Rec	%
2.0-2.2	0	0.0	0	0.0	0	0.0	0	0.0	0	0.0	0	0.0	0	0.0	0	0.0	0	0.0	0	0.0
1.8-2.0	1	0.8	0	0.0	4	1.6	0	0.0	0	0.0	0	0.0	0	0.0	0	0.0	0	0.0	0	0.0
1.6-1.8	6	4.8	4	1.9	20	8.1	3	1.2	9	3.8	0	0.0	6	2.5	0	0.0	0	0.0	0	0.0
1.4-1.6	69	55.2	18	8.7	62	25.1	21	8.5	33	13.8	6	2.4	18	7.6	0	0.0	0	0.0	0	0.0
1.2-1.4	46	36.8	88	42.5	88	35.6	81	32.7	60	25.1	49	19.9	19	8.1	10	4.0	10	4.0	6	2.7
1.0-1.2	3	2.4	82	39.6	59	23.9	127	51.2	85	35.6	114	46.3	53	22.5	56	22.7	83	33.5	42	18.8
0.8-1.0	0	0.0	15	7.2	14	5.7	16	6.5	49	20.5	70	28.5	66	28.0	96	38.9	120	48.4	93	41.7
0.6-0.8	0	0.0	0	0.0	0	0.0	0	0.0	3	1.3	7	2.8	46	19.5	82	33.2	35	14.1	81	36.3
0.4-0.6	0	0.0	0	0.0	0	0.0	0	0.0	0	0.0	0	0.0	28	11.9	3	1.2	0	0.0	1	0.4
0.2-0.4	0	0.0	0	0.0	0	0.0	0	0.0	0	0.0	0	0.0	0	0.0	0	0.0	0	0.0	0	0.0
0.0-0.2	0	0.0	0	0.0	0	0.0	0	0.0	0	0.0	0	0.0	0	0.0	0	0.0	0	0.0	0	0.0
Total	125	100.0	207	100.0	247	100.0	248	100.0	239	100.0	246	100.0	236	100.0	247	100.0	248	100.0	223	100.0

Table 2.2.3 (2) Seasonal Frequency Distribution of Wave Height

Wave Height Hs (m)	Total Period May '88-Feb '89		S.W. Monsoon May '88-Sep '88		N.E. Monsoon Dec '88-Feb '89	
	Rec	%	Rec	%	Rec	%
	2.0-2.2	0	0.0	0	0.0	0
1.8-2.0	5	0.2	5	0.5	0	0.0
1.6-1.8	48	2.1	42	3.9	0	0.0
1.4-1.6	227	10.0	203	19.0	0	0.0
1.2-1.4	457	20.2	363	34.1	26	3.6
1.0-1.2	704	31.1	356	33.4	181	25.2
0.8-1.0	539	23.8	94	8.8	309	43.0
0.6-0.8	254	11.2	3	0.3	198	27.6
0.4-0.6	32	1.4	0	0.0	4	0.6
0.2-0.4	0	0.0	0	0.0	0	0.0
0.0-0.2	0	0.0	0	0.0	0	0.0
Total	2266	100.0	1066	100.0	718	100.0

Table 2.2.4 Maximum and Minimum of Monthly Wave Height and Period

Wave Parameter	Month										
	May '88	Jun '88	Jul '88	Aug '88	Sep '88	Oct '88	Nov '88	Dec '88	Jan '89	Feb '89	
Hmax (m)	max	3.21	3.10	3.21	2.93	3.36	2.82	2.88	2.39	2.46	2.15
	min	1.72	1.40	1.37	1.45	1.19	1.09	0.68	0.94	1.06	0.86
H10% (m)	max	2.44	2.15	2.58	2.14	2.20	1.95	2.23	1.75	1.65	1.58
	min	1.45	1.07	1.09	1.13	0.93	0.90	0.56	0.71	0.82	0.72
Hs (m)	max	1.95	1.78	1.87	1.64	1.78	1.57	1.70	1.38	1.33	1.28
	min	1.15	0.87	0.86	0.85	0.76	0.69	0.47	0.55	0.60	0.58
Tz (s)	max	7.38	9.00	10.70	8.94	8.00	9.00	9.90	8.82	6.85	8.83
	min	5.12	5.04	4.62	4.49	4.39	4.50	5.11	3.75	4.14	3.84
Ts (s)	max	10.77	12.30	14.38	15.23	12.08	12.61	13.85	10.66	10.31	10.33
	min	6.23	6.11	6.06	5.50	5.41	5.58	7.17	5.22	5.04	4.80

Table 2.2.5 (1) Monthly Frequency Distribution of Wave Period

Wave Pd Ts(sec)	May '88		Jun '88		Jul '88		Aug '88		Sep '88		Oct '88		Nov '88		Dec '88		Jan '89		Feb '89	
	Rec	%	Rec	%	Rec	%	Rec	%	Rec	%	Rec	%	Rec	%	Rec	%	Rec	%	Rec	%
16-	0	0.0	0	0.0	0	0.0	0	0.0	0	0.0	0	0.0	0	0.0	0	0.0	0	0.0	0	0.0
15-16	0	0.0	0	0.0	0	0.0	1	0.4	0	0.0	0	0.0	0	0.0	0	0.0	0	0.0	0	0.0
14-15	0	0.0	0	0.0	2	0.8	0	0.0	0	0.0	0	0.0	0	0.0	0	0.0	0	0.0	0	0.0
13-14	0	0.0	0	0.0	7	2.8	1	0.4	0	0.0	0	0.0	1	0.4	0	0.0	0	0.0	0	0.0
12-13	0	0.0	3	1.6	5	2.0	3	1.2	1	0.4	4	1.6	3	1.3	0	0.0	0	0.0	0	0.0
11-12	0	0.0	6	3.1	13	5.3	10	4.1	1	0.4	23	9.3	25	10.5	0	0.0	0	0.0	0	0.0
10-11	4	3.3	19	9.7	39	15.9	17	7.0	15	6.5	25	10.2	55	23.3	4	1.6	1	0.4	3	1.3
9-10	15	12.3	47	24.0	68	27.6	45	18.4	27	11.6	44	17.9	79	33.5	23	9.3	7	2.8	7	3.1
8-9	47	38.5	46	23.5	54	22.0	75	30.7	54	23.3	52	21.1	66	28.0	28	11.3	21	8.5	19	8.5
7-8	49	40.2	67	34.2	42	17.1	68	27.9	80	34.5	55	22.4	7	3.0	58	23.5	66	26.2	51	22.9
6-7	7	5.7	8	4.1	16	6.5	21	8.6	44	19.0	40	16.3	0	0.0	61	24.7	122	49.2	71	31.8
5-6	0	0.0	0	0.0	0	0.0	3	1.2	10	4.3	3	1.2	0	0.0	62	25.1	32	12.9	65	29.1
-5	0	0.0	0	0.0	0	0.0	0	0.0	0	0.0	0	0.0	0	0.0	11	4.5	0	0.0	7	3.1
Total	122	100.0	196	100.0	246	100.0	244	100.0	232	100.0	245	100.0	238	100.0	247	100.0	248	100.0	223	100.0

Table 2.2.5 (2) Seasonal Frequency Distribution of Wave Period

Wave Pd Ts(sec)	Total Period		S.W. Monsoon		N.E. Monsoon	
	May '88-Feb '89		May '88-Sep '88		Dec '88-Feb '89	
	Rec	%	Rec	%	Rec	%
16-	0	0.0	0	0.0	0	0.0
15-16	1	0.1	1	0.1	0	0.0
14-15	2	0.1	2	0.2	0	0.0
13-14	9	0.5	8	0.8	0	0.0
12-13	19	1.0	12	1.2	0	0.0
11-12	78	4.1	30	2.9	0	0.0
10-11	182	9.5	94	9.0	8	1.1
9-10	362	19.0	202	19.4	37	5.2
8-9	462	24.2	276	26.5	68	9.5
7-8	541	28.3	306	29.4	174	24.2
6-7	390	20.4	96	9.2	254	35.4
5-6	175	9.2	13	1.3	159	22.1
-5	18	0.9	0	0.0	18	2.5
Total	1909	100.0	1040	100.0	718	100.0

Table 2.2.6 Comparison of Wave Period Obtained by Buoy Type Wave Recorder and Magnetic Current Meter

Wave Period Tz(s)	Total Period		S.W. Monsoon		N.E. Monsoon	
	May '88-Feb '89		May '88-Sep '88		Dec '88-Feb '89	
	Rec	%	Rec	%	Rec	%
10-12	4	0.2	4	0.4	0	0.0
8-10	133	5.9	57	5.3	5	0.7
6-8	799	35.3	476	44.7	69	9.6
4-6	1326	58.5	529	49.6	640	89.3
2-4	3	0.1	0	0.0	3	0.4
0-2	0	0.0	0	0.0	0	0.0
Total	2265	100.0	1066	100.0	717	100.0

(1) Seasonal Distribution of Zero Crossing Period (Tz).

Wave Period To2(s)	Total Period		S.W. Monsoon		N.E. Monsoon	
	May '88-Feb '89		May '88-Sep '88		Dec '88-Feb '89	
	Rec	%	Rec	%	Rec	%
14-16	0	0.0	0	0.0	0	0.0
12-14	22	2.1	17	2.9	4	1.8
10-12	285	27.0	179	30.4	57	25.4
8-10	671	63.5	358	60.8	129	57.6
6-8	77	7.3	35	5.9	33	14.7
4-6	2	0.2	0	0.0	1	0.4
2-4	0	0.0	0	0.0	0	0.0
Total	1057	100.0	589	100.0	224	100.0

(2) Seasonal Distribution of Orbital Period (To2).

Table 2.2.7 Monthly and Seasonal Wave Direction

Orbital Dir Deg	May '88		Jun '88		Jul '88		Aug '88		Sep '88		Oct '88		Nov '88		Dec '88		Jan '89		Feb '89	
	Rec	%	Rec	%	Rec	%	Rec	%	Rec	%	Rec	%	Rec	%	Rec	%	Rec	%	Rec	%
165-180	62	61.4	112	93.3	108	87.1	118	95.2	91	75.8	98	79.0	96	80.0	7	70.0	41	40.2	69	61.6
135-165	0	0.0	7	5.8	0	0.0	6	4.8	12	10.0	10	8.1	8	6.7	2	20.0	19	18.6	13	11.6
105-135	0	0.0	0	0.0	0	0.0	0	0.0	0	0.0	0	0.0	0	0.0	0	0.0	18	17.6	0	0.0
75-105	0	0.0	0	0.0	1	0.8	0	0.0	0	0.0	1	0.8	0	0.0	0	0.0	7	6.9	0	0.0
45-75	0	0.0	0	0.0	0	0.0	0	0.0	0	0.0	0	0.0	0	0.0	0	0.0	0	0.0	0	0.0
15-45	0	0.0	0	0.0	0	0.0	0	0.0	0	0.0	0	0.0	0	0.0	0	0.0	0	0.0	0	0.0
0-15	39	38.6	1	0.8	15	12.1	0	0.0	17	14.2	15	12.1	16	13.3	1	10.0	17	16.7	30	26.8
Total	101	100.0	120	100.0	124	100.0	124	100.0	120	100.0	124	100.0	120	100.0	10	100.0	102	100.0	112	100.0

(1) Monthly Distribution of Orbital Direction (modulus).

Orbital Dir Deg	Total Period		S.W. Monsoon		N.E. Monsoon	
	Rec	%	May '88-Feb '89	May '88-Sep '88	Dec '88-Feb '89	Dec '88-Feb '89
165-180	802	75.9	491	88.4	117	52.2
135-165	77	7.3	25	4.2	34	15.2
105-135	18	1.7	0	0.0	18	8.0
75-105	9	0.9	1	0.2	7	3.1
45-75	0	0.0	0	0.0	0	0.0
15-45	0	0.1	0	0.0	0	0.0
0-15	151	14.3	72	12.2	48	21.4
Total	1057	100.0	589	100.0	224	100.0

(2) Seasonal Distribution of Orbital Direction.

Table 2.2.8 (1) Frequency Distribution of Swells in NE Monsoon Season

Wave Height (m)	Wave Period (s)	Calm	0-8	8-9	9-10	10-11	11-12	12-13	13-14	14-15	15-16	16-	Total
		0	0	0	0	0	0	0	0	0	0	0	0
		0.0	0.0	0.0	0.0	0.0	0.0	0.0	0.0	0.0	0.0	0.0	0.0
0.00-0.25	0	0	0	0	0	0	0	0	0	0	0	0	0
		0.0	0.0	0.0	0.0	0.0	0.0	0.0	0.0	0.0	0.0	0.0	0.0
0.25-0.50	0	0	0	0	0	2	4	0	0	0	0	0	6
		0.0	0.0	0.0	0.0	0.0	1.2	2.4	0.0	0.0	0.0	0.0	3.6
0.50-0.75	0	0	0	1	23	29	29	18	10	2	0	0	112
		0.0	0.0	0.6	13.7	17.3	17.3	10.7	6.0	1.2	0.0	0.0	66.7
0.75-1.00	0	0	0	1	17	8	18	5	1	0	0	0	50
		0.0	0.0	0.6	10.1	4.8	10.7	3.0	0.6	0.0	0.0	0.0	29.8
1.00-1.25	0	0	0	0	0	0	0	0	0	0	0	0	0
		0.0	0.0	0.0	0.0	0.0	0.0	0.0	0.0	0.0	0.0	0.0	0.0
1.25-1.50	0	0	0	0	0	0	0	0	0	0	0	0	0
		0.0	0.0	0.0	0.0	0.0	0.0	0.0	0.0	0.0	0.0	0.0	0.0
1.50-	0	0	0	0	0	0	0	0	0	0	0	0	0
		0.0	0.0	0.0	0.0	0.0	0.0	0.0	0.0	0.0	0.0	0.0	0.0
Total	0	0	0	2	40	39	51	23	11	2	0	0	168
		0.0	0.0	1.2	23.8	23.2	30.4	13.7	6.5	1.2	0.0	0.0	100.0

* Figures in lower columns show the percentage of frequency

Table 2.2.8 (2) Frequency Distribution Wind Waves in NE Monsoon Season

Wave Height (m)	Wave Period (s)	Calm	0-3	3-4	4-5	5-6	6-7	7-8	8-	Total
		0	0	0	0	0	0	0	0	0
		0.0	0.0	0.0	0.0	0.0	0.0	0.0	0.0	0.0
0.00-0.25	0	0	0	0	0	0	0	0	0	0
		0.0	0.0	0.0	0.0	0.0	0.0	0.0	0.0	0.0
0.25-0.50	0	0	1	4	1	0	0	0	0	6
		0.0	0.6	2.4	0.6	0.0	0.0	0.0	0.0	3.6
0.50-0.75	0	0	7	30	8	0	0	0	0	45
		0.0	4.2	17.9	4.8	0.0	0.0	0.0	0.0	26.8
0.75-1.00	0	0	0	47	42	0	0	0	0	89
		0.0	0.0	28.0	25.0	0.0	0.0	0.0	0.0	53.0
1.00-1.25	0	0	0	17	10	0	0	0	0	27
		0.0	0.0	10.1	6.0	0.0	0.0	0.0	0.0	16.1
1.25-1.50	0	0	0	1	0	0	0	0	0	1
		0.0	0.0	0.6	0.0	0.0	0.0	0.0	0.0	0.6
1.50-	0	0	0	0	0	0	0	0	0	0
		0.0	0.0	0.0	0.0	0.0	0.0	0.0	0.0	0.0
Total	0	0	8	99	61	0	0	0	0	168
		0.0	4.8	58.9	36.3	0.0	0.0	0.0	0.0	100.0

* Figures in lower columns show the percentage of frequency

(2) Characteristics of Nearshore Waves

Correlations between the offshore and nearshore waves are shown in Fig.2.2.11 (1) - (2). The nearshore wave heights in the SW monsoon season decreased 80 % of the offshore wave height due to refraction and diffraction by the Point and waves breaking. However in the NE monsoon season, there were no changes between the nearshore waves and the offshore waves.

The wave periods at the nearshore were longer than those of the offshore in both seasons. The real reason of this difference is not clear as different measuring instruments and different calculation methods for the nearshore and offshore waves were used.

The relations between the nearshore and offshore average wave directions are shown in Table 2.2.9. It is apparent that in the SW monsoon season, the wave direction from S at the offshore changed to SE at the nearshore, while in the NE monsoon season, SSE to ESE.

Table 2.2.9 Average Wave Direction at
Nearshore and Offshore

	SW season	NE season
Offshore	173 ° (S)	161 ° (SSE)
Nearshore	141 ° (SE)	119 ° (ESE)
Changes	32 °	42 °

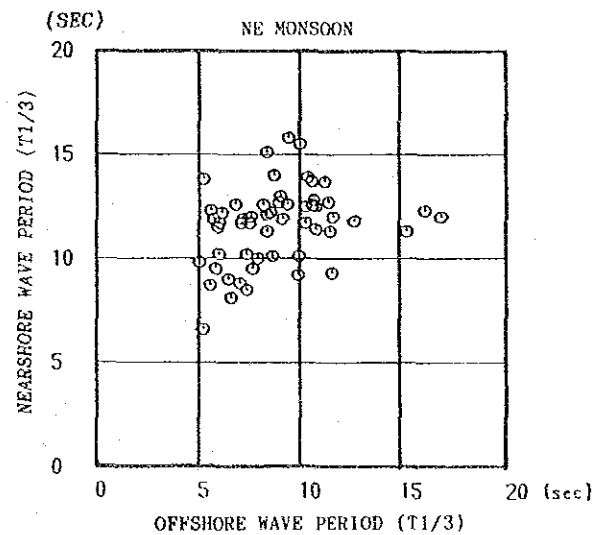
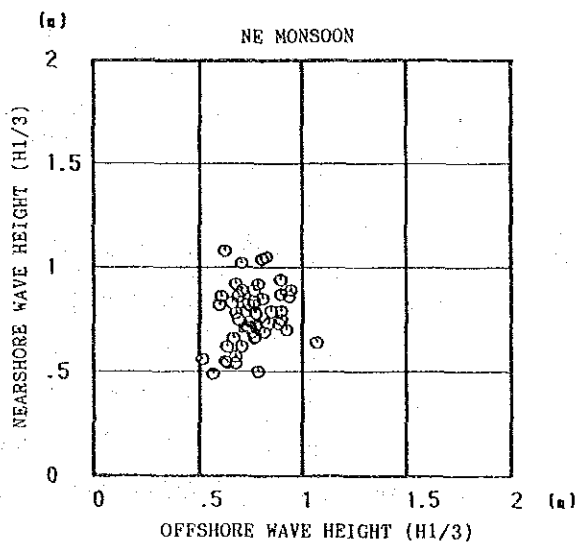
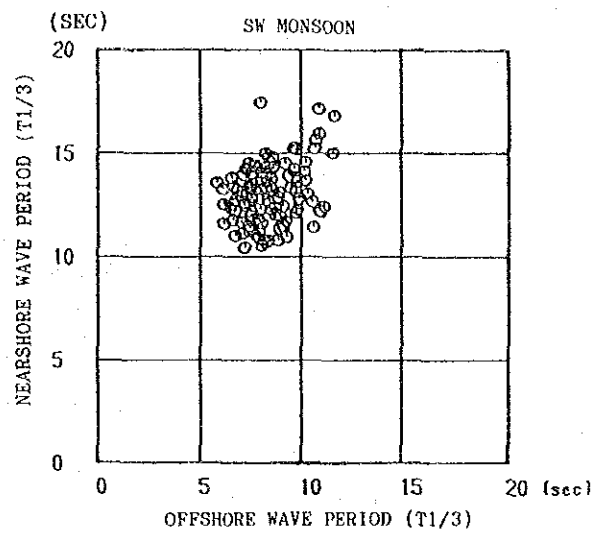
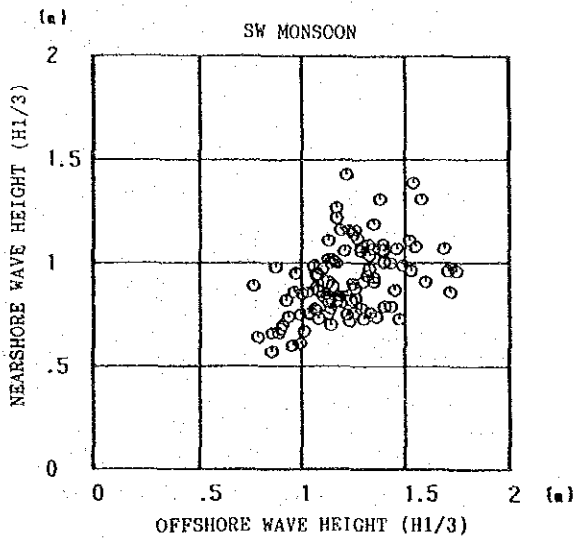


Fig. 2.2.11 (1) Comparison of Significant Wave Height at Offshore and Nearshore

Fig. 2.2.11 (2) Comparison of Significant Wave Period at Offshore and Nearshore

2.2.5 Longshore current

Longshore current measurements using magnetic current meters and ball floats were conducted in one month field surveys in September 1988 and March 1989. In the case where magnetic current meters were used, the longshore current was measured 70 cm above the sea bottom while ball floats were used to measure 1 m under the water surface.

(1) Results using current meters

The relations between the speeds and directions of the longshore currents measured by current meters is shown in Fig.2.2.12. In this Figure, the current direction zero refers to a current flowing north direction, 90 degrees is west and 180 degrees is south. It is apparent that in the SW monsoon season, the maximum current speed observed was 28 cm/sec. There was a tendency for the direction of the longshore current to be toward the NE in the case of a strong current and this was random in the case of weak current below 10 cm/sec. On the other hand, in the NE monsoon season, the current was weak and current direction random. Also, there were two current directions toward the W and N-NE. The NE direction is almost parallel to the Main Breakwater.

Relations between the longshore current and nearshore wave heights and periods are shown in Figs.2.2.13 and 2.2.14 respectively. It was found that the longshore current became stronger as the nearshore wave height and nearshore wave period in the SW monsoon season became larger. There was no correlation between the longshore current and nearshore waves due to the weak current in the NE monsoon season.

(2) Results using ball floats

The results of ball tracking in the SW and NE monsoon seasons are shown in Figs.2.2.15 and 2.2.16 respectively. The results in the SW monsoon season showed a tendency for all the balls to flow north along the front of the Main Breakwater in the same current direction

at about 100 m offshore. While in the NE monsoon season, the current was weak and there was no obvious tendency except at the head of the Main Breakwater and offshore where the current was toward the south.

Comparison between the average current speeds obtained by ball floats tracking as the data observed at the front of the Main Breakwater, mouth of the Harbour and north side coast of the Harbour in September 1988 and those obtained with a current meter with wave recorder at the same time and same locations are listed in Table 2.2.10. Also a correlation between the average current speeds obtained by balls tracking and those with the magnetic current meter, and a correlation between the average current speeds and nearshore wave heights are shown in Fig.2.2.17 (1) -(2), respectively. There was a weak correlation between them.

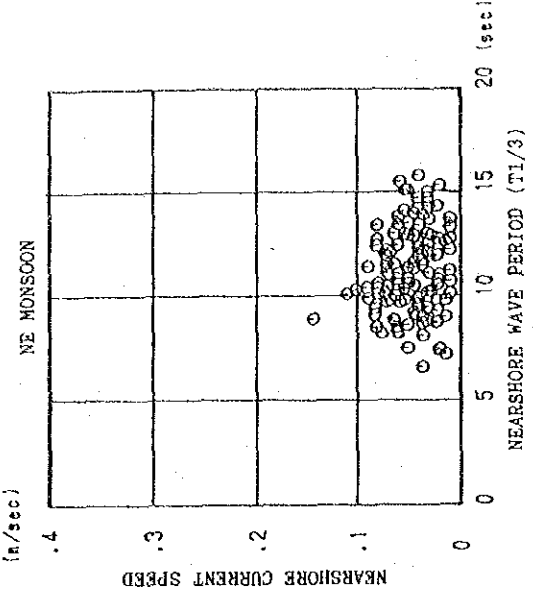
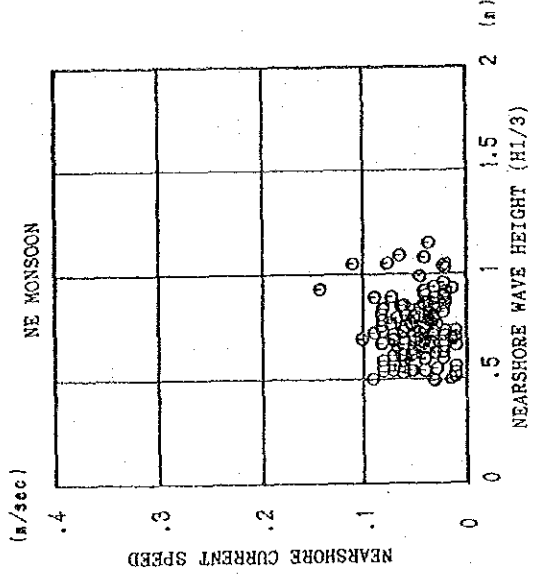
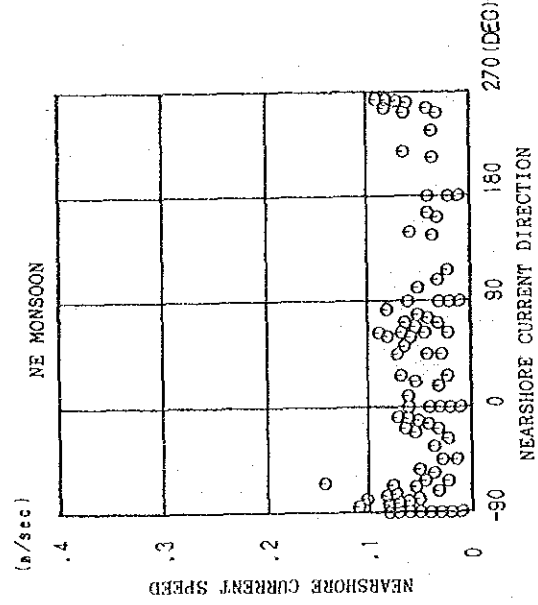
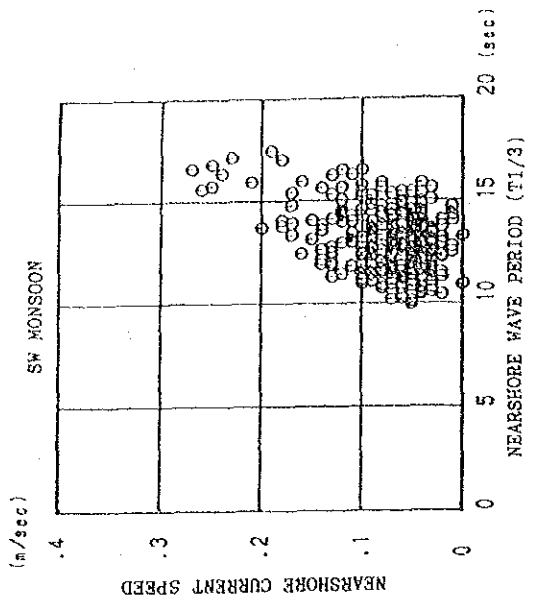
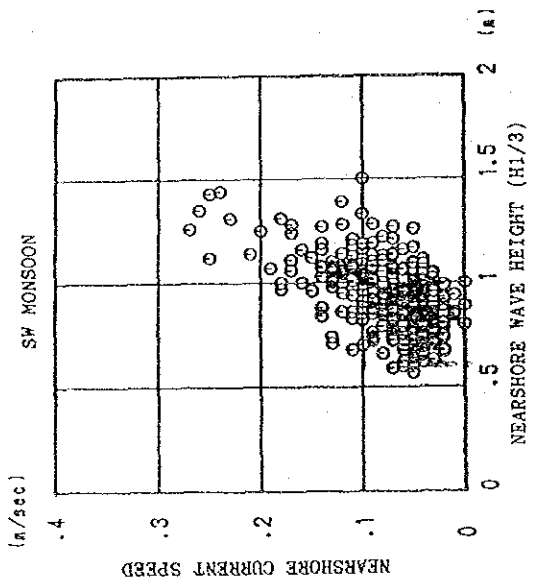
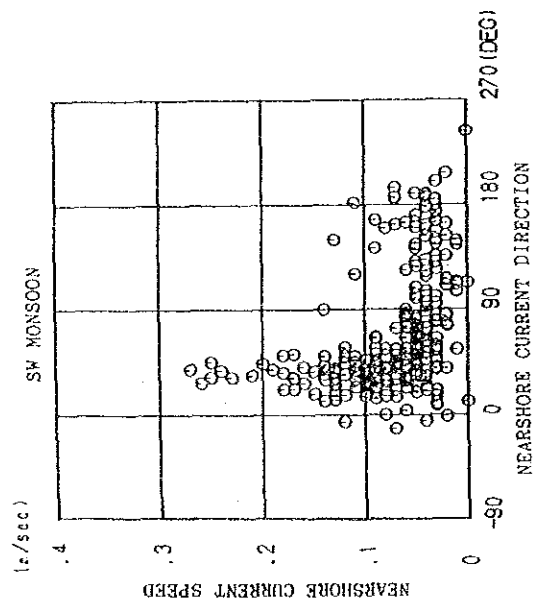


Fig. 2.2.12 Relation between Nearshore Current Direction and Speed

Fig. 2.2.13 Relation between Nearshore Current Speed and Wave Height

Fig. 2.2.14 Relation between Nearshore Current Speed and Wave Period

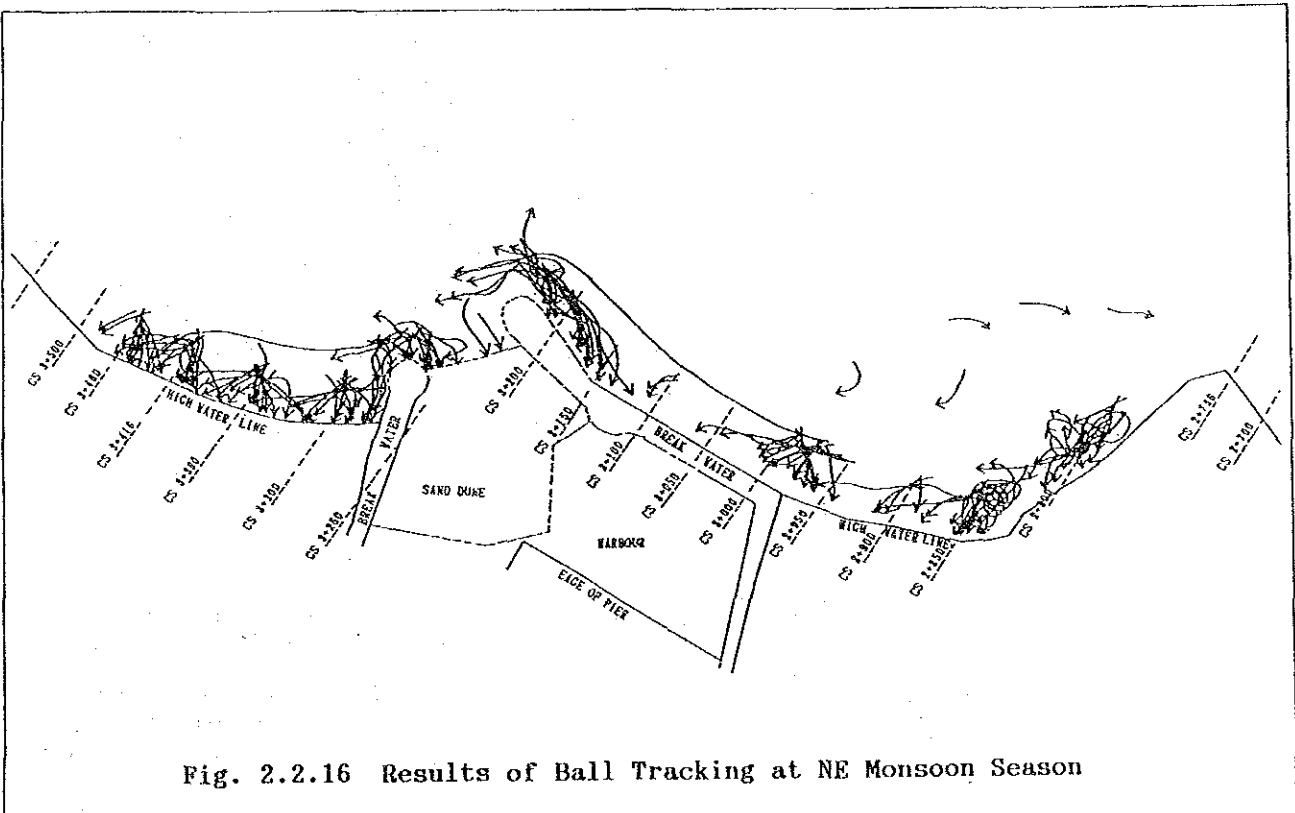
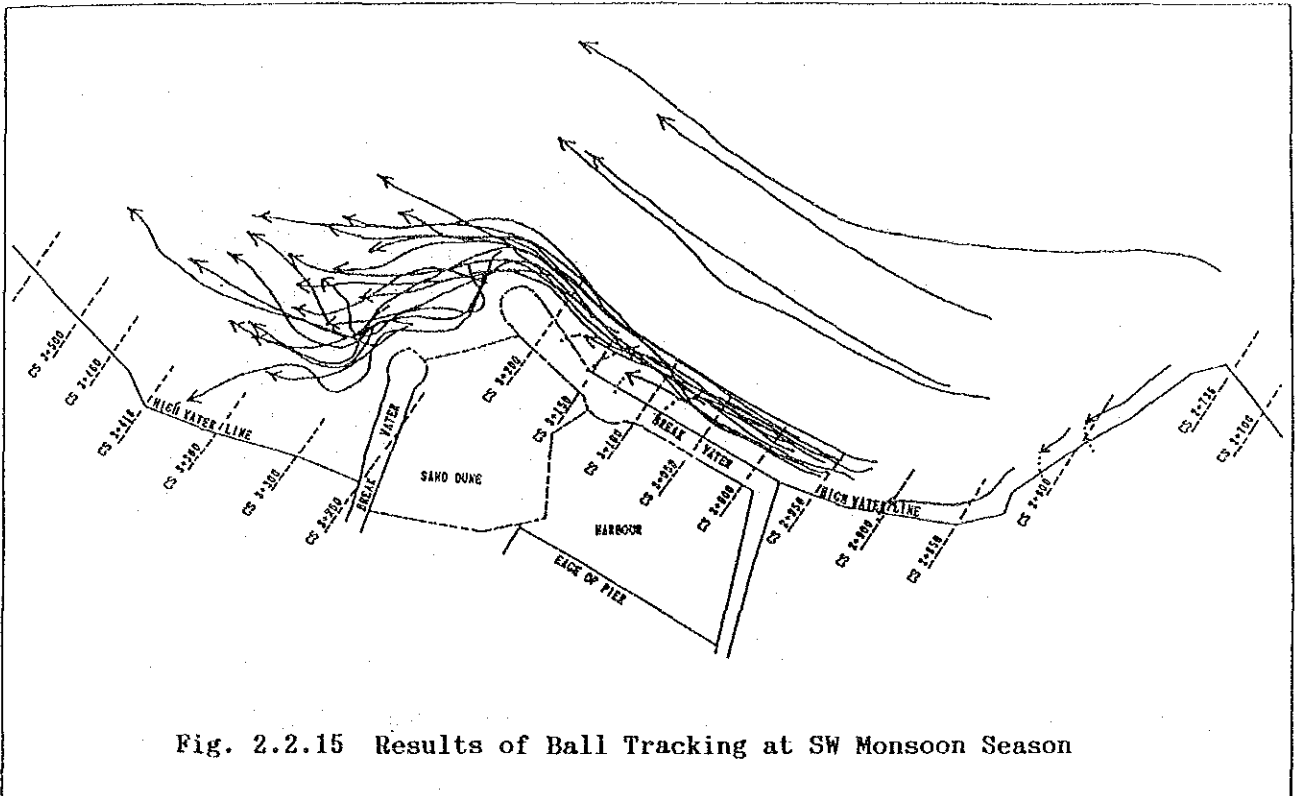


Table 2.2.10 Relation between Current Measured by Magnetic Current Meter,
Ball Tracking and Offshore Wave Height

Year	Month	Day	Time	Current Measured by Ball Tracking			Magnetic Current Meter with Wave Recorder			Offshore wave	
				Front of Main Breakwater	Front of Breakwater Mouth	East Coast	Current (m/sec)	Wave Height (m)	Wave Period (sec)	H1/3(m)	T1/3(sec)
88	8	24	9:00	0.52 (20)	0.30 (50)	----	0.16	1.15	15.96	1.23	10.49
88	8	26	11:10	0.32 (30)	0.32 (60)	----	0.08	0.81	12.84	1.02	9.02
88	8	28	15:30	0.22 (20)	----	0.15 (90)	0.14	0.88	13.84	1.28	8.01
88	8	30	16:00	0.42 (30)	----	----	0.14	0.84	13.84	1.38	7.51
88	9	1	14:30	0.42 (30)	0.30 (30)	0.30 (80)	0.13	1.06	11.32	1.39	7.46
88	9	3	14:00	0.46 (30)	0.50 (30)	0.30 (90)	0.07	1.14	13.60	1.25	8.28
88	9	5	9:00	0.27(200)			0.07	0.94	10.97	1.07	9.23
			15:00	0.32 (30)	0.20 (60)	0.23 (90)	0.05	0.76	11.06	1.04	7.66
88	9	8	10:30	0.13(130)	----	----	0.04	0.81	13.19	1.47	7.43
				0.21(200)							
88	9	9	14:00	0.34 (30)	0.30(100)	0.15(100)	0.09	0.87	13.29	1.08	8.02
88	9	11	15:30	0.25 (40)	0.27 (90)	----	0.05	0.65	13.19	0.95	6.84
88	9	14	9:00	0.19(100)	----	----	0.03	0.82	12.25	1.12	6.73
88	9	15	15:00	0.34 (30)	0.27 (90)	0.16(100)	0.13	1.07	12.03	1.69	8.69
88	9	17	14:30	0.36 (40)	0.25(100)		0.10	0.91	10.97	1.52	7.06
					0.17 (60)	----					
88	9	19	10:00	0.40 (30)	0.22 (70)	----	0.13	1.10	14.11	1.54	8.45
88	9	21	9:00	0.38 (30)	0.21 (30)	----	----	----	----	1.00	9.24

() means distance from shoreline

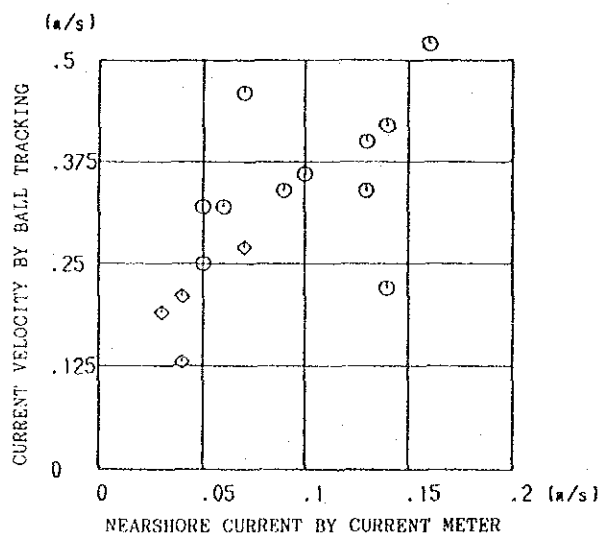


Fig. 2.2.17 (1) Relation between Current by Ball Tracking and Current Meter

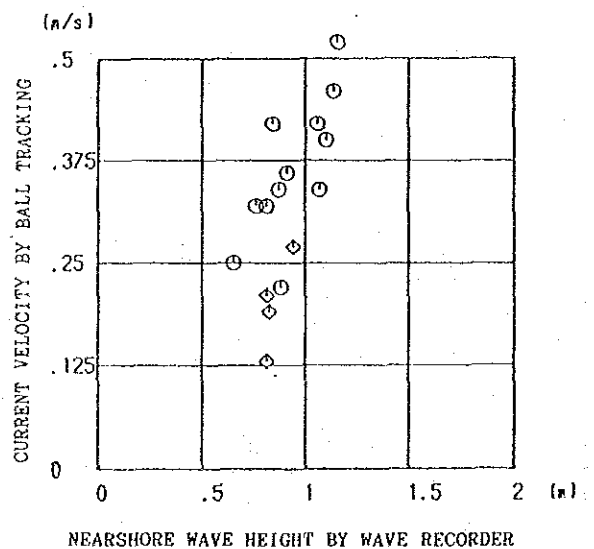
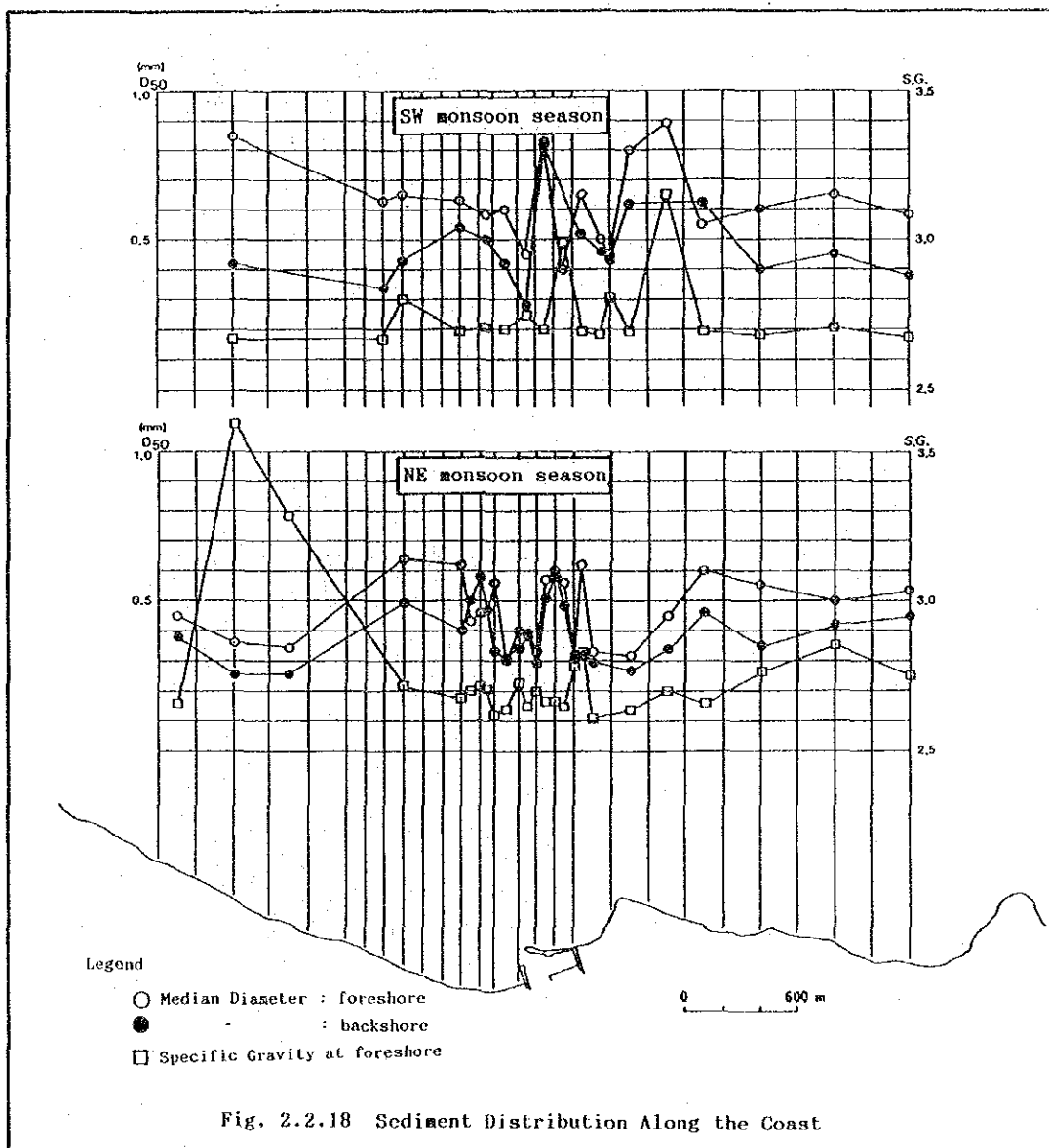


Fig. 2.2.17 (2) Relation between Current by Ball Tracking and Nearshore Wave Height

2.2.6 Bed Material

Sieve analysis and measurements of the specific gravity were conducted using samples which had been collected from the coast of the north and south sides of the Harbour in the one month surveys in September 1988 and March 1989. Distribution along the coast is shown in Fig.2.2.18. The median diameter was 0.4 - 0.8 mm at the foreshore and 0.3 - 0.8 mm at the backshore in the SW monsoon season except for the area south of the Point. The specific gravity was 2.7 - 3.0. In the NE monsoon season, the median diameter around the Harbour was a little larger than in the SW monsoon season.



2.2.7 Littoral Drift and Shoreline Changes

(1) Process of Siltation in the Harbour and Shoreline Changes

The process of siltation in the Harbour after construction is shown in Fig.2.2.19 and a transition of the amount of siltation is shown in Fig.2.2.20. As shown in these figures, the pocket beach had already been occupied by sand on completion of the construction after the NE monsoon season. During the following SW monsoon season, siltation in front of the Main Breakwater had progressed to an amount of about 100 thousand m³. However the mouth of the Harbour was still available for use. In the NE monsoon season from 1985 to 1986 the front of the Main Breakwater suffered erosion of 40 thousand m³ and some of this sand came through or over the Main Breakwater into the basin to an amount of 13 thousand m³. The siltation at the front of the Main Breakwater started again in the SW monsoon season of 1986, and in the June of 1986 a sand bank connecting the north side of the quay and the back side of the Main Breakwater had appeared, the result of sand being transported via the mouth of the Harbour. In this period, siltation in the basin caused by sedimentation and overtopping had amounted to 120 thousand m³. By May 1988, siltation in the basin had increased up to the mouth and the shoreline connecting the Main and Sub Breakwaters advanced to the mouth.

The changes in water depth in the basin for the period between April 1985 and August 1986 are shown in Fig.2.2.21. As mentioned formerly, as a sand bank had appeared in the basin connecting the north side of the quay and the back side of the Main Breakwater in June 1986. Sand accumulated in front of the quay either through the mouth or over the Main Breakwater or as wind-blown sand. Even though the mouth of the Harbour was eventually effectively blocked, the area behind the sand bank continued to fill up. This was taken as proof that some sand was indeed transported through or over the Main Breakwater or was wind-borne.

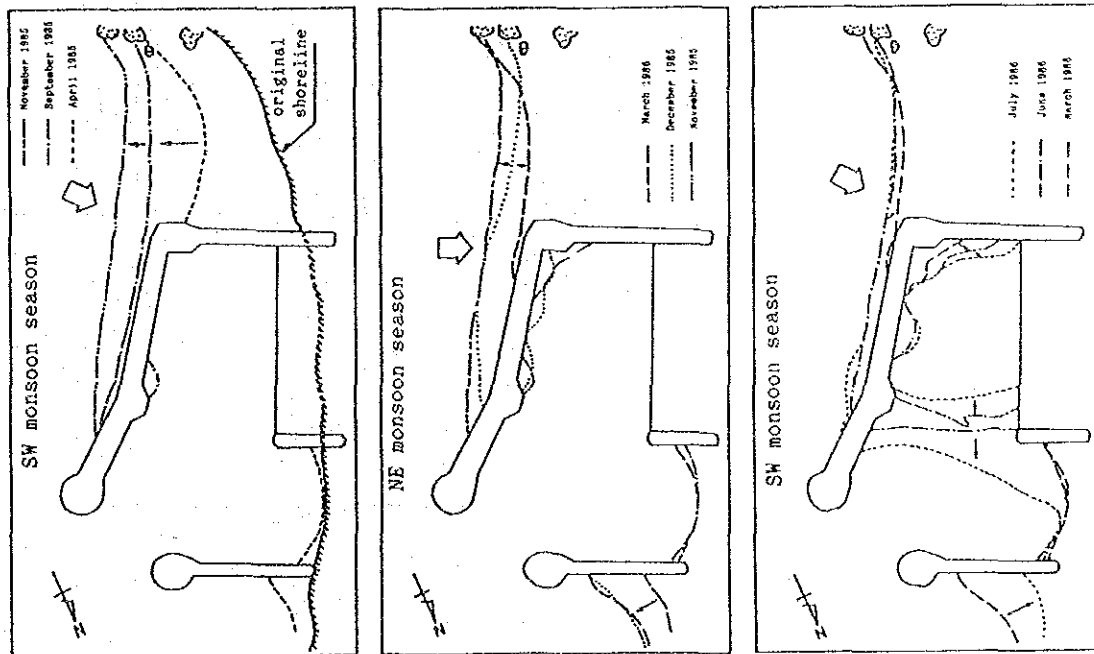


Fig. 2.2.19 Transition of Shoreline in Front of Main Breakwater

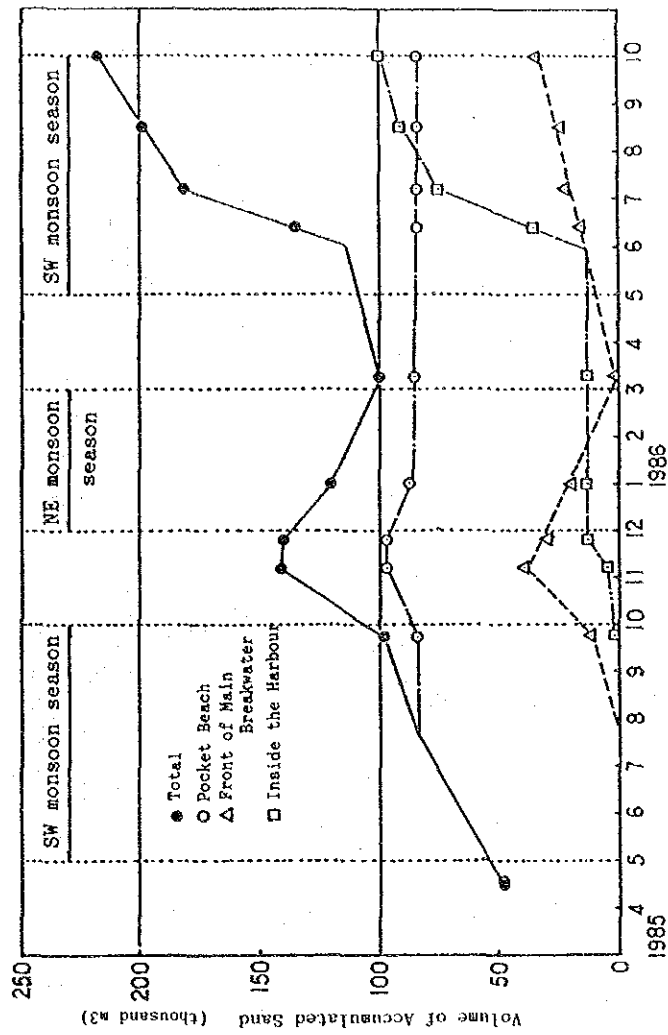


Fig. 2.2.20 Transition of Sand Accumulation

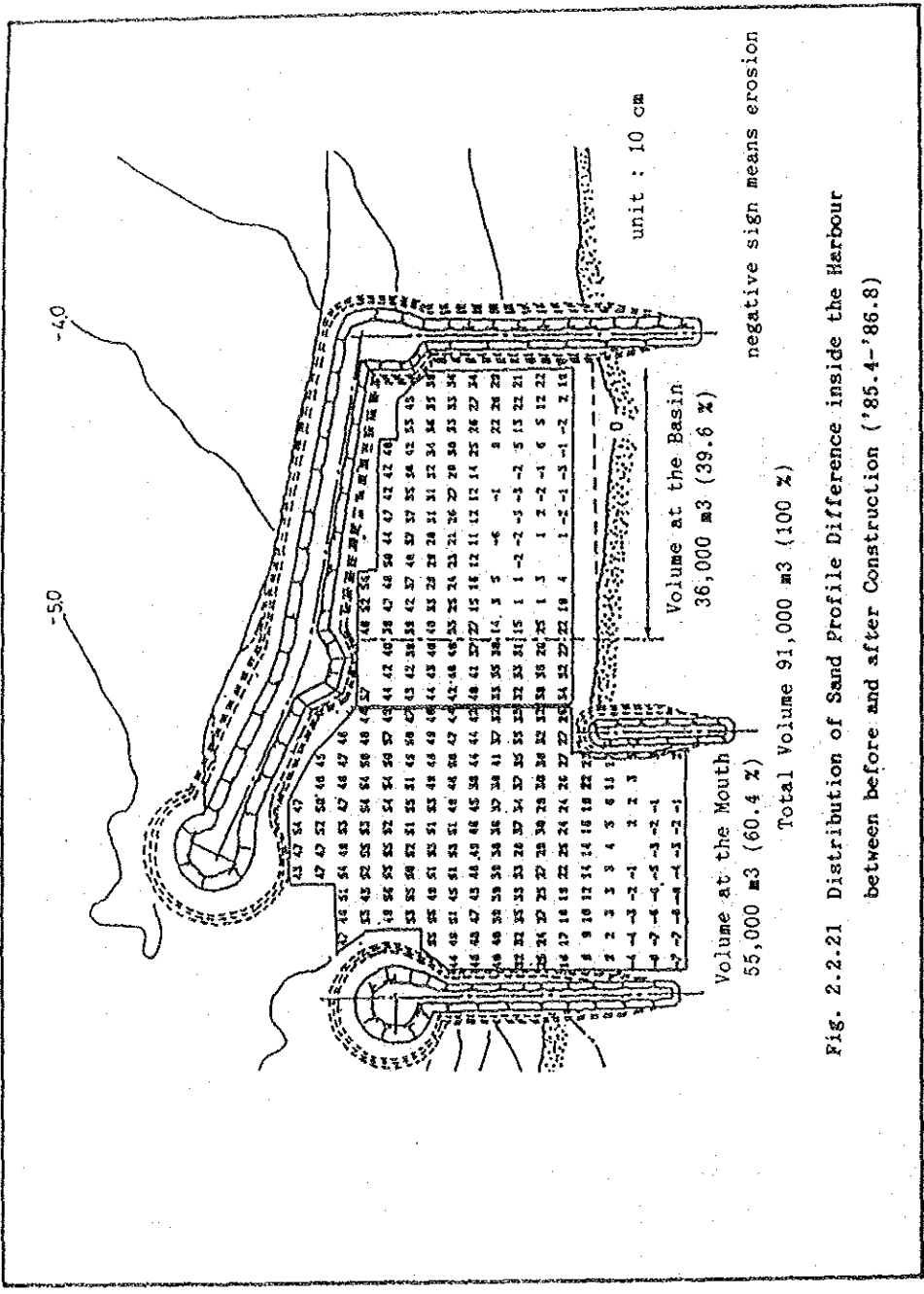


Fig. 2.2.21 Distribution of Sand Profile Difference inside the Harbour between before and after Construction ('85.4-'86.8)

(2) Vertical Distribution of Suspended Sand

A collection of suspended sand was conducted in the field surveys. Samplers attached to bamboos were installed at water depths of 5 and 5.5 m. The results of the vertical distribution of suspended sand is shown in Fig.2.2.22. "A" refers to data for water depth 5.5 m and "B" is 5 m. It is apparent that the amount of suspended sand in the SW monsoon season was about ten times that of the NE monsoon season.

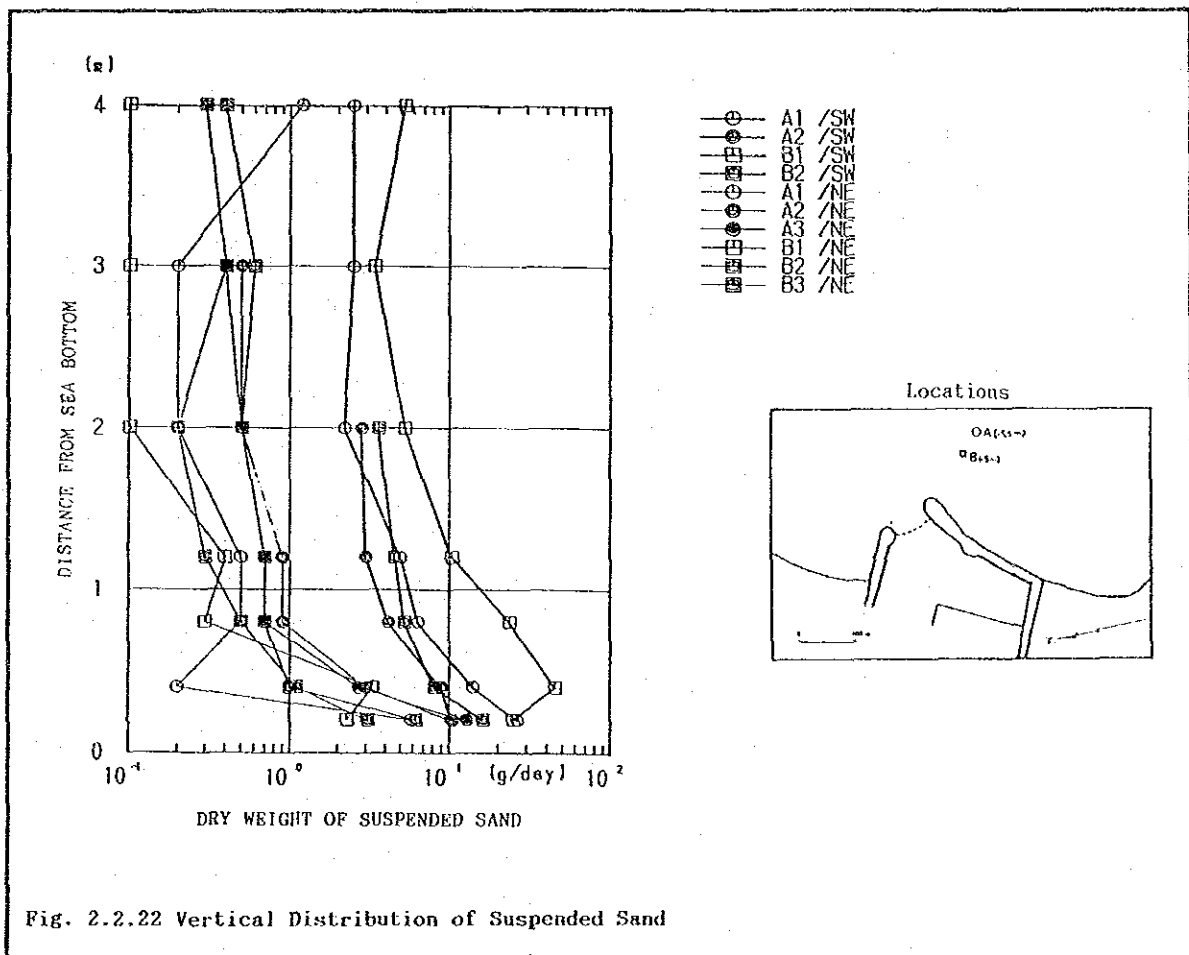


Fig. 2.2.22 Vertical Distribution of Suspended Sand

CHAPTER 3 COUNTERMEASURES AGAINST SILTATION AND THEIR EFFECTIVENESS

CHAPTER 3 COUNTERMEASURES AGAINST SILTATION AND THEIR EFFECTIVENESS

3.1 Method of Investigation

3.1.1 Adoption of Hybrid Method

Hydraulic experiments are often conducted to investigate the phenomena related to waves and currents. The adoption of hydraulic experiments is based on the geometrical and dynamic similitude of the hydraulic phenomena in the model and in the prototype.

The similitude of sediment transport can not be realized in the scale model test utilizing movable bed material. Therefore, problems would result if the movable bed experiments are adopted alone as the method to investigate the sedimentation problem.

Equations which express the mechanism of the sedimentation phenomena are indispensable to establish the numerical simulation method. A lot of phenomena on waves and currents can be expressed as the numerical equations, but some phenomena on waves and currents are difficult to express as equations due to their complexity. Wave breaking, the distribution of current speed along the water depth and wave overtopping are typical examples.

In front of the Kirinda Point, wave breaking occurs on the offshore rocky reef and strong currents exist around this area. Regarding information on waves and currents in the above situation, data obtained from the hydraulic experiments are considered to be more reliable than those obtained by numerical calculations.

Sedimentation is known as one of the most complex phenomena treated in coastal and ports & harbour engineering. It includes many unsolved problems. However, in recent years, progress has been made in deducing numerical equations which express the mechanism of sediment transport.

Taking the problem of similitude of sediment transport into consideration, a numerical simulation is more reliable than a movable bed experiment as a quantitative prediction method.

Attempts to predict sedimentation with more accuracy utilizing a hybrid method which combines the advantages of both hydraulic experiments of fixed bed and numerical simulations are being carried out.

Data on waves and currents obtained from the fixed bed hydraulic model test were utilized to calculate the forces which caused the sediment transport. Quantitative predictions of sand transport were also performed by conducting numerical simulations.

In this study, the sedimentation problem was investigated mainly by adopting the hybrid model and some detailed phenomena such as the possibility of the sand bar occurring at the harbour mouth were taken into account in the movable bed experiments.

This hybrid method was considered to be the most adequate means for investigation at the present technical level. However, taking the complexity of sedimentation into consideration, a judgment based only on the results obtained by this method would not be enough. Therefore, the final judgment should be formed by considering both the results obtained from the hybrid method and technical judgment based on experience.

3.1.2 Outline of Hybrid Method

The physical model test (hydraulic model test) was conducted first and the numerical simulation then conducted utilizing the results obtained.

In adopting this procedure, a hybrid method containing the advantages such as good reproducibility of the hydraulic characteristics in the physical model and the good applicability of the numerical model was combined. The flowchart is shown in Fig.3.1.1 and the relations between the site survey, hydraulic model test and numerical simulation are shown in Fig.3.1.2.

The current velocities, wave heights and wave directions were measured in the hydraulic model test to calculate the forces which were the cause of the sand transport. These hydraulic characteristics were interpolated onto the grid points and utilized as input data in the numerical calculations.

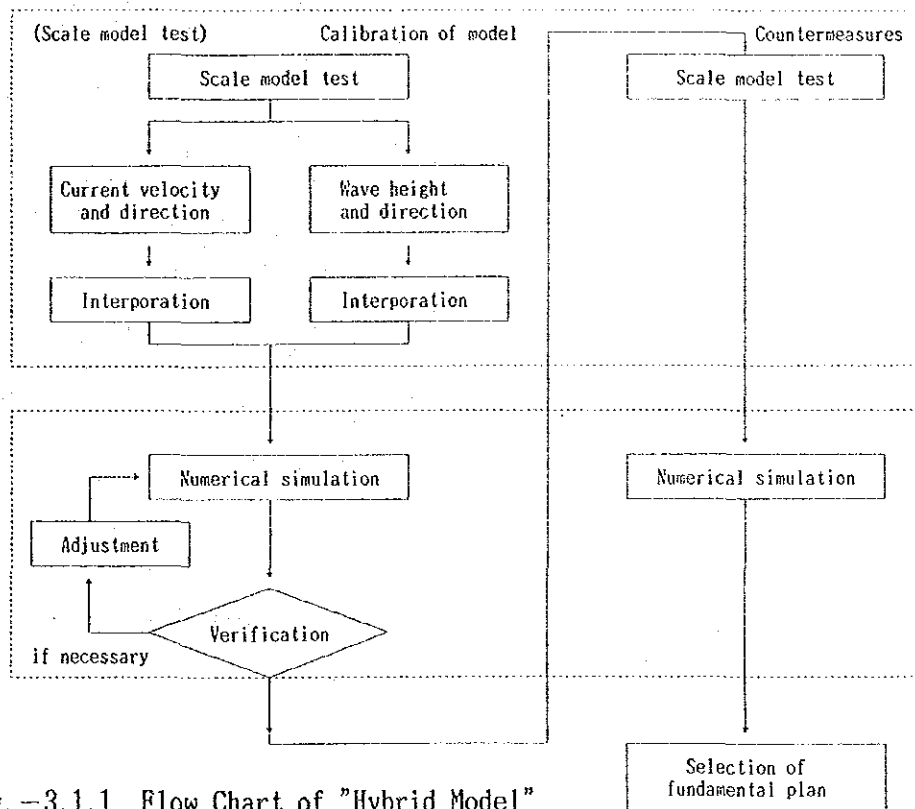


Fig.-3.1.1 Flow Chart of "Hybrid Model"

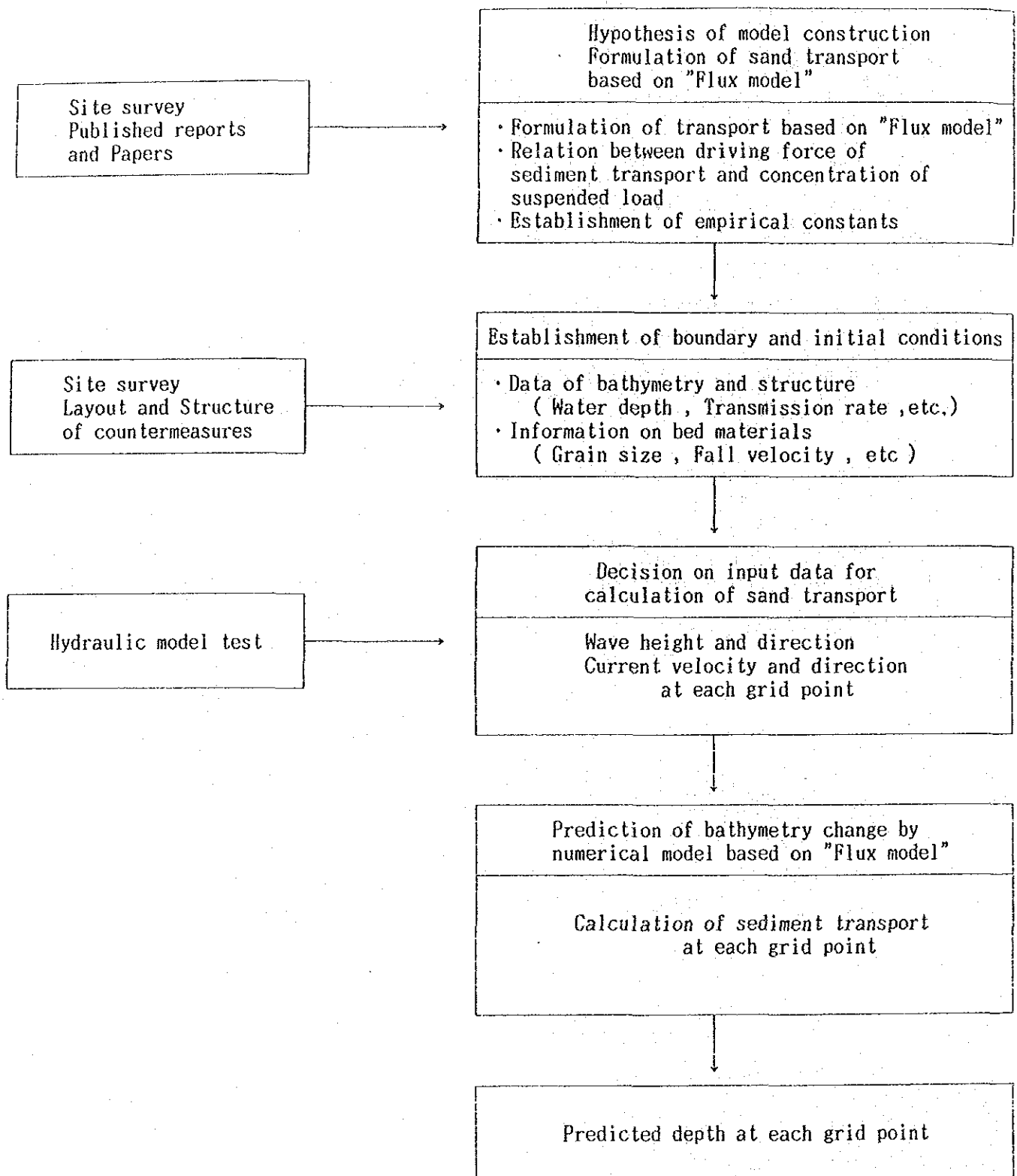


Fig. 3.1.2 Procedure of Numerical Simulation

3.1.3 Testing Method of Hydraulic Experiments

(1) Outline of Experiments

Two types of model bed conditions were adopted in this study. One was a fixed bed condition and the other a movable bed condition.

In the fixed bed experiment, the wave heights, wave directions and current velocities were measured and an analysis of these data was conducted to obtain the mean values of the wave heights, current velocities and superior wave directions. The values were used to calculate the sand transport in the numerical simulation.

The movable bed experiments were conducted for that layout which was confirmed to have the highest effectiveness through the fixed bed experiments and numerical simulations.

In the area which is shadowed in Fig.3.1.3, movable material was used to make a bed surface. The topographical changes near the harbour entrance, main breakwater and sub breakwater were focused on in the investigation.

(2) Test Facilities and Measuring Equipment

Test facilities and measuring equipment are described below with photographs ;Photo 3.1 to 3.8.

1) Wave basin and wave generator

Dimensions of the wave basin and wave generator utilized in the study were as follows.

Details of wave generator

Type : Pendulum type

Paddle length : 32m (8 m * 4)

Max.wave height : 25cm (Reg. wave)

Wave period : 0.4-4sec (Reg. wave)

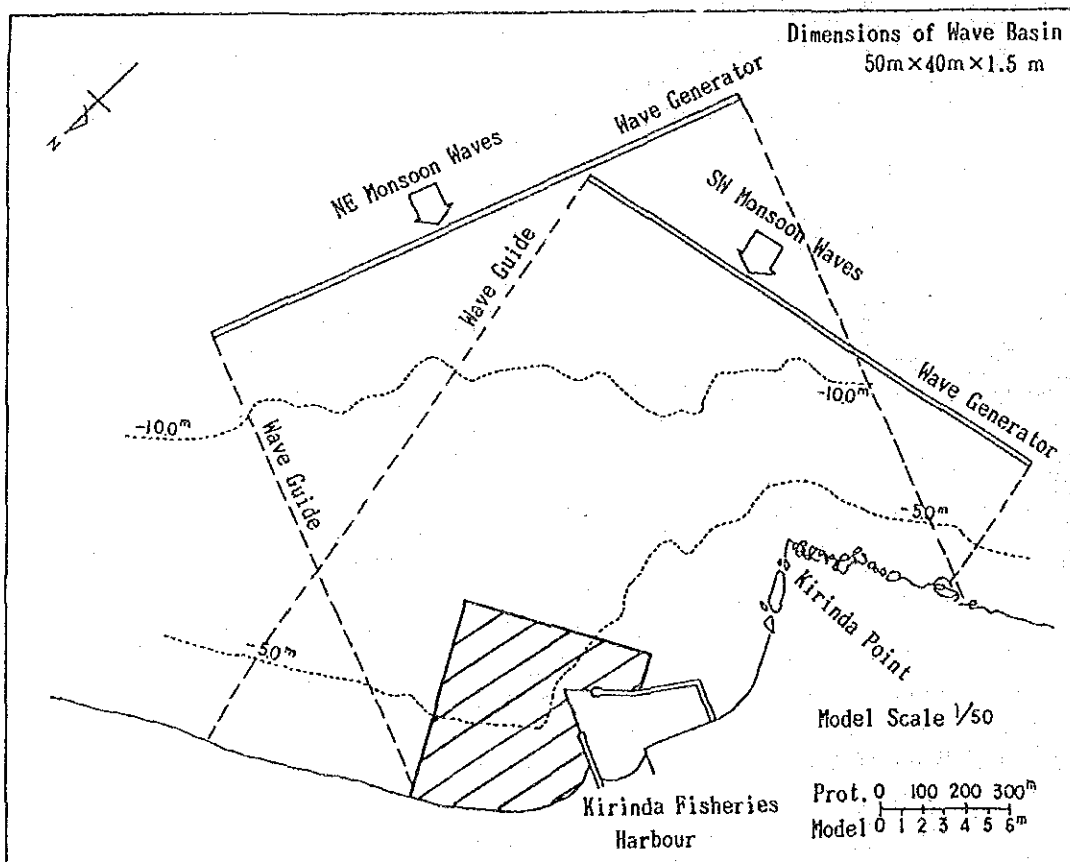


Fig.-3.1.3 Model Layout

2) Measuring Equipment and Computer

- 1 Servo-type wave gages
- 2 Electro-magnetic current meters
- 3 Bottom profile meters(Sandy surface meters)
- 4 Digital data recorder
- 5 Oscillograph
- 6 Video camera & editing system
- 7 J.A.C.150 Computer system

(3) Test Conditions of Scale Model (3-D,Regular Wave)

The model scale was 1/50 in the vertical and horizontal directions. This scale was adopted in both the fixed and movable bed experiments. According to Froude's similarity law, the scale of wave height and period was as follows.

Model scale: 1/50

Wave height: 1/50

Wave period: $\sqrt{1/50}=1/7.07$

M.S.L. was adopted as the water level in this study. A cover of mortar was applied over a gravel bed in the case of the fixed bed experiment. The topography of the model bed was renovated to suit each investigation step. The model material for breakwater, groin and submerged groyne was of two types of gravel.

One type consisted of 3g stones (equivalent to 375Kg at the site) and this was used to make the core section, the other type had stones of almost 60g weight (about 7.5 t at the site) and this was used to make the outer layer.

(4) Measurement

1) Fixed Bed Experiment

The main measurement items of this experiment were the wave heights, directions and current velocities. The location of the wave breaking line and the observation of current field using a dye tracer were also conducted. The wave and currents were measured simultaneously at the points shown in Fig. 3.1.4.

The currents were measured at points of 15mm height (0.75m height at the site) from the bottom.

Small floats were utilized as tracers in the very shallow area where a current meter could not be used.

2) Movable Bed Experiment

The surface level of sea bottom and the changes in shoreline were measured using a bottom profile meter.

Measurement points of 25cm intervals were shown in Fig. 3.1.5.

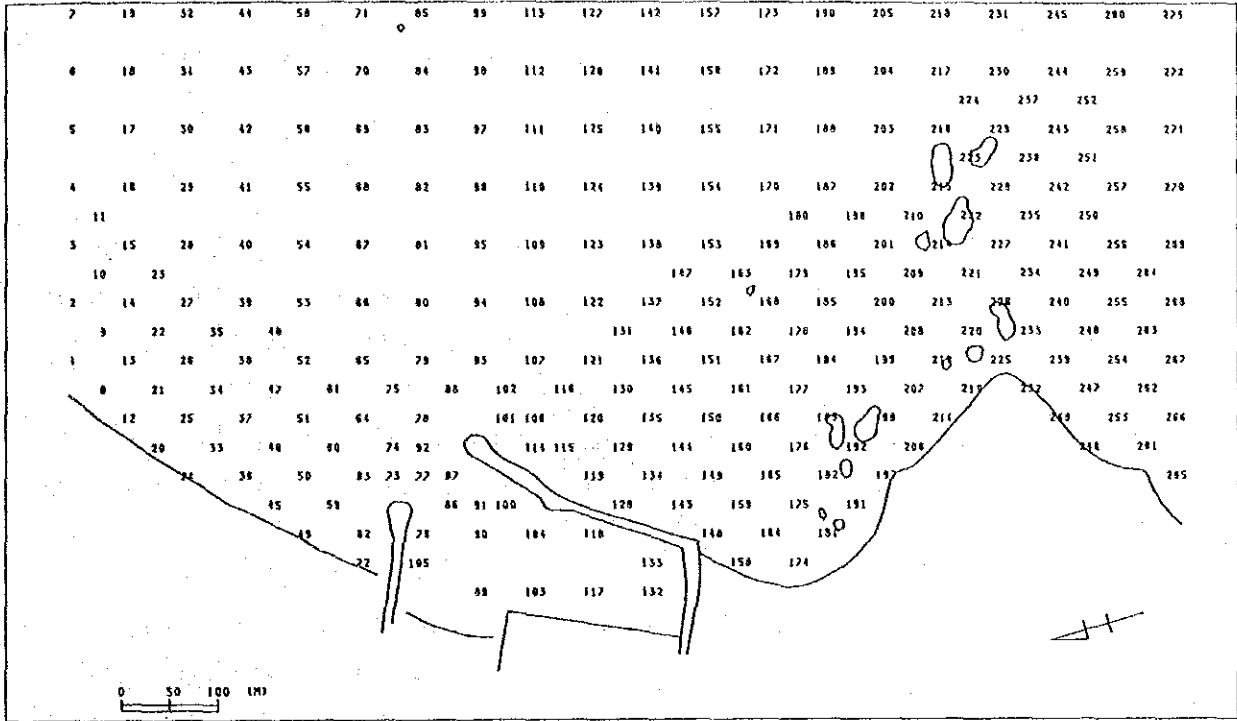


Fig.-3.1.4 Measurement Points (Fixed Bed Exp.)

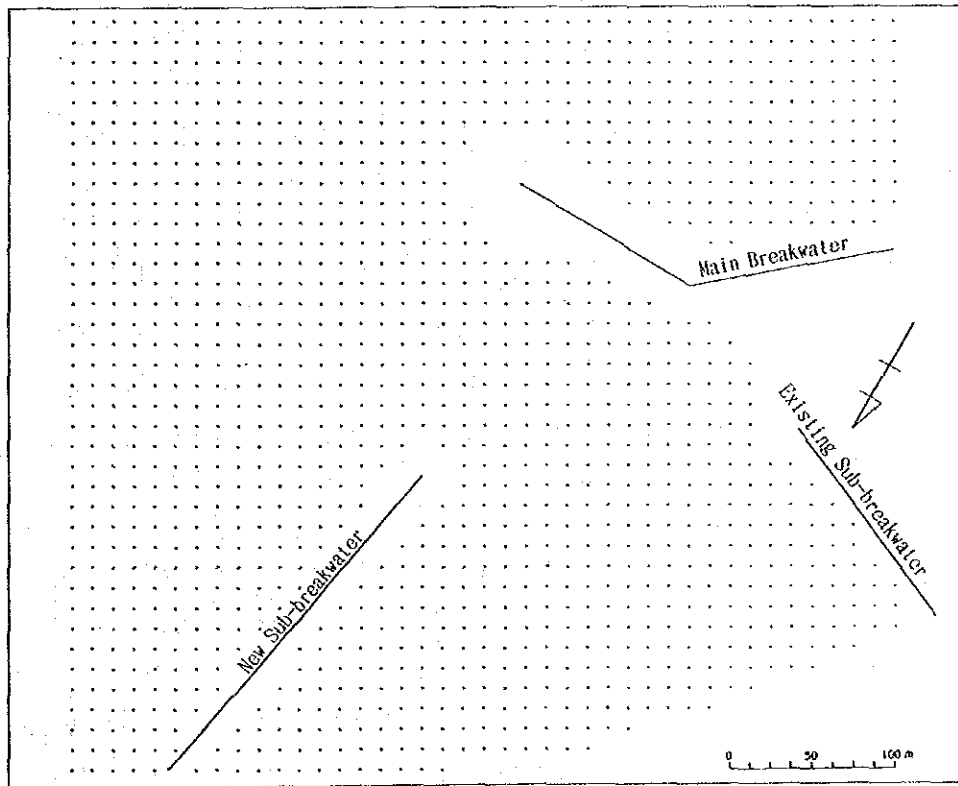


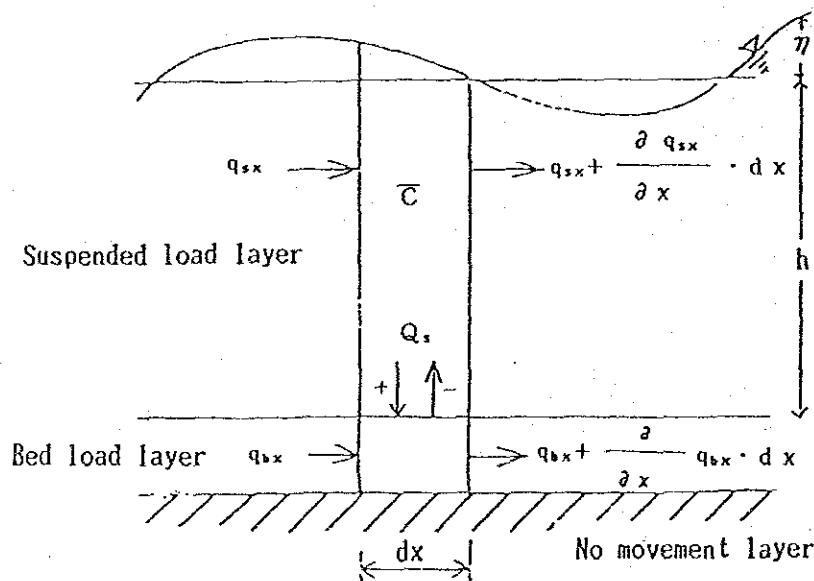
Fig.-3.1.5 Measurement Points (Movable Bed Exp.)

3.1.4 Procedure of Numerical Simulation

(1) Outline of Numerical Model

The numerical calculations were conducted by adopting the measured values obtained from the 3-D hydraulic experiments used as input data. The formula to calculate the volume of sand transport was that established by Sawaragi and Deguchi based on the "Flux model concept". The change in current speed caused by a water depth change was considered in the calculation on the premise of conservation of flow volume at the same point.

Change in water depth was the result of the difference of resuspended and deposited sand and the net inflowing bed load volume. A definition sketch of this situation is shown below. The bottom was defined as the boundary between the suspended layer and bed load layer.



Sketch of the Mechanism of Bottom Changes

The change of water depth was defined as follows.

$$\frac{\partial h}{\partial t} = \frac{1}{1-\lambda} \left(-Q_s + \left(\frac{\partial q_{bx}}{\partial x} + \frac{\partial q_{by}}{\partial y} \right) \right) \quad \dots(3.1.1)$$

in which

x, y : coordinates

t : time

h : water depth

λ : porosity of sediment

Q_s : the net vertical flux of sediment

q_{bx}, q_{by} : bed load fluxes in the direction of the x and y axis

where Q_s and q_{bx}, q_{by} were calculated as follows.

(a) Q_s : net vertical flux of sediment

Net vertical flux of sediment Q_s was calculated by the following expressions.

$$Q_s = \left[(1-\gamma) C_0 w_f \alpha \left(1 - \frac{u_*}{w_f} \right) + \bar{C} w_f \right] \quad \dots(3.1.2)$$

in which

$\gamma = 0$ for $u_* > w_f$

$\gamma = 1$ for $u_* < w_f$

ϵ_z : Vertical diffusion coefficient

h : water depth

\bar{C} : depth and time averaged concentration of suspended sediment

C_0 : concentration at the reference level defined at the top of the bed load layer

u_* : shear velocity at the bottom

w_f : fall velocity of sediment

α : coefficient, $0 < \alpha < 1$

\bar{C} was estimated by solving the two-dimensional advection-diffusion equation. And C_0 was evaluated utilizing the following equations.

$$C_0 = 0.347 Nc^{1.77} \quad \dots(3.1.3)$$

in which

$$Nc = \frac{0.688 u_w^2}{1.13 (\rho_s / \rho - 1) g W_f T}$$

u_w : maximum flow velocity at the bottom

$(\rho_s / \rho - 1)$: specific gravity of sediment in the water

g : acceleration due to gravity

T : wave period

ε_z was evaluated as follows

out of the surf zone

$$\varepsilon_z / w_f = \min [0.021 \exp(0.5 u_*), h] \quad \dots(3.1.4)$$

in the surf zone

$$\varepsilon_z / w_f = \beta \cdot h \quad (\beta : \text{coefficient, } 0 < \beta < 1) \quad \dots(3.1.5)$$

(b) q_{bx} , q_{by} : bed load flux

The bed load fluxes were evaluated using the following expressions as proposed by Sleath.

$$\begin{aligned} q_{bx} &= 47 \sigma d^2 (\psi - \psi_c)^{3/2} \{ \cos \theta_w + \pi (U/u_w) \} \\ q_{by} &= 47 \sigma d^2 (\psi - \psi_c)^{3/2} \{ \sin \theta_w + \pi (V/u_w) \} \dots (3.1.6) \end{aligned}$$

in which

- σ : $2\pi / T$
- d : median diameter of sediment
- u_w : maximum flow velocity at the bottom
- θ_w : wave direction
- ψ : Shield's parameter
- ψ_c : Critical value of Shield's parameter of sediment movement

(2) 1-line Model

Generally, a 1-line model is utilized to obtain the shoreline changes over a long term. Changes in a shoreline can be obtained by solving the sand continuity equation (eq.3.1.7) numerically.

The Ozasa-Brampton formula (eq.3.1.8) was adopted to calculate the volume of littoral sand drift (Q_x) in a continuity equation.

< sand continuity equation >

$$\frac{\partial Y_s}{\partial t} + \frac{1}{D} \frac{\partial Q_x}{\partial x} = 0 \quad \dots(3.1.7)$$

< littoral sand drift equation >

$$Q_x = \frac{K_1}{\gamma_s} (E \cdot C_g)_b \cdot (\sin 2\theta_b - \frac{K_2}{\tan \beta} \cdot \frac{\partial H_b}{\partial x} \cdot \cos \theta_b) \quad \dots(3.1.8)$$

in which

Y_s : shoreline location

D : vertical range of profile change

Q_x : littoral sand drift velocity

K_1, K_2 : coefficient ($K_1 = 0.2$, $K_2 = 3.0$ were adopted in this study

$(E \cdot C_g)_b$: littoral component of breaking wave energy
 $= (1/8 \rho g H_b^2 C_{gb})$

ρ, g : the density of sea water and acceleration due to gravity

H_b, C_{gb}, θ_b : wave height ,group velocity ,wave direction at breaking point

$\tan \beta$: slope of beach

γ_s : specific gravity of sediment in the water

In this 1-line model calculation, it was necessary to calculate the wave deformation and obtain breaking wave characteristics. In the study, an energy equilibrium equation was adopted for wave deformation.

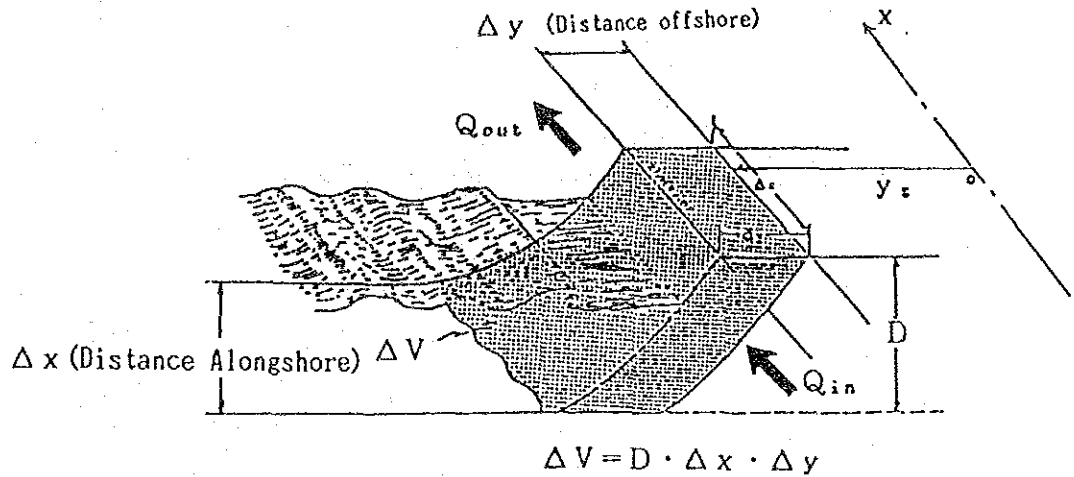


Fig.-3.1.6 Definition Sketch for Sand Continuity Equation

(3) Conditions for Calculation

1) Calculation Area

The calculation area was as shown in Fig. 3.1.7. It had 1100 m alongshore length and 700 m offshore length, and included Kirinda Point and Kirinda Fisheries Harbour.

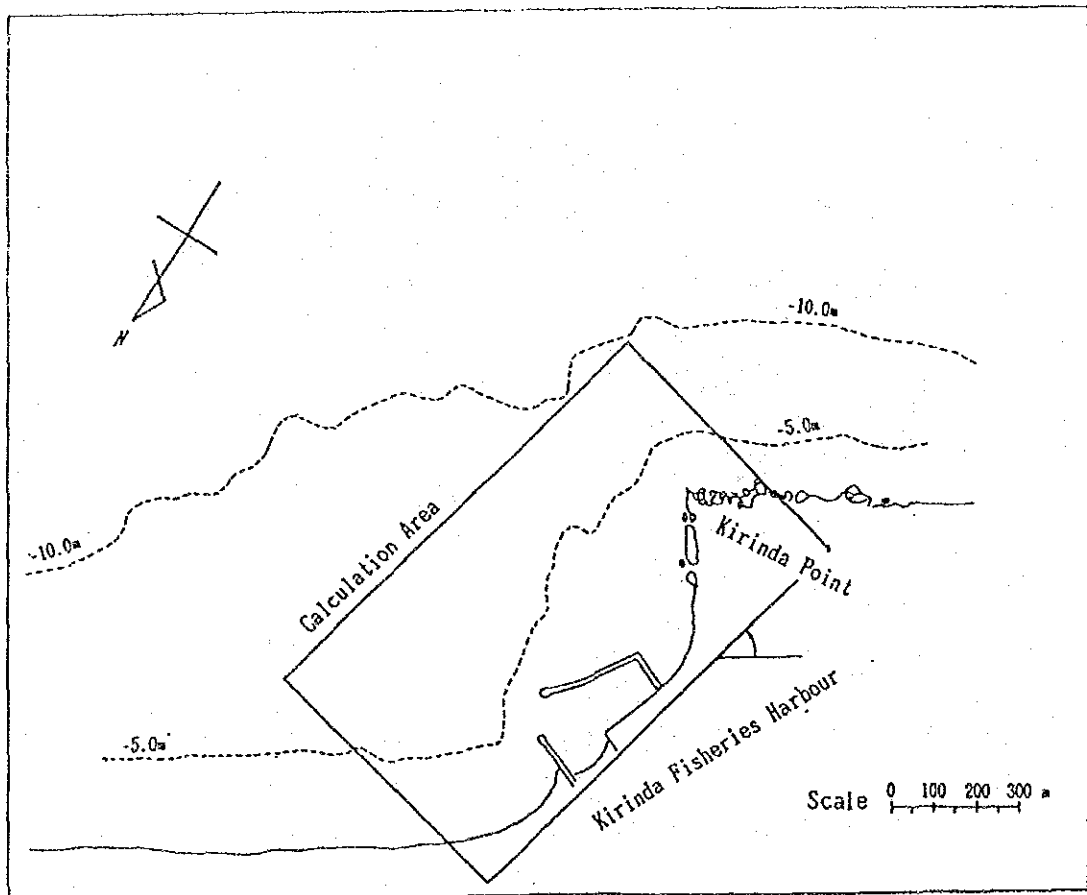


Fig.-3.1.7 Calculation Area

2) The Period of Wave Action adopted in the Calculation

The results obtained from the 3-D hydraulic model test were utilized as input data in the calculation of the water depth change. The period of wave action considered in the calculation was established as follows. From the data observed at the site, the accumulation of the wave energy flux was calculated for each monsoon season. The period of wave action was decided as that period in which the total energy flux was equal to the total energy flux in the period in which the representative wave continued. (Details on the decision on this period are discussed in the Appendix D)

a) SW Monsoon Season

The period of wave action utilized in the numerical simulation was decided for two cases. For one case, only one representative wave (1.8m) was assumed. In the other, two representative waves (1.8m & 1.25m) were adopted.

In the latter case, the group with wave heights exceeding 1.5m were represented by the 1.8m wave height and the rest were represented by the 1.25m wave height.

The periods decided for these two cases are shown in Table.3.1.1.

Table.-3.1.1 Period of Wave Action in the Calculation
(SW Monsoon Season)

Representative Wave (adopted in Exp.)	Wave Height 1.8m Period 14sec	Wave Height 1.25m Period 14sec
Period of Wave Action (One Representative Wave)	94 days	-----
Period of Wave Action (Two Representative Waves)	17 days	159 days

b) NE Monsoon Season

In the NE monsoon season, it is considered that both wind waves from the NE direction and swells from the SW direction are observed in the same season. Wind waves were separated and their energy fluxes calculated to decide the period of wave action for the numerical simulation.

The period is shown in Table.3.1.2.

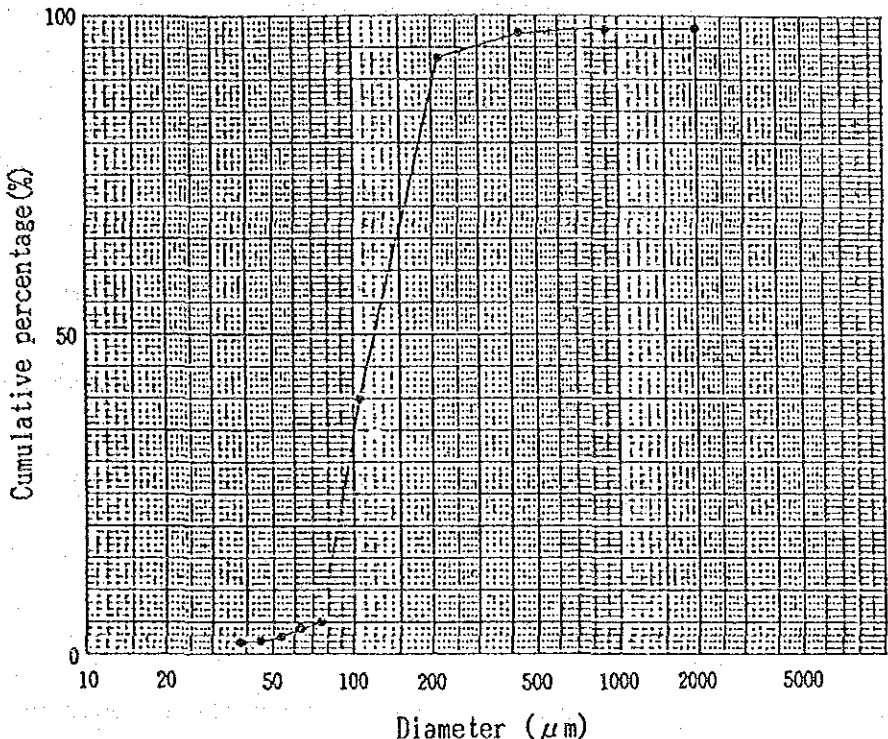
Table 3.1.2 Period of Wave Action in the Calculation
(NE Monsoon Season)

Representative Wave	;	Wave Height	0.86m
	;	Period	6sec
Period of Wave Action	!		59 days

3) Sediment Condition

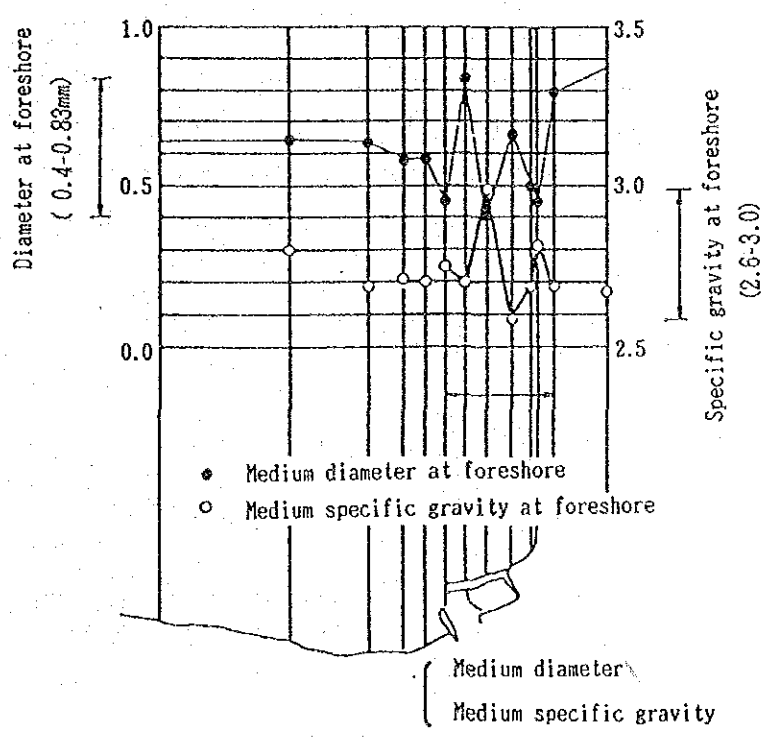
The median diameter and specific gravity of the sediment were settled on the basis of analysis of data obtained in the site survey. (Bed materials examination and suspended sand measurement) The fall velocity of the material was calculated using Rubey's formula. Settled values were as follows.

Suspended Sand : $D_{50}=0.12\text{mm}$, $\rho =2.63$, Fall Velocity= 1.1cm/sec
Bed Load : $D_{50}=0.5\text{ mm}$, $\rho =2.70$, Fall Velocity= 6.2cm/sec



B.S. sieve size(mm)	Specific gravity
over 0.425	2.65
0.425 - 0.212	2.57
0.212 - 0.106	2.63
Medium diameter	$D_{50} = 0.12\text{mm}$
Medium specific gravity	$\rho_s = 2.63$

Particle size distribution of suspended sediment



Medium diameter	$D_{50} = 0.5-0.6\text{mm}$
Medium specific gravity	$\rho_s = 2.7-2.8$

Grain size distribution at foreshore

Fig.-3.1.8 Observed Grain Size Distribution

3.2 Effectiveness of Investigation Method

3.2.1 Aspects of Investigation

Reproducibility of the waves and currents was confirmed through a comparison between the data observed in the site survey and that measured in the hydraulic experiments. The effectiveness of the prediction method was investigated by comparing the estimated sand volume and that actually observed in the pocket beach, the front area of the main breakwater, and inside the harbour.

(1) Objective Period and Areas for Calibration

The sand volume deposited and shoreline changes near the harbour were studied in the 1st and 2nd follow up studies. The objective period and area chosen for calibration were settled on the basis of a study of the results which were summarized in the summation report on the follow up studies on the Kirinda harbour siltation.

For the SW monsoon, two objective periods were considered. The 1st period corresponded to the SW monsoon period of 1985 (April, 1985 - Oct., 1985), and 2nd to the SW monsoon period of 1986 (Mar., 1986 - Sept., 1986). In the 1st, the area between Kirinda Point and the main breakwater was saturated by sand and the pocket beach formed. In the 2nd period, the sand deposit expanded along the front of the main breakwater and the siltation inside the harbour began.

For the NE monsoon, one objective period was decided upon. This corresponded to the NE monsoon period of 1986 (Sept., 1986 - Mar., 1987).

From above examinations the three periods can therefore be summarized as follows.

- 1st Period (April, 1985 - Oct., 1985); SW Monsoon Season
- 2nd Period (Mar., 1986 - Sept., 1986); SW Monsoon Season
- 3rd Period (Sept., 1986 - Mar., 1987); NE Monsoon Season

The area near the harbour was separated into the three regions shown in Fig.3.2.1.(i.e.pocket beach,front area of the breakwater and inside the harbour).

The sand volumes of accretion and erosion around the harbour in the SW and NE monsoon seasons of 1985 and 1986 are shown in Table 3.2.1.

The transitions of the sand accretion volume in the SW monsoon seasons of 1985 and 1986 are shown in Fig.3.2.2 and shoreline changes at the pocket beach are shown in Fig.3.2.3.

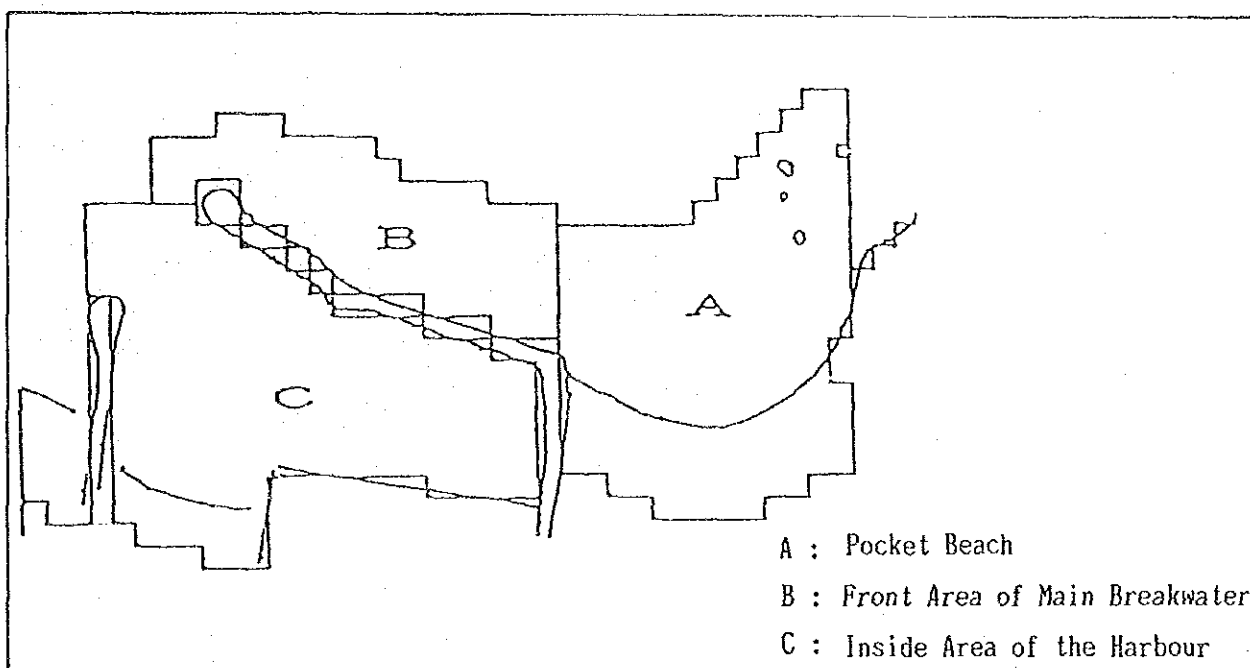


Fig.-3.2.1 Examination Area of Deposited Sand Volume

Table 3.2.1 Sand Volume of Accretion and Erosion

Area	SW Monsoon		NE Monsoon
	1st Stage	2nd Stage	3rd Stage
Pocket Beach	49,000 m ³	0	22,500 m ³
Breakwater outside	39,000 m ³	32,000 m ³	-20,000 m ³
Inside harbour	5,000 m ³	87,000 m ³	3,500 m ³
Total	93,000 m ³	119,000 m ³	6,000 m ³

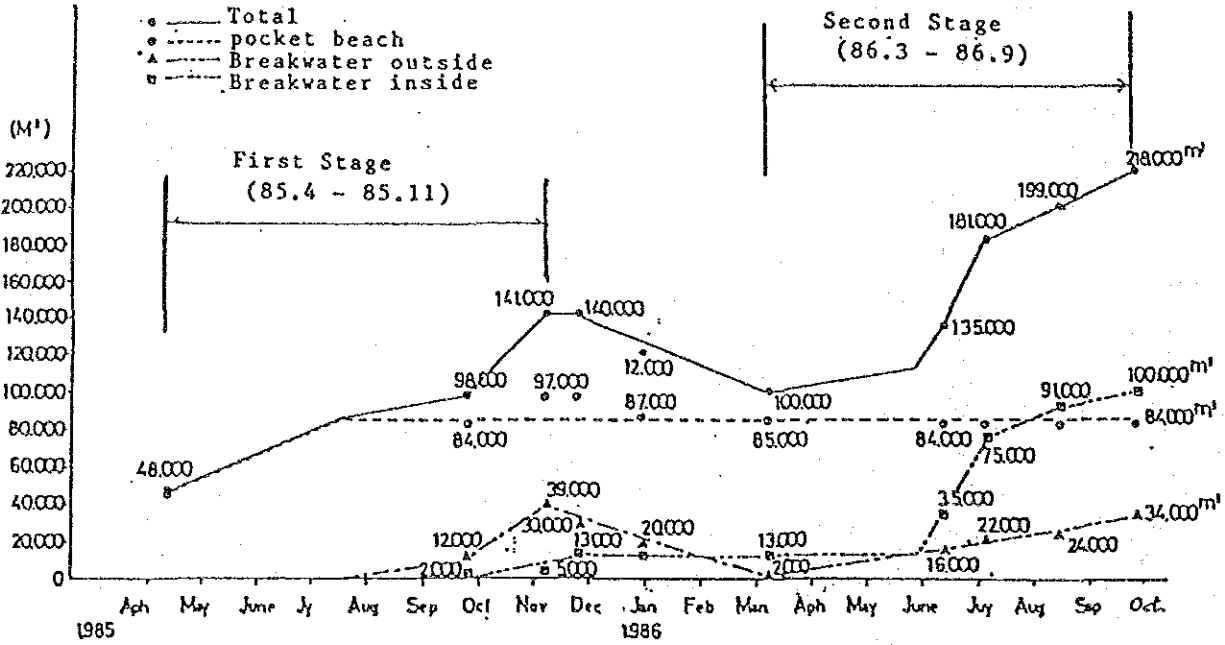


Fig.-3.2.2 Transition of Sand Accretion Volume

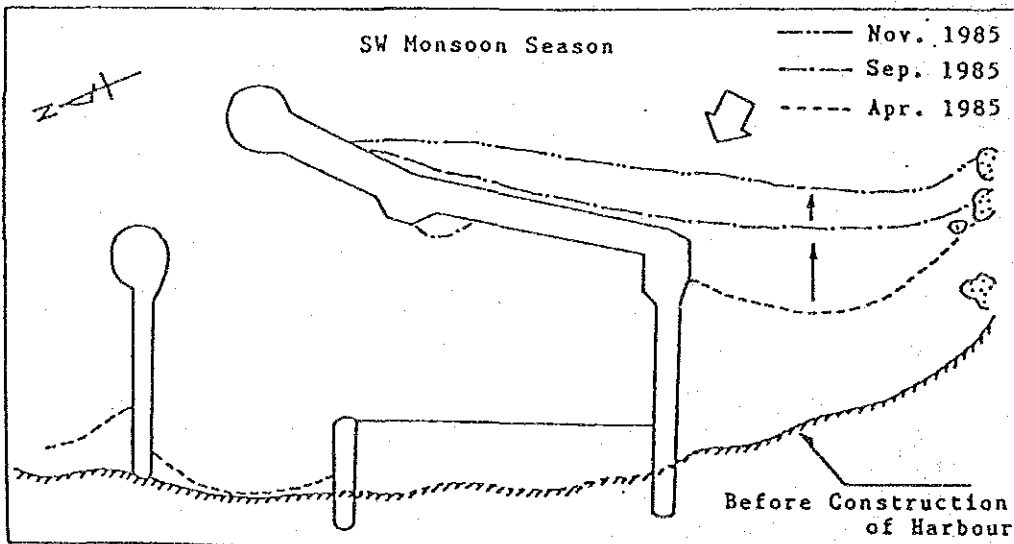


Fig.-3.2.3 Transition of Shoreline

As for the sand volume deposited inside the harbour, it was considered that the volume of sand being brought in via the overtopping waves and transmitted waves was very significant.

In order to investigate the ratio between the sand volume which flowed in through the harbour mouth and that via overtopping or transmitted waves, a distribution of the sand volume deposited from April, 1985 to Aug., 1986 was calculated by comparing the water depth data. (See Fig. 3.2.4)

The sand which flowed in from the harbour mouth was considered to have deposited mainly near the harbour mouth as was described in 2.2.7. On the other hand, after the harbour mouth had been closed, sand deposition continued and the rate of deposited sand became an almost constant $190 \text{ m}^3/\text{m}$ along the main breakwater at the inner part of the harbour.

Also, the rate of deposited sand decreased according to the distance from the main breakwater alignment. This sand deposition along the main breakwater was considered to have been carried in via overtopping and transmitted waves.

The total sand volume which was carried in with overtopping and transmitted waves was estimated to be about $47,000 \text{ m}^3$ by multiplying the rate of deposited sand and main breakwater length (from turning point to the head of breakwater). While the sand volume which flowed in through the harbour mouth was estimated to be about $44,000 \text{ m}^3$ by subtracting $47,000 \text{ m}^3$ from $91,000 \text{ m}^3$ which is total sand volume deposited during this period.

The sand volumes despite coming into the harbour via different paths were found to be almost the same.

(2) Investigation of Effectiveness of Method

The effectiveness of the method adopted in the study was examined for the 3 items described below.

- 1) A comparison of the currents observed at the site and those obtained in the experiments was conducted for both the SW and NE monsoon seasons.
- 2) A comparison of the estimated sand volume deposited obtained from the site survey with that obtained from the numerical calculations was conducted for in the regions around the harbour for the 3 stages described in 3.2.1.(See Figs.3.2.1 ,3.2.2 and Table 3.2.1)
- 3) A comparison of the observed shoreline changes at the site and those calculated by utilizing the l-line model was conducted. The objective period of this comparison was from April,1985 to Nov.,1985.

3.2.2 Waves and Topographical Conditions

(1) Wave Conditions

1) SW monsoon season

Representative waves for the SW monsoon season were decided on the basis of analysis of observed data obtained at offshore (20m depth) and nearshore points (5m depth).

Dimensions of representative waves are shown below. Details on the decision on these waves are presented in Appendix D.

a) $H=1.80$ m, $T=14$ sec, S 10 E

(equivalent to the monthly maximum of the significant wave)

b) $H=1.25$ m, $T=14$ sec, S 10 E

(equivalent to the seasonal mean of the significant wave)

2) NE monsoon season

Representative waves for the NE monsoon season were decided on the basis of analysis of observed data obtained at the offshore and nearshore points. (Dec., 1988 - Feb., 1989)

In the NE monsoon season, the wind concentrating NNE to ENE and wind waves were also observed in these directions as was described in 2.2.4.

On the other hand, swells were observed in the S direction throughout the year. These two types of waves exist together in the NE monsoon season. Because of this situation, the wind waves and swells had to be separated from the spectrum of sea waves and dimensions of the representative waves of NE monsoon season then decided upon. (Details on the decision on representative waves are presented in the Appendix D)

a) $H= 0.86$ m, $T= 6$ sec, S 80 E

(equivalent to the mean value in wind waves)

b) $H=0.69$ m, $T= 14$ sec, S 10 E

(equivalent to the mean value in swells)

Experiments were conducted for wind wave conditions and effects of swells were considered in the numerical calculations.

(2) Initial Topography

The topography in April, 1985 and the topography in April, 1986 were adopted as the initial sea bed topographies for the 1st and 2nd stages of the calibration experiments.

The topography in May, 1988 was adopted as the initial sea bed topography for the 3rd stage of the calibration experiment.

3.2.3 Investigation of Calibration Results Obtained from Experiments and Numerical Calculations

The hydraulic experiments for calibration were conducted for the cases shown in Table 3.2.2. In the calculation for calibration, the results of experiments were utilized to calculate the sand transport.

Also, the frequency of occurrence of wave height was taken into consideration in the calculations. The group with wave heights exceeding 1.5 m were represented by the 1.8 m wave height and the rest were represented by the 1.25 m wave height as was described in 3.1.4 (3).

Table 3.2.2 Test Cases (Calibration)

No.	Case	Wave condition			Remarks
		Height	Period	Direction	
1	A-1	1.80m	14sec	S 10° E	1st stage
2	A-2	1.25m	14sec	S 10° E	ditto.
3	AA-1	1.80m	14sec	S 10° E	2nd stage
4	AA-2	1.25m	14sec	S 10° E	ditto.
5	B	0.86m	6sec	S 80° E	3rd stage

(1) Reproducibility of Waves and Currents in the Experiments

Wave observation at the site was conducted in the offshore and near shore points in the period May, 1988 to Nov., 1988. Locations of observation are shown in Fig. 3.2.5.

Relations of the offshore waves and nearshore waves are shown in Fig. 3.2.6 along with the relations obtained in the experiments.

Good reproducibility was confirmed through this comparison of the experiment results and observed data.

As for the currents, a comparison between experimented results and observed data was also conducted. The comparison for the SW monsoon season is shown in Fig. 3.2.7 and that for the NE monsoon season

season is shown in Fig.3.2.7 and that for the NE monsoon season is shown in Fig.3.2.8. A comparison of the current speeds at the representative points are shown in Table 3.2.3.

The existence of a strong current in the NE direction along the main breakwater in SW monsoon was confirmed in the experiment. The existence of currents 100 -200 m offshore from the main breakwater was also confirmed in the experiments.

Currents measured at the harbour mouth in the experiments were weaker than those observed at the site. The harbour mouth was already closed by a sand bar at the site when the observation was conducted so nearshore currents flowed continuously along the north coast.

On the other hand ,the harbour mouth had more than 3 m of water depth at the objective time in the experiments so the current speed had become weaker at the harbour mouth.

A comparison of the current observed at the site in the NE monsoon season and those measured in the experiment showed good agreement as given in Fig.3.2.7 and Table 3.2.3.

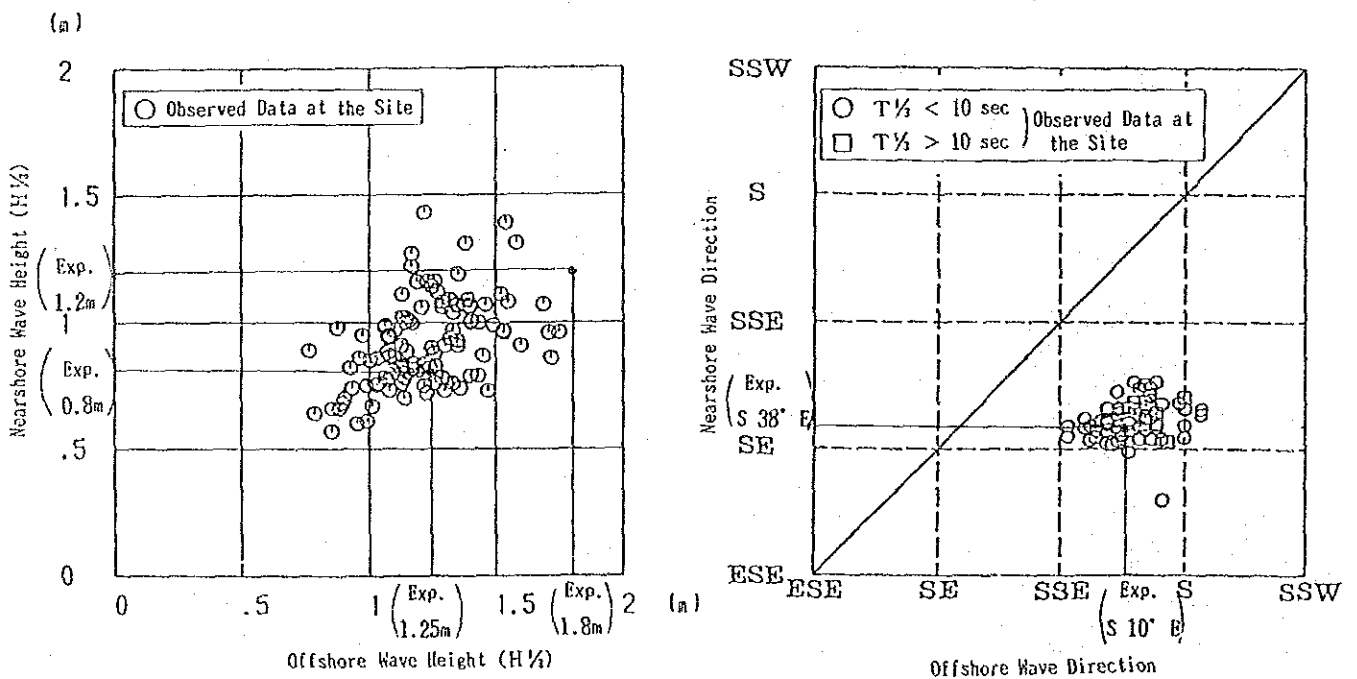
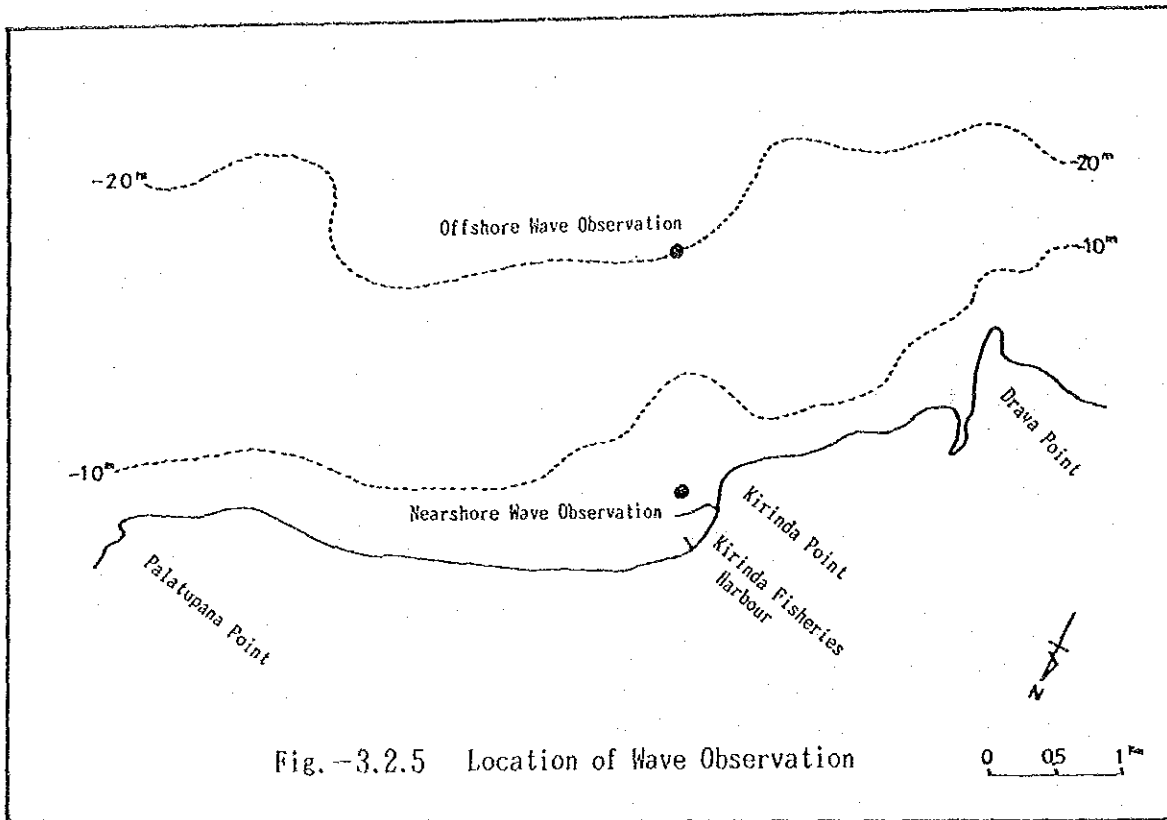
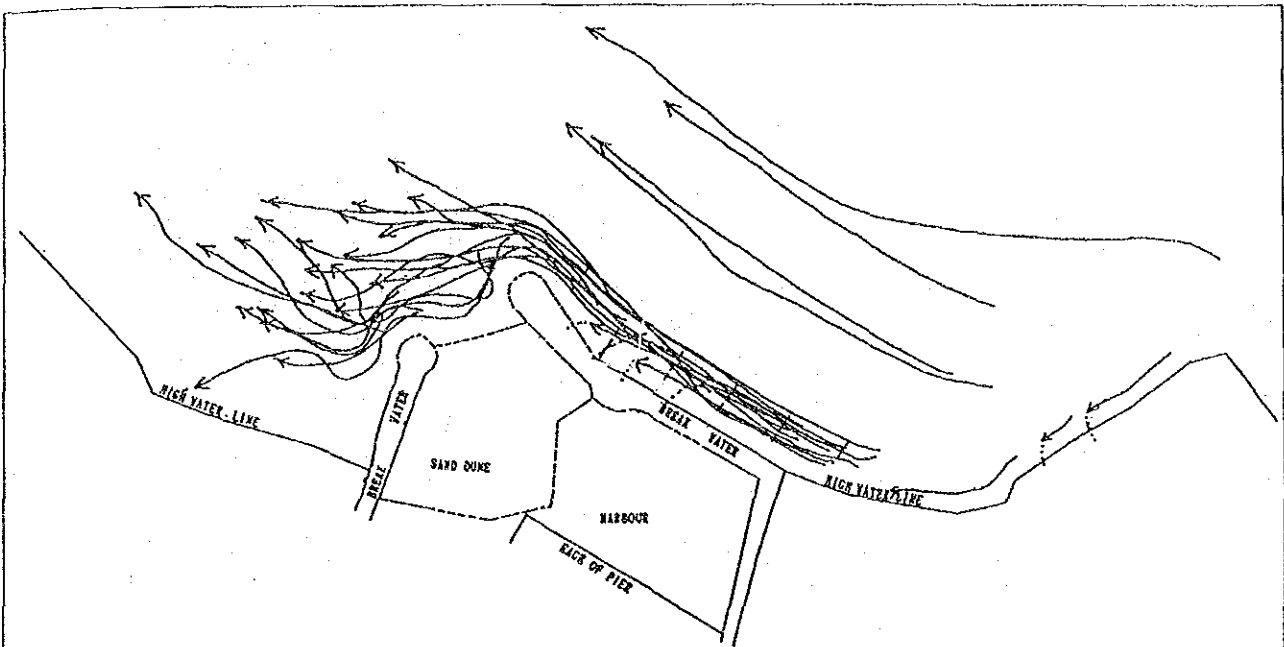
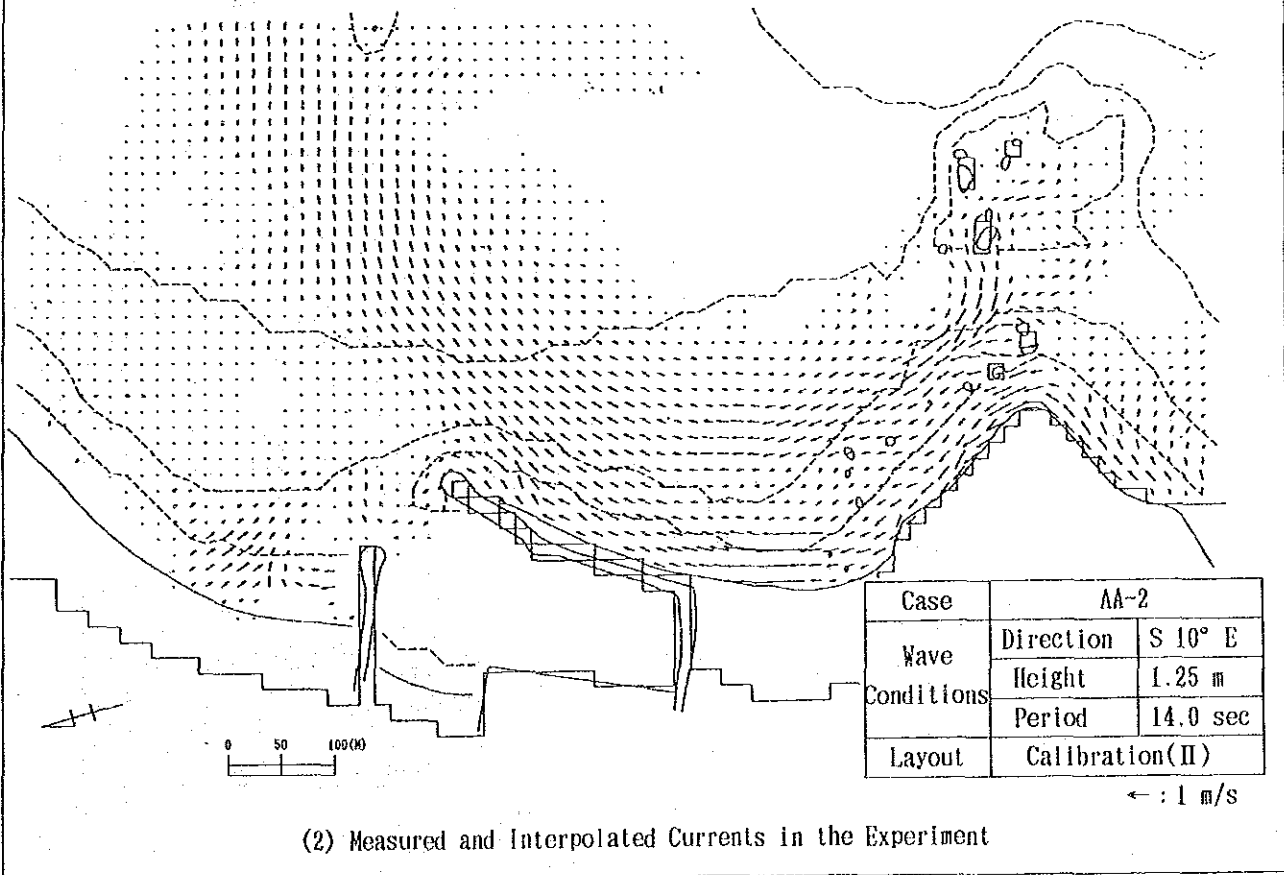


Fig.-3.2.6 Comparison of Observed Waves at the Site and Measured Waves in the Experiment

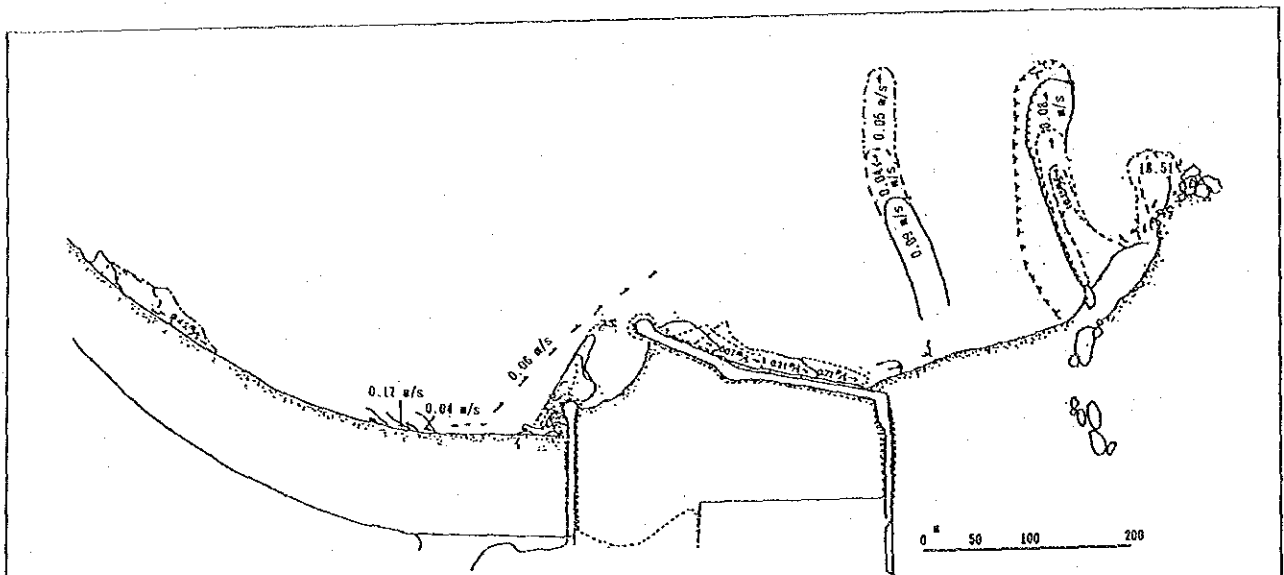


(1) Observed Currents near Harbour by Ball Float Tracking (88' 24th Aug. ~21th Sept.)

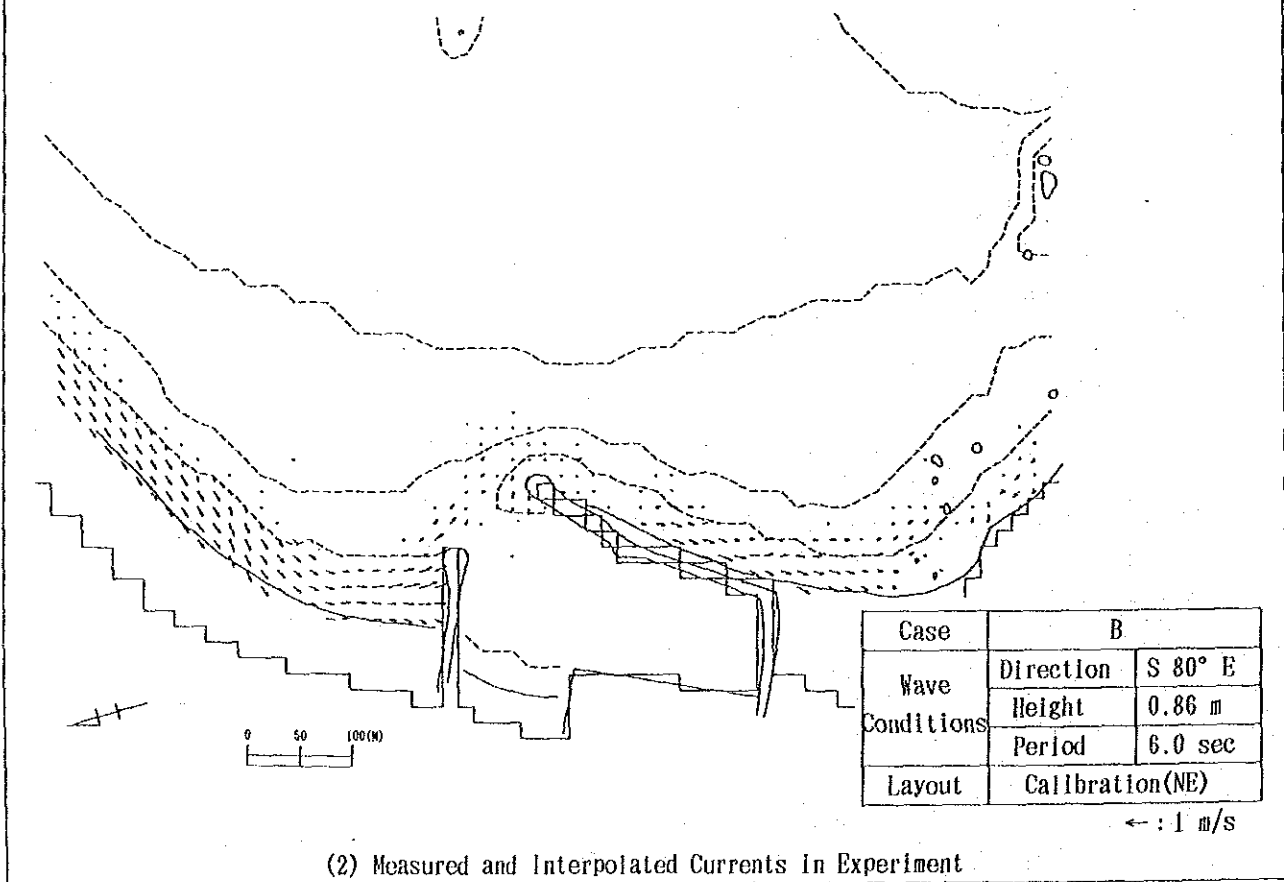


(2) Measured and Interpolated Currents in the Experiment

Fig.-3.2.7 Comparison of Observed and Measured Currents (SW Monsoon Period)



(1) Observed Currents at Site by Dye Tracing (87' 8th Mar.)



(2) Measured and Interpolated Currents in Experiment

Fig.-3.2.8 Comparison of Observed and Measured Currents (NE Monsoon Period)

Table 3.2.3 Comparison of Current Speed

(1) SW Monsoon Season

(Observed at the site)

Date\Location	Current Speed (m/sec)				Wave Condition		
	a	b	c	d	e	d	d
24th Aug.1988	0.52	0.30	----	0.16	1.23	1.16	16.0
28th Aug.1988	0.22	----	0.15	0.14	1.26	0.88	13.6
30th Aug.1988	0.42	----	----	0.14	1.33	0.84	13.8
3th Sept.1988	0.46	0.50	0.30	0.07	1.25	1.14	13.6
Average	0.41	0.40	0.23	0.13	1.27	1.01	14.3

(Measured in the experiment)

Location	Current Speed (m/sec)				Wave Condition		
	a	b	c	d	e	d	d
Experiment	0.36	0.25	0.21	0.20	1.25	0.87	14.0

(2) NE Monsoon Season

(Observed at the site)

Date\Location	Current Speed (m/sec)				Wave Condition		
	a	b	c	d	e	d	d
8th Mar.1987	0.07	----	0.17	----	----	----	----
	- 0.21						

(Measured in the experiment)

Location	Current Speed (m/sec)				Wave Condition		
	a	b	c	d	e	d	d
Experiment	0.10	----	0.25	----	0.86	0.84	6.0
	- 0.29						

- a: In front of the main breakwater
- b: In front of the harbour entrance
- c: North coast of the harbour
- d: About 100 m offshore from breakwater
- e: Offshore point(20m depth)

(2) Investigation of Reproducibility of Deposited Sand Volume Studies

Areas near the harbour were divided into 11 small regions as shown in Fig.3.2.9. Calculated results of sand deposition are shown in Table 3.2.4 and compared to the actual deposition in the site.

1) The 1st Stage (April,1985 - Oct.,1985)

The amount of calculated sand volume deposited in the pocket beach and front area of the main breakwater was 72,000 m³ while that estimated from the site survey was 88,000 m³.

The calculated value was therefore about 82 % that of the one estimated from the site survey and this degree of accuracy was considered to be sufficient.

2) The 2nd Stage (Mar.,1986 - Oct.,1986)

The amount of calculated sand volume deposited in the front area of the main breakwater was 37,000 m³ while that estimated from the site survey was 32,000 m³.

The sand volume which flowed into the harbour was calculated to be 10,000 m³ in this stage while that estimated from the site survey was 40,000 m³.

Not included in this volume was the sand volume which came into the harbour with overtopping and transmitted waves which was estimated to be about 47,000 m³ in the site.

3) The 3rd Stage (Nov.,1986 - Feb.,1987)

From the site survey, it was estimated that the 20,000 m³ of sand was transported from the front area of main break water to the pocket beach by waves and currents.

In the simulation, 12,000 m³ of sand was calculated to have been transported from the front area of the main breakwater to the pocket beach while 10,000 m³ of sand was calculated to have been transported and deposited inside the harbour from the northern areas.

Additionally 10,000 m³ of sand was calculated to have been deposited in the adjacent north region of the existing sub

breakwater.

At the site, as the harbour mouth was already almost closed by the sand bar by this stage, it would be reasonable to consider that the sand volume calculated to have deposited inside the harbour would actually have deposited just to the north of the existing sub breakwater.

Considering this, the $20,000 \text{ m}^3$ of sand was taken as having deposited in the region adjacent to the sub breakwater in the calculation.

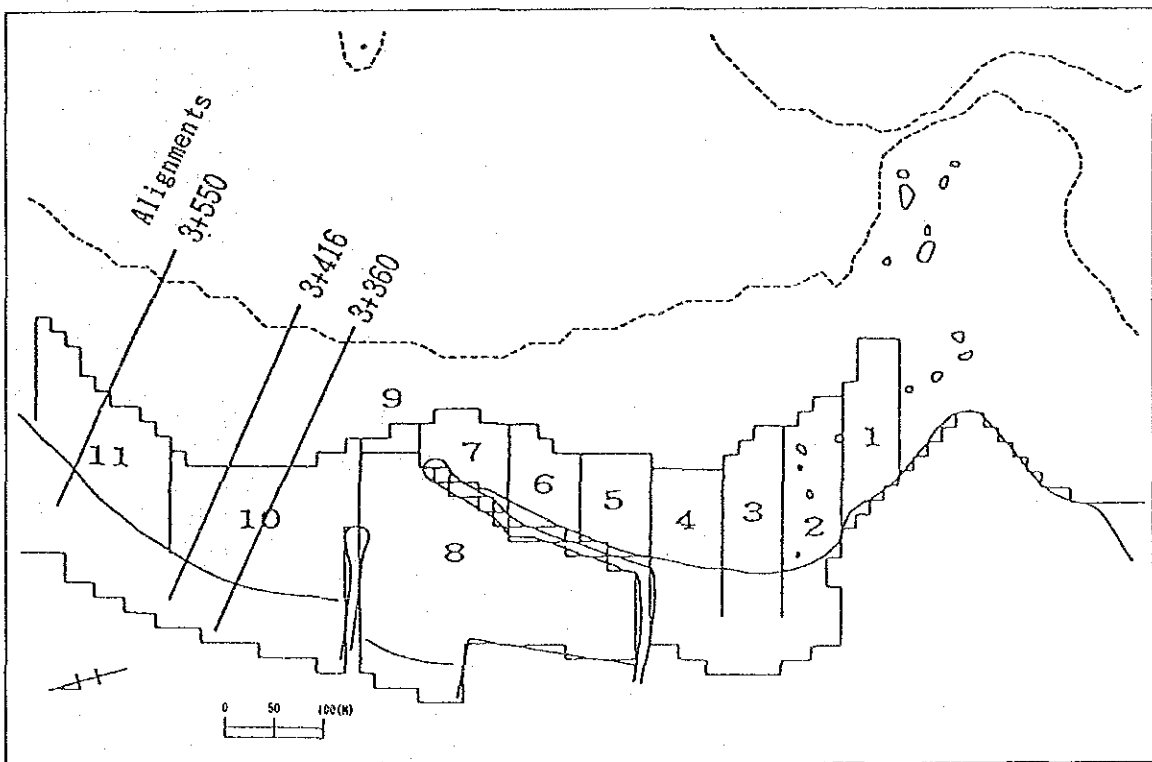


Fig. -3.2.9 Examination Area for Bathymetry Changes (Calibration)

Table-3.2.4 Accretion Volumes in Each Area (Calibration)

(unit: $\times 10^3 \text{ m}^3$)

+ : Accretion
- : Erosion

Area	SW monsoon season				NE monsoon season			
	1st stage (1985.4 ~ 1985.10)		2nd stage (1986.3 ~ 1986.10)		3rd stage (1986.11 ~ 1987.2)			
	Calculated Results	Actual * Deposits	Calculated Results	Actual * Deposits	Calculated Results	Actual** Deposits	Calculated Results	Actual** Deposits
1	5.2		12.5		2.8			
2	7.1	29.6	8.1	28.1	5.8	9.1		22.5
3	8.2		4.5		0.5			
4	9.1		3.0		-3.7			
5	11.6		6.0		-3.0			
6	11.5	42.4	3.6	9.0	-2.8		-12.2	-20.0
7	19.3		-0.6		-2.7			
8	0	0	10.3	10.3	10.5	10.5		3.5
9	1.0		1.2		1.5			
10	-11.4	-22.1	-16.9	-23.0	6.9	9.5	20.0	100.0
11	-11.7		-7.3		1.1			(84.0)

* Actual deposits are quoted from the first follow up study (Oct.1986)

** Actual deposits are quoted from the second follow up study (Mar.1987)

*** Actual deposits in northern beach of Kirinda port were estimated by

sounding data of the 3 lines (3+360, 3+416, 3+550, shown in Fig.3.1.9),

where data were from examination areas, and sea bottoms changes in

areas shallower than D.L. from Nov.1988 to Mar.1989.

In areas deeper than D.L., the sea bottom profiles were estimated

at 2 m heights parallelgram shapes, on the basis of Hallimeter's

Formula for critical water depth of sand movement (D_{SH})

as follows (1983).

$$D_{SH} = 2.9 H_0 / (\rho_s / \rho - 1)^{1/2} - 110 H_0^2 / \{ (\rho_s / \rho - 1) g T^2 \}$$

in which

ρ_s : density of sand and water

g : acceleration due to gravity

T : wave period

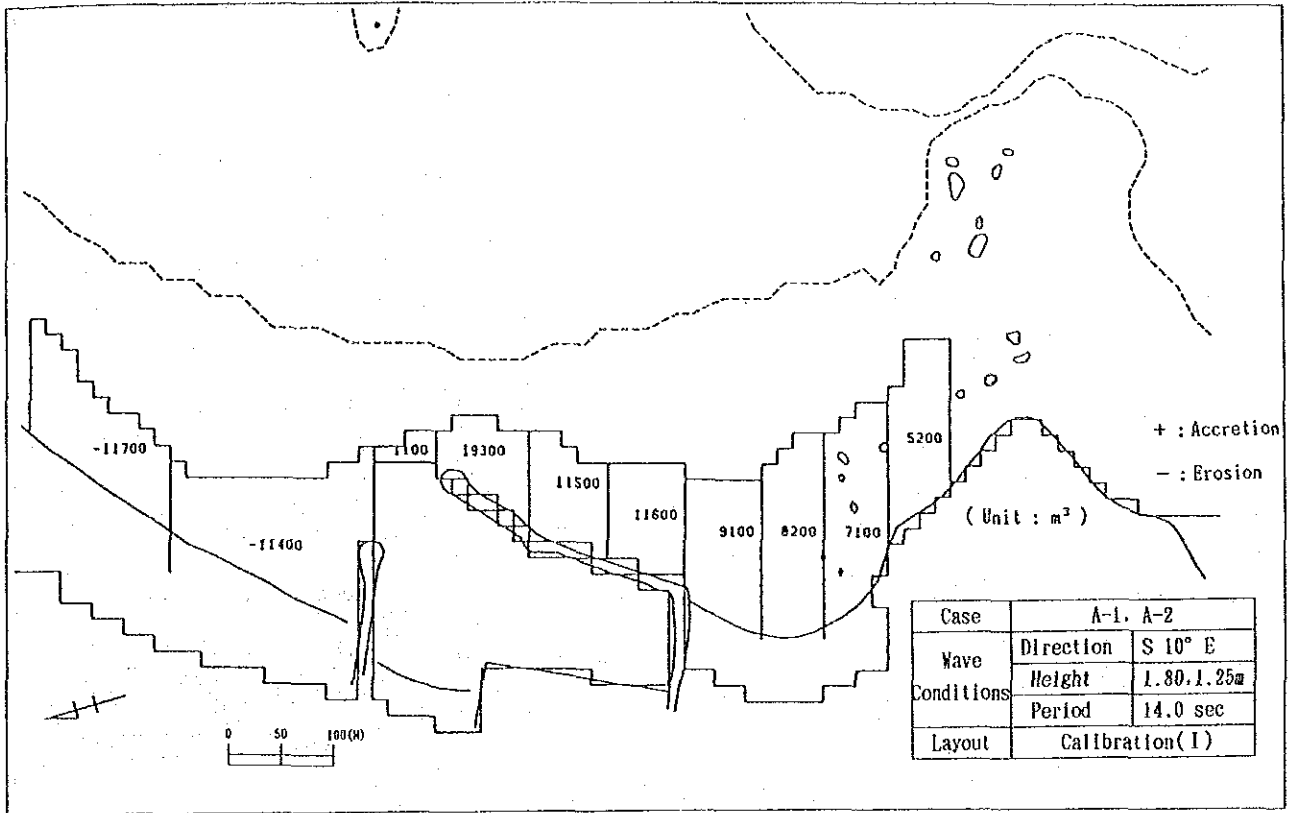


Fig.-3.2.10 Accretion Volumes (Calibration(I) SW. 1.8m, 1.25m, 1 season)

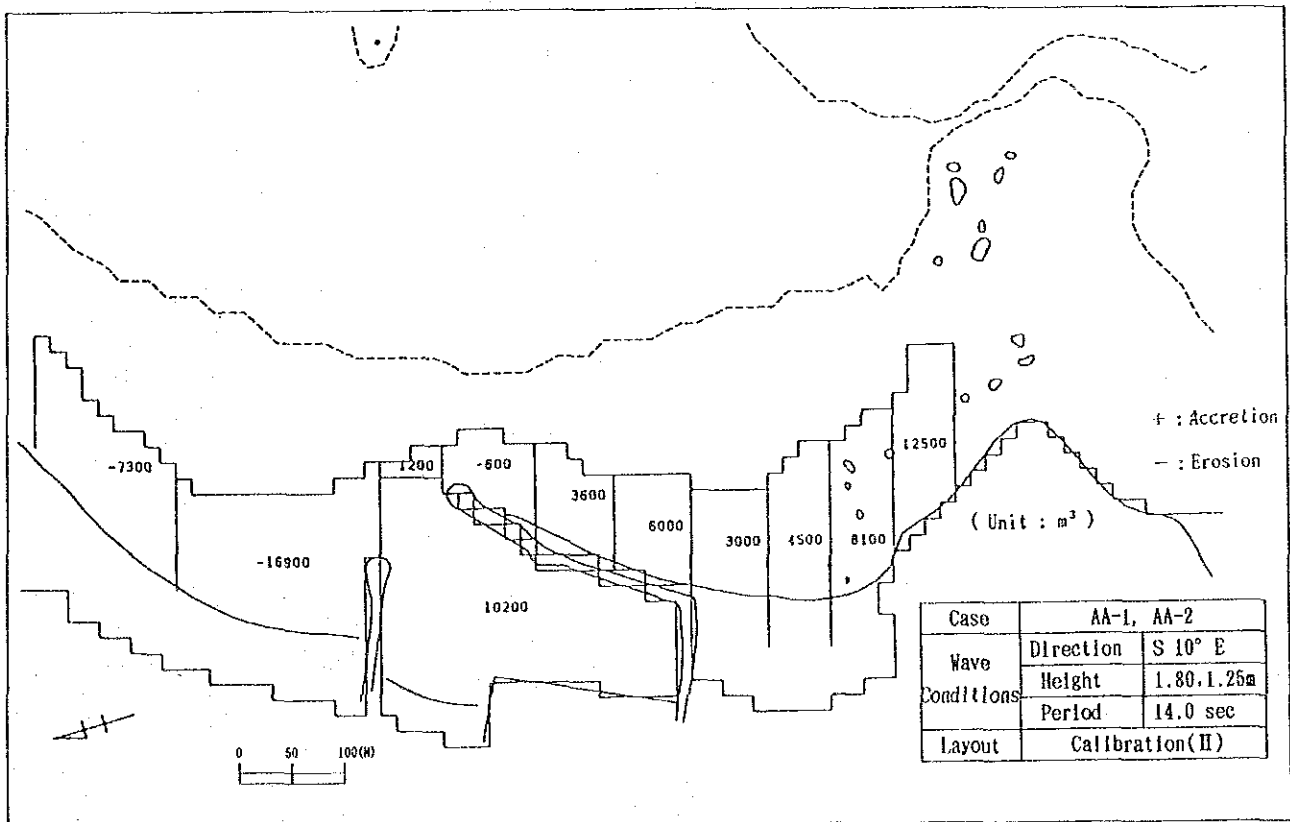


Fig.-3.2.11 Accretion Volumes (Calibration(II) SW. 1.8m, 1.25m, 1 season)

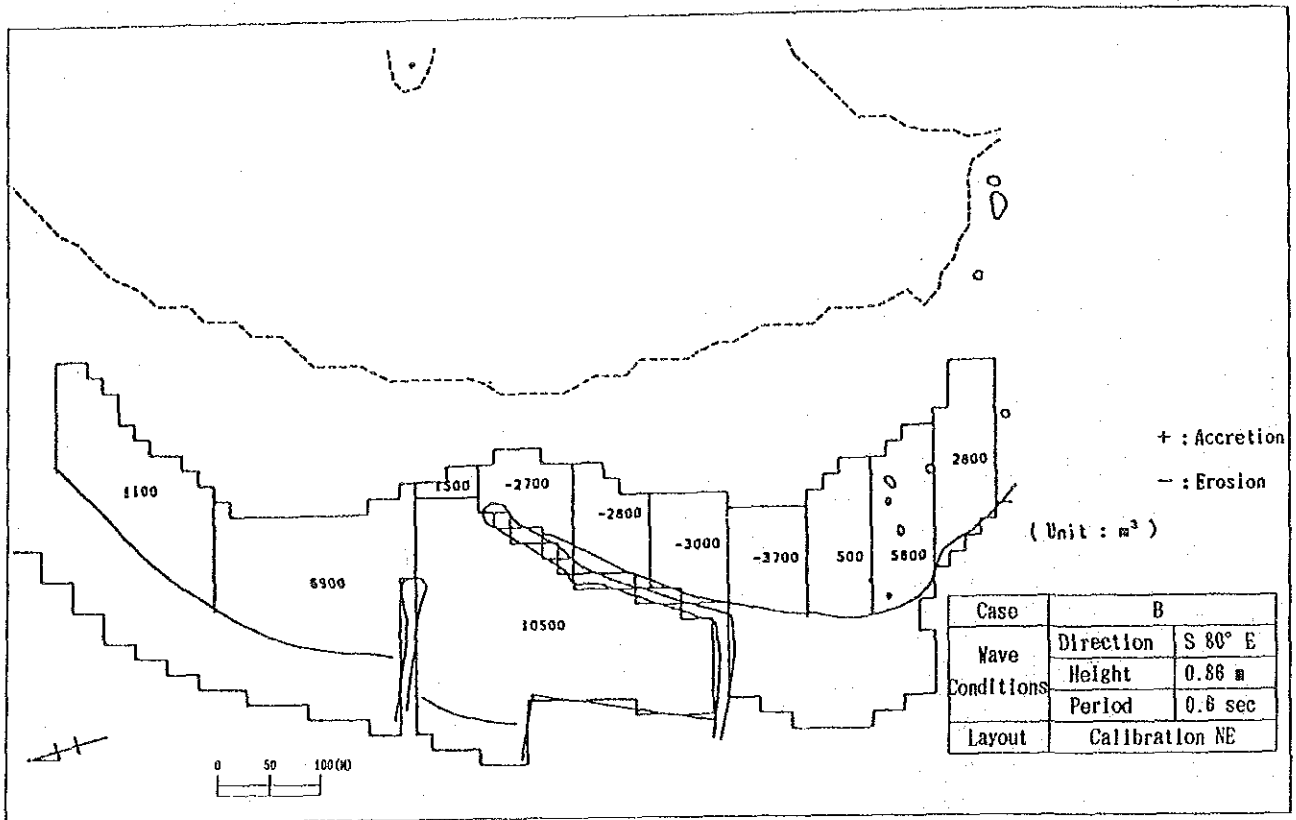


Fig.-3.2.12 Accretion Volumes (Calibration NE. 0.88m. 1 season)

(3) Investigation of Reproducibility of Shoreline Changes

An investigation of reproducibility of shoreline changes was conducted by utilizing a 1-line model.

The objective areas were the front areas of the main breakwater and pocket beach shown in Fig.3.2.13 and the objective period was the 1st stage(April,1985 - Nov.,1985) as described previously.

In the 1-line model,the wave heights and directions at breaking were obtained from the results of calculation with some references made to the result of hydraulic experiments as shown in Fig.3.2.14.

The adopted wave conditions which approximated to the mean value in the SW monsoon season were as follows.

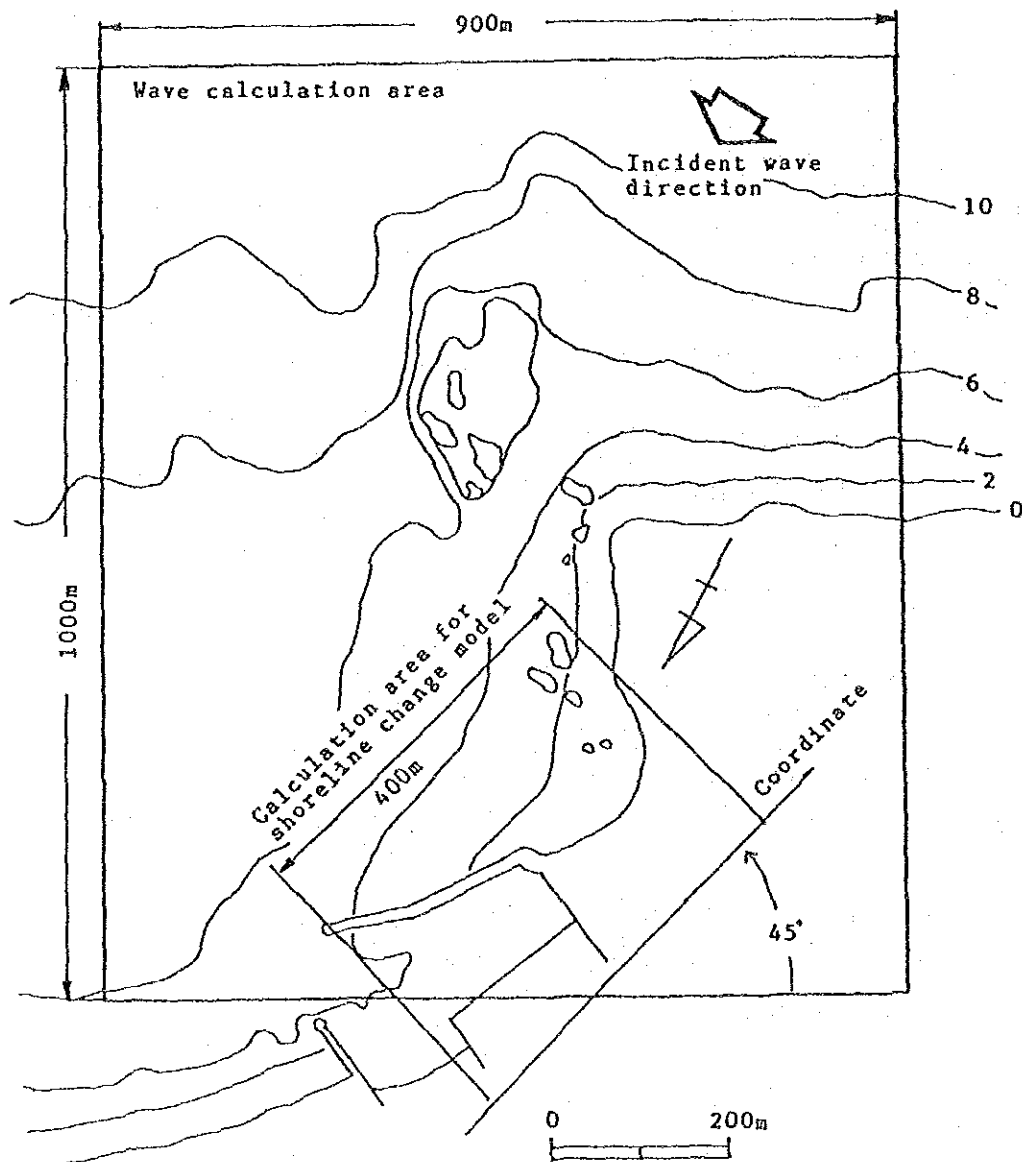
Wave Height : 1 m

Wave Period : 14 sec

Wave Direction : S 10° E

The depth of closure (Ds) and the rate of sand volume supply from Kirinda Point were settled on at 5.6 m and 430 m³ /day respectively on the basis of the relation between the deposited sand volume and the increase in area.

A comparison of the calculated shoreline changes and those observed in the site showed that good reproducibility had been achieved in this hindcast simulation.(See Fig.3.2.15 and Fig.3.2.16)



Grid space of 15m was taken in calculation

Fig.-3.2.13 Calculation Area for Shoreline Change Model Simulation

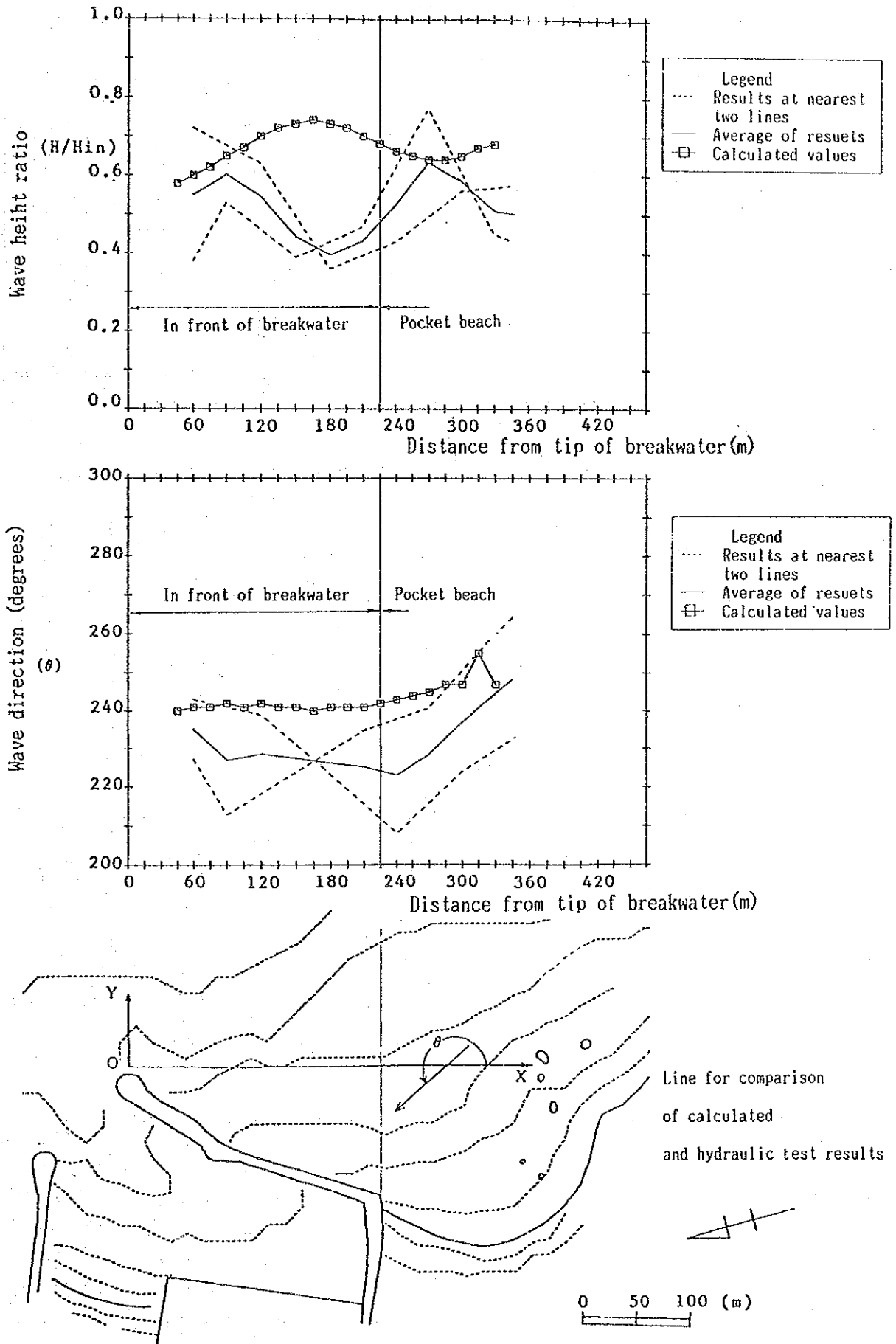


Fig.-3.2.14 Comparison of Wave Heights and Direction in front of Breakwater

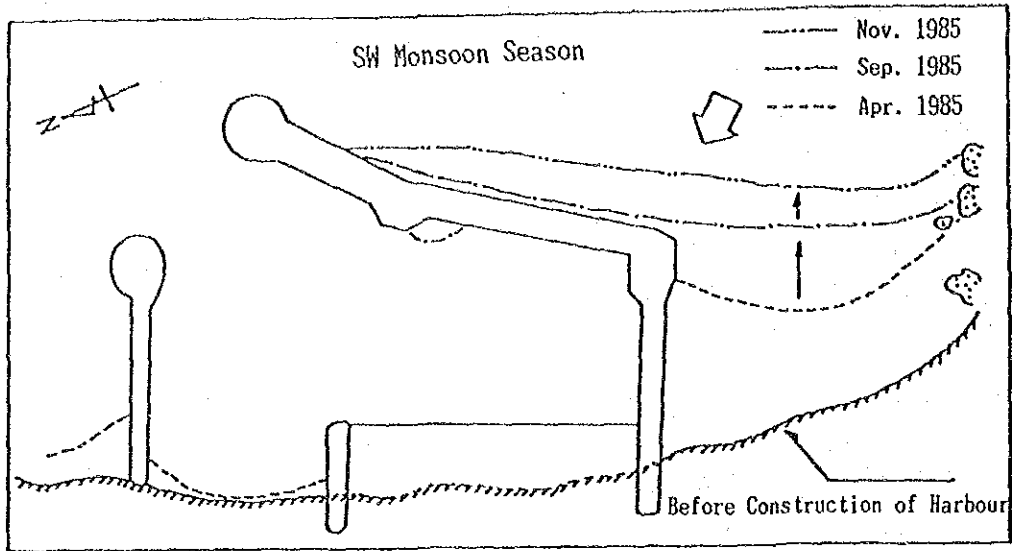


Fig.-3.2.15 Transition of Shoreline

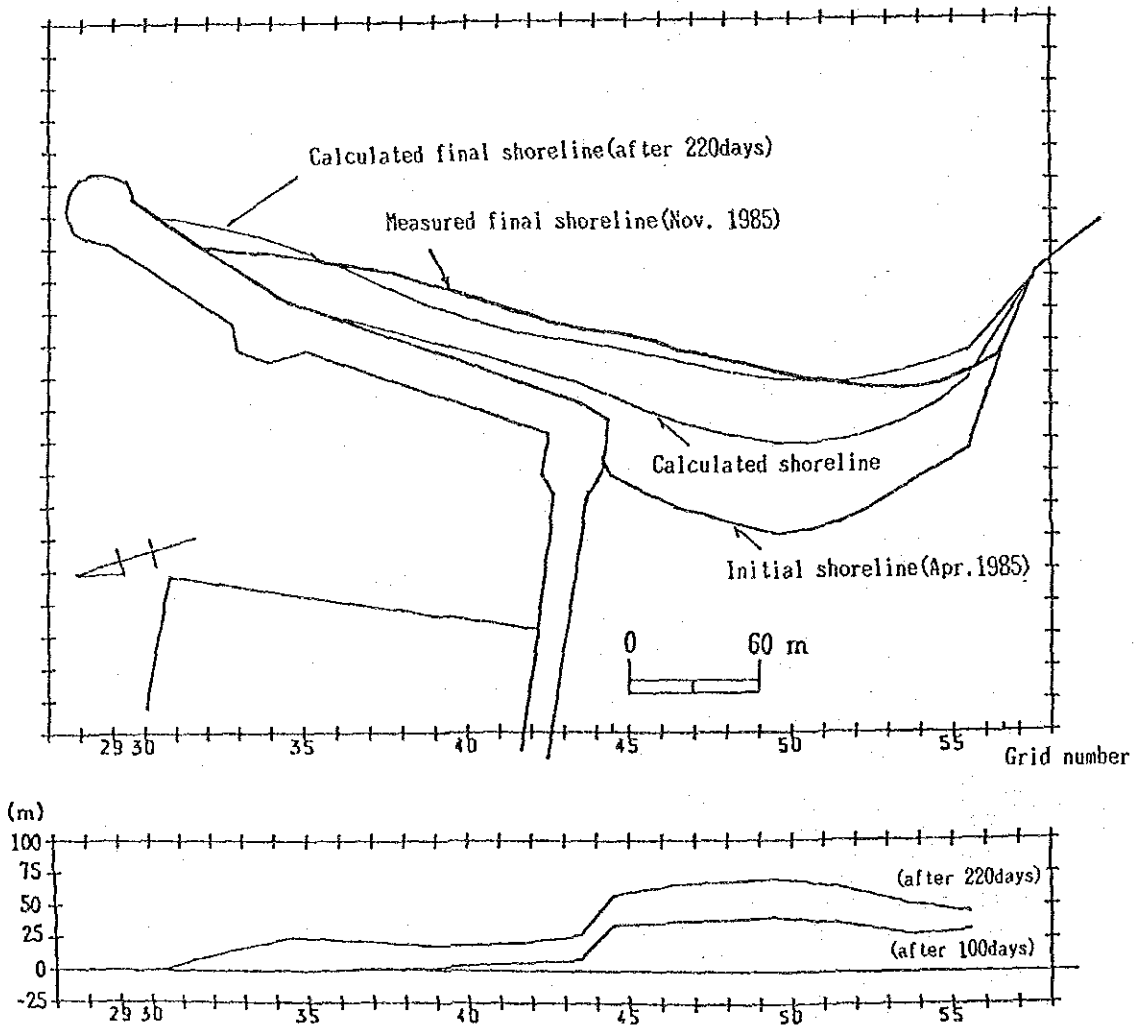


Fig.-3.2.16 Comparison of Calculated and Measured Shoreline

3.3 Investigation Cases

3.3.1 Procedure to Investigate the Efficiency of Countermeasures

- (1) Hydraulic experiments were conducted for several different layouts of countermeasures first and layouts were selected roughly by comparing the results of the experiments. (Topography in May, 1988)
- (2) On consideration of the reliability of the prediction method, it was decided that the best approach was to include the change of wave and current condition caused by the change of sea bottom bathymetry. New hydraulic conditions would then be obtained by conducting the hydraulic experiment, adopting the new predicted bathymetry. For this reason, the procedure to select the countermeasures which would produce the highest efficiency was decided as follows.

```
-----  
| Prediction for bathymetry change by hybrid model |  
| (topography in May, 1988) |  
| Prediction for shoreline change by 1-line model |  
-----
```

|

```
-----  
| Performance of hydraulic experiment |  
| (topography in predicted situation) |  
-----
```

|

```
-----  
| Prediction for bathymetry change by hybrid model |  
| (usage of newly obtained hydraulic data) |  
| Prediction for shoreline changes by 1-line model |  
-----
```

|

```
-----  
| Evaluation of efficiency of countermeasures |  
-----
```

3.3.2 Investigation Cases by means of Hybrid Model

All cases investigated by means of the hybrid model are shown in Tables 3.3.1 and 3.3.2 relating to countermeasure plans. All 11 layouts are shown in Figs.3.3.1 to 3.3.4 with their beneficial effects listed.

The sea bottom topography for May,1988 was adopted as the initial topography and expressed as topography II, while the sea bottom topography predicted after five SW monsoon periods was expressed as topography III.

Construction of a submerged breakwater or a groyne at Kirinda Point was confirmed to be very efficient as a countermeasure. The success of the plans for countermeasures could only be assured with a groyne of some sort in place.

As to the possibility of establishment some kind of countermeasure in front of Kirinda Point, the Study Team was informed by the Government of Sri Lanka concerned that they had gotten a basic agreement with priests of Kirinda Temple and that a groyne rather than a submerged breakwater should be adopted to take into account the safe navigation of boats. Therefore, in the middle of the study, the Study Team started examination of a groyne instead of a submerged breakwater.

Table 3.3.1 Countermeasure Test Cases for SW Monsoon Season

No	Case	Wave conditions			Countermeasure	Sea Bottom Topography	Hydraulic Experiment	Numerical Simulation
		Height	Period	Direction †				
1	C-1	1.80 m	14 sec	S10°E	Layout 1: Extension of Main Breakwater (200m, 40°)	II	○	○
2	C-2	1.80 m	14 sec	S10°E	Layout 2: Extension of Main Breakwater (300m, 40°)	II	○	○
3	C-3	1.80 m	14 sec	S10°E	Layout 3: Extension of Main Breakwater (200m, 20°) : Submerged Groyne at Kirinda Point	II	○	
4	C-4	1.80 m	14 sec	S10°E	Layout 4: Extension of Main Breakwater (200m, 40°) : Submerged Groyne at Kirinda Point	II	○	
5	C-5	1.80 m	14 sec	S10°E	Layout 5: Extension of Main Breakwater (300m, 40°) : Submerged Groyne at Kirinda Point	II	○	
6	C-6	1.80 m	14 sec	S10°E	Layout 6: Extension of Main Breakwater (200m, 40°) : Submerged Groyne at Kirinda Point : New Sub Breakwater (Type b)	II	○	
7	C-7	1.25m	14 sec	S10°E	Layout 6: Extension of Main Breakwater (200m, 40°) : Submerged Groyne at Kirinda Point : New Sub Breakwater (Type b)	II	○	
8	C-8	1.80m	14 sec	S10°E	Layout 7: Extension of Main Breakwater (300m, 40°) : Submerged Groyne at Kirinda Point : New Sub Breakwater (Type a)	II	○	
9	C-9	1.25m	14 sec	S10°E	Layout 7: (ditto)	II	○	
10	C-10	1.80m	14 sec	S10°E	Layout 8: Extension of Main Breakwater (200m, 40°) : Groyne at Kirinda Point : New Sub Breakwater (Type a)	II	○	
11	C-11	1.25m	14 sec	S10°E	Layout 8: (ditto)	II	○	
12	C-12	1.80m	14 sec	S10°E	Layout 9: Extension of Main Breakwater (200m, 40°) : Groyne at Kirinda Point : New Sub Breakwater (Type c)	II	○	○
13	C-13	1.25m	14 sec	S10°E	Layout 9: (ditto)	II	○	○
14	C-14	1.80m	14 sec	S10°E	Layout 9: (ditto)	III	○	○
15	C-15	1.25m	14 sec	S10°E	Layout 9: (ditto)	III	○	○

Table 3.3.2 Countermeasure Test Cases for NE Monsoon Season

No	Case	Wave conditions			Countermeasure	Sea Bottom Topography	Hydraulic Experiment	Numerical Simulation
		Height	Period	Direction †				
16	D-1	0.86 m	6 sec	S80°E	Layout 9: Extension of Main Breakwater (200m, 40°) : Groyne at Kirinda Point : New Sub Breakwater (Type c)	III	○	○
17	D-2	0.86 m	6 sec	S80°E	Layout 10: Extension of Main Breakwater (200m, 40°) : Groyne at Kirinda Point : New Sub Breakwater (Type c) : Groyne at Northern Coast	III	○	
18	D-3	0.86 m	6 sec	S80°E	Layout 11: Extension of Main Breakwater (200m, 20°) : Groyne at Kirinda Point : New Sub Breakwater (Type d)	III	○	○

†Direction at wave generator

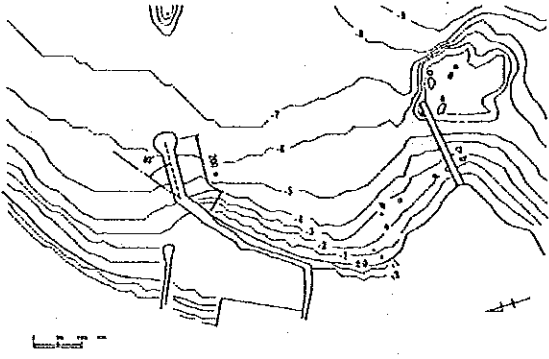
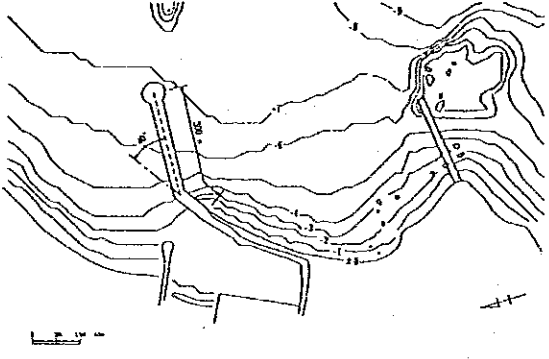
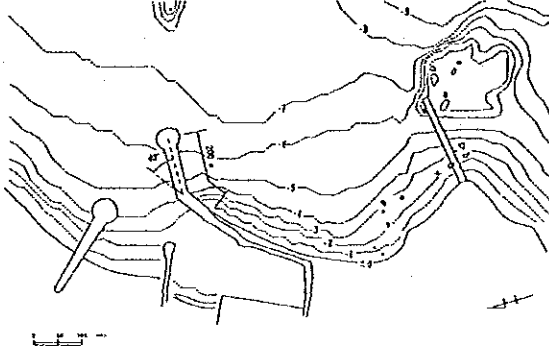
Countermeasure	Aim	No.	Layout
Main breakwater extension (200m, 40°) + Submerged groyne at Kirinda Point	To effect more suppression of deposition near the head of the main breakwater by shifting the direction of the main breakwater extension to the offshore side.	4	
Main breakwater extension (300m, 40°) + Submerged groyne at Kirinda Point	To enhance the effects 1)~4) through a 300m extension of main breakwater.	5	
Main breakwater extension (200m, 40°) + Submerged groyne at Kirinda Point + New sub breakwater (Type b)	6) To reduce the sand deposited near the harbour mouth resulting from circulation currents in the SW monsoon season by constructing a new sub breakwater. 7) To prevent littoral sand transport into the harbour.	6	

Fig. -3.3.2 Layouts of Countermeasures(2)

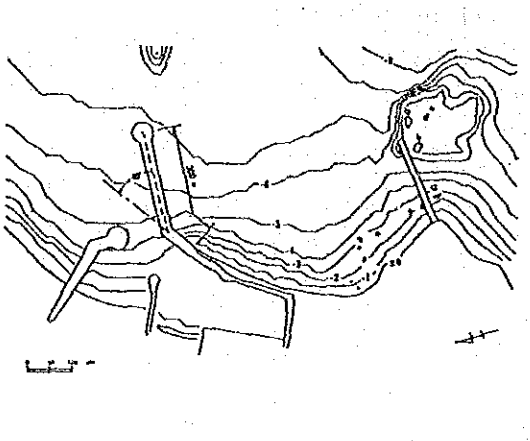
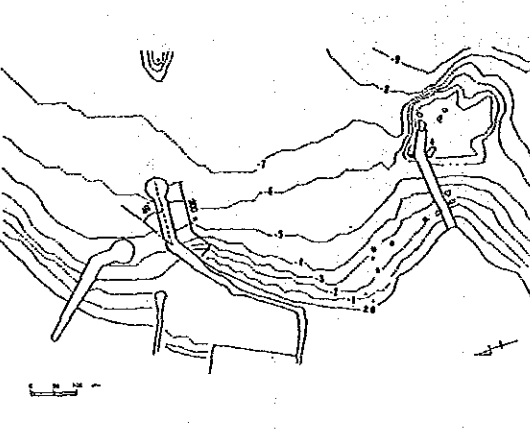
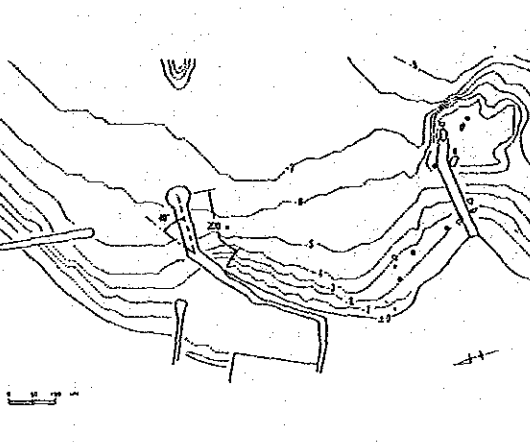
Countermeasure	Aim	No.	Layout
Main breakwater extension (300m, 40°) + Submerged groyne at Kirinda Point + New sub breakwater (Type a)	To intensify effects 1)~ 4) by a 300m extension of main breakwater in addition to layout 6.	7	
Main breakwater extension (200m, 40°) + Groyne at Kirinda Point + New sub breakwater (Type a)	To enhance the ability to inhibit sand transport at Kirinda Point by adopting an extended groyne. (not submerged)	8	
Main breakwater extension (200m, 40°) + Groyne at Kirinda Point + New sub breakwater (Type c)	6) To reduce the sand deposited near the harbour mouth resulting from circulation currents in the SW monsoon season by constructing a new sub breakwater. 7) To prevent littoral sand transport into the harbour.	9	

Fig. -3.3.3 Layouts of Countermeasures(3)

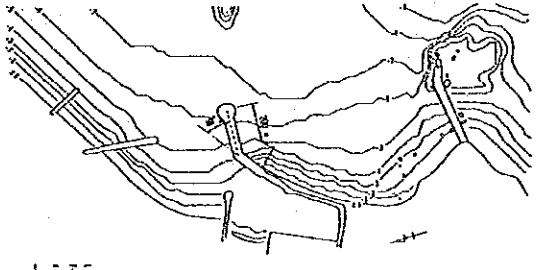
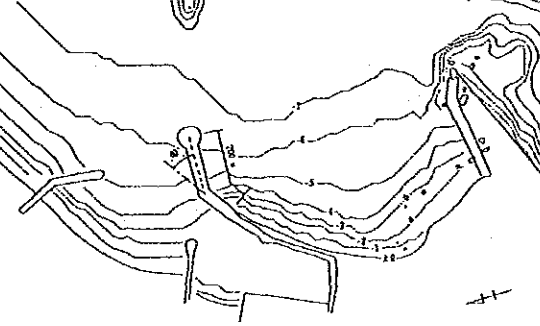
Countermeasure	Aim	No.	Layout
Main breakwater extension (200m, 40°) + Groyne at Kirinda Point + New sub breakwater (Type c) + Groyne at northern coast	To enhance the ability to reduce littoral sand transport in the NE monsoon season.	10	
Main breakwater extension (200m, 40°) + Groyne at Kirinda Point + New sub breakwater (Type d)	To investigate the intensified effect of a variation in alignment of new sub breakwater in the NE monsoon season.	11	

Fig. -3.3.4 Layouts of Countermeasures (4)

3.3.3 Investigation Cases of Hydraulic Experiments using Movable Bed

Layout 9 was selected and confirmed to have high efficiency as a countermeasure as a result of investigation by utilizing the hybrid model.

Movable bed experiments were also conducted for this layout 9 .

Cases are summarized in Table.3.3.3.

Table-3.3.3 Cases of Movable Bed Experiments

No.	Case	Wave Condition			Layout Case	Remarks
		Height	Period	Direction		
1	E-1	0.86m	6sec	S 80° E	9	NE monsoon
		1.20m	6sec	S 80° E	9	NE monsoon
2	E-2	1.25m	14sec	S 10° E	9	SW monsoon